# SEASONAL HYDROLOGICAL PREDICTION IN GREAT BRITAIN – AN ASSESSMENT

by

DAVID ANTHONY LAVERS

A thesis submitted to The University of Birmingham for the degree of DOCTOR OF PHILOSOPHY

School of Geography, Earth and Environmental Sciences

College of Life and Environmental Sciences

The University of Birmingham

October 2010

UNIVERSITY OF
BIRMINGHAM

## University of Birmingham Research Archive

### e-theses repository

This unpublished thesis/dissertation is copyright of the author and/or third parties. The intellectual property rights of the author or third parties in respect of this work are as defined by The Copyright Designs and Patents Act 1988 or as modified by any successor legislation.

Any use made of information contained in this thesis/dissertation must be in accordance with that legislation and must be properly acknowledged. Further distribution or reproduction in any format is prohibited without the permission of the copyright holder.

## ABSTRACT

This thesis assesses seasonal hydrological prediction in Great Britain. Firstly, the study evaluates river flow prediction using climate model output to drive a rainfall-runoff model in the Dyfi basin, Wales. Results show that climate model precipitation can not skilfully simulate Dyfi discharge. When a downscaling process is employed to generate precipitation time series, river flow forecast skill improves, but historical river flows still provide superior forecasts. Secondly, large-scale climatic control on British precipitation/discharge and European precipitation is investigated by correlation analysis. Results show spatiotemporal hydroclimatological variation, with western regions generally having stronger empirical relationships. River flow has weaker associations because of basin controls and evapotranspiration. The dynamic nature of precipitation/discharge generating mechanisms is not captured by the North Atlantic Oscillation Index. Thirdly, seasonal climate model forecast skill is evaluated. Limited skill exists over land and over all extratropical regions for forecasts beyond month-1; precipitation has lower skill than 2-metre air temperature and mean sea level pressure. Seasonal climate models exhibit higher idealised predictive skill indicating potential for future increases in actual predictive skill. In conclusion, seasonal hydrological prediction using a climate-to-river modelling chain could be improved through consideration of the uncovered spatiotemporal hydroclimatological variability and through seasonal climate modelling improvements.

‘If any of you lacks wisdom, he should ask God, who gives generously to all without finding fault, and it will be given to him.’ James 1:5 (New International Version)

‘Difficulties mastered are opportunities won.’ Winston Churchill

## ACKNOWLEDGEMENTS

This PhD research has been made possible by support, financial and otherwise, from many people during the last four years. I am grateful for the financial support from the United Kingdom Natural Environment Research Council (NER/S/A/2005/13646A) and the supportive environment of the Centre for Ecology and Hydrology (CEH) Wallingford that made this work possible. In particular, I sincerely thank my supervisors, Dr. Christel Prudhomme at CEH Wallingford and Dr. David M. Hannah at the University of Birmingham, for their continual guidance and friendship throughout the PhD.

I deeply thank Professor Eric F. Wood of Princeton University USA for the wonderful opportunity to work within his research group on a 9 month placement during 2009, and Professor Wood's and Dr. Lifeng Luo's advice and discussions that helped to generate the research presented in Chapter 7. I recognise the departmental and computer support in Princeton and acknowledge NOAA grants NA06OAR4310051 and NA17RJ2612 that also made the work in Chapter 7 possible.

I acknowledge the following groups/institutions/projects that provided the data used in this research: the National River Flow Archive (NRFA) at CEH Wallingford for providing river basin precipitation and discharge, the ECMWF data server that provided the DEMETER and ERA-40 datasets, and the ENSEMBLES project that produced an E-OBS observed precipitation dataset across Europe. I would also like to thank the following people for stimulating discussions during my PhD: Sue Crooks, Jamie Hannaford, Thomas Kjeldsen, Ming Pan, Ian D. Phillips, John Schaake, Alberto Troccoli, Gabriele Villarini and Raghuveer Vinukollu. I acknowledge the vital support from my family and friends, and I finally thank God for giving me the strength and ability to complete this project.

# TABLE OF CONTENTS

# LIST OF ILLUSTRATIONS

# LIST OF TABLES

# LIST OF ABBREVIATIONS

| | |
|---|---|
| AI | Artificial Influence |
| ALO | Atmosphere-land-ocean |
| ANN | Artificial Neural Network |
| ARMA | Autoregressive Moving Average |
| BFI | Base Flow Index |
| CCA | Canonical Correlation Analysis |
| CERFACS | European Centre for Research and Advanced Training in Scientific Computation |
| CFS | Climate Forecast System |
| COLA | Centre for Ocean-Land-Atmosphere |
| CRU | Climatic Research Unit |
| DEMETER | Development of a European Multimodel Ensemble system for seasonal to interannual prediction |
| DJF | December, January and February |
| ECHAM | European Centre/Hamburg Model |
| ECMWF | European Centre for Medium-Range Weather Forecasts |
| ENSEMBLES | EU-funded integrated project to develop an ensemble prediction system for climate change |
| ENSO | El Niño Southern Oscillation |
| ERA-40 | ECMWF Re-analysis–40 |
| ES | Expert Systems |
| EU | European Union |
| FDC | Flow Duration Curve |
| GCM | General Circulation Model |
| GEWEX | Global Energy and Water Cycle Experiment |
| GLACE | Global Land-Atmosphere Coupling Experiment |
| GM | Genetic Algorithm |
| GPCC | Global Precipitation Climatology Centre |
| GSM | Global Spectral Model |
| HEPEX | Hydrologic Ensemble Prediction Experiment |
| INGV | Istituto Nazionale de Geofisica e Vulcanologia |
| JJA | June, July and August |
| JMA | Japan Meteorological Agency |
| KNN | K-Nearest Neighbour |
| LODYC | Laboratoire d'Océanographie Dynamique et de Climatologie |
| LWP | Locally Weighted Polynomial |
| MAM | March, April and May |
| MEI | Multivariate Index |
| Météo-France | French Meteorological Service |
| MORECS | UK Meteorological Office Rainfall and Evaporation Calculation System |
| MPI | Max-Planck Institut für Meteorologie |
| MRF | Medium-Range Forecast |
| MSLP | Mean Sea Level Pressure |
| NAO(I) | North Atlantic Oscillation (Index) |
| NCEP | National Centers for Environmental Prediction |

| | |
|---|---|
| NOAA | National Oceanic and Atmospheric Administration |
| NRFA | National River Flow Archive |
| PCR | Principal components regression |
| PDM | Probability Distributed Model |
| PE | Potential Evapotranspiration |
| POL | Polar-Eurasian teleconnection |
| RCM | Regional Climate Model |
| RCSM | Regional Climate System Model |
| SAAR | Standard Annual Average Rainfall |
| SNAO | Summer North Atlantic Oscillation |
| SOI | Southern Oscillation Index |
| SON | September, October and November |
| SST | Sea Surface Temperature |
| SVD | Singular Value Decomposition |
| UCLA | University of California, Los Angeles |
| UEA | University of East Anglia |
| UK | United Kingdom |
| UKMO | United Kingdom Meteorological Office |
| USA | United States of America |
| VIC | Variable Infiltration Capacity |

# 1. INTRODUCTION

## 1.1 Background and rationale

Hydrological extremes, or floods and droughts, have adverse socio-economic effects that threaten human and animal life, cause property damage and insurance losses, and disrupt agricultural production and water supply. These recurrent hydrological hazards affect both the developed and less-developed world and are a natural part of hydroclimatological variability. In Great Britain over the last decade, flood (e.g. January 2003 (Marsh, 2004) and summer 2007 (Marsh, 2008)) and drought (such as 2004–06 (Marsh *et al.*, 2007)) events have been prominent and thus of great public concern. As flooding and drought events are expected to become more commonplace in a changing climate (Kundzewicz *et al*., 2007), the need to improve understanding of the hydroclimatological process chain across Great Britain and the capability to skilfully predict hydrological extremes months in advance has been brought into sharp focus.

Seasonal climate forecasting (defined here as up to six months lead time) is undertaken with two main approaches (Troccoli, 2010). First, statistical modelling uses historical observations to develop predictive relationships between a predictor variable (e.g. sea surface temperature SST) and a predictand (e.g. precipitation). Second, dynamical modelling uses coupled General Circulation Models (GCMs) of the atmosphere-land-ocean (ALO) system (Palmer *et al.*, 2004) to integrate in to the future a truncated set of partial differential equations (that describe the ALO system processes) to predict future climate. Many meteorological forecast centres now produce their seasonal climate forecasts using dynamical modelling and these include the European Centre for Medium-Range Weather Forecasts (ECMWF) and UK Meteorological Office (UKMO). Seasonal climate forecasts have potential socio-economic benefits across many sectors, including energy, agriculture, health, and water resource

management (Barnston *et al.*, 2005). In the field of water resources, reliable forecasts of precipitation and river flow at seasonal time scales can help mitigate the detrimental effects of hydrological extremes by increasing human preparedness for future anomalous conditions (Wedgbrow *et al.*, 2002), and informing the decision making process for land and water resources management (Kirono *et al.*, 2010). For example, seasonal hydrological forecasts can inform more appropriate allocation of water for hydroelectric power generation (Cardoso and Silva Dias, 2006, Coelho *et al.*, 2006). Improved water management, in turn, has potential to reduce economic losses associated with floods and droughts (Wood and Lettenmaier, 2006).

This thesis focuses on seasonal hydrological prediction in Great Britain because of the (1) paucity of studies undertaken for this region, (2) situation of Great Britain, with respect to the westerly atmospheric circulation that travels over the North Atlantic Ocean heat and moisture source, which holds potential for strong climate-hydrology connections and (3) great economic damage that hydrological extremes cause to the high population of Great Britain. Furthermore, with the recent success of the 2005–06 UKMO seasonal winter climate forecast for Britain/Europe (Graham *et al.*, 2006), it is timely to undertake a study that attempts to assess and improve the state-of-the-art of seasonal hydrological prediction.

## 1.2 Research gaps and objectives

The literature review of seasonal climate and river flow prediction in Chapter 2 identifies three research gaps for investigation as follows:

1) GCMs have been shown to be useful tools for river flow simulation in certain parts of the World, but the use of an end-to-end physically realistic modelling system using a rainfall-runoff model forced with GCM data has not been tested in Great Britain.

2) There is a lack of knowledge on the spatiotemporal variability of hydroclimatological relationships across Great Britain.

3) There are few published studies that assess global-scale seasonal climate model predictive skill.

In view of these research gaps, the overarching *aim* of this thesis is to evaluate the potential for seasonal hydrological prediction in Great Britain. To address each of the recognised gaps, the objectives of this thesis are:

1) To evaluate river flow predictive skill using a rainfall-runoff model forced with GCM data in a test British river basin (Chapter 4).

2) To identify and quantify spatiotemporal variability in hydroclimatological relationships across Great Britain and Europe (Chapters 5 and 6, respectively).

3) To assess at the global scale the current level of seasonal climate model predictive skill (specifically 2-metre temperature, precipitation and mean sea level pressure) for potential applications in sectors such as hydrology (Chapter 7).

### 1.3 Thesis structure

The thesis layout is discussed below and an illustration of the thesis structure together with the inter-relationships between the chapters is shown in Figure 1.1. Chapter 2 provides the literature review and teases out the research gaps aforementioned in section 1.2. The research design and an overview of the data and methods used in the thesis are presented in Chapter 3. Chapter 4 evaluates river flow forecasting using a rainfall-runoff model forced with GCM data. Chapters 5 and 6 investigate the nature and dynamics of hydroclimatological relationships across Great Britain and Europe respectively. An assessment of the current level

of seasonal climate model predictive skill for applications is undertaken in Chapter 7. Chapter 8 synthesises findings and draws conclusions on the research undertaken, and ends with suggestions for future research.

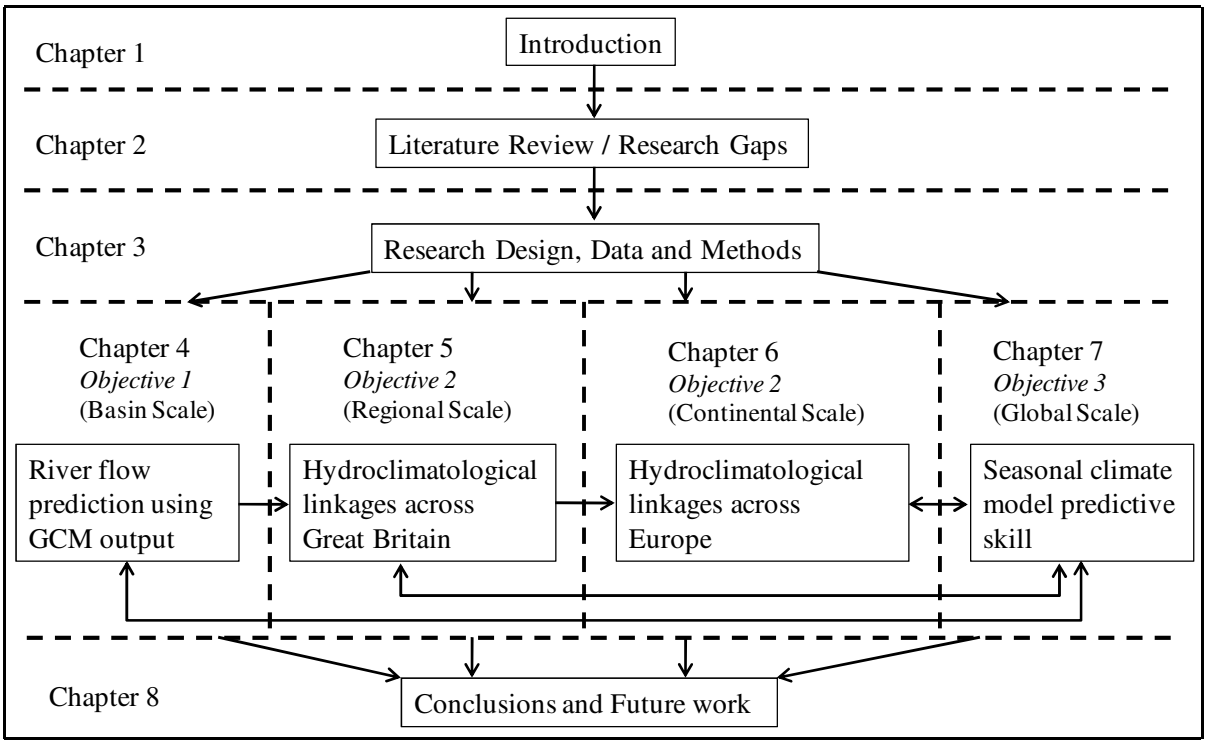


Figure 1.1: Schematic diagram of the thesis. The arrows show the inter-relationships between chapters.

## 1.4 Chapter summary

This chapter has provided a background and rationale to conduct research on seasonal hydrological prediction and hydroclimatological variability in Great Britain and Europe. The research gaps and the objectives to address have been listed, and an outline of the thesis has been given. Chapter 2 undertakes the literature review, which provides the research context for the thesis and identifies research gaps for investigation in subsequent chapters.

Elements of this thesis have been published in peer-reviewed journals. Research from Chapter 4 was presented in a CLIVAR Newsletter. A *Hydrological Processes* paper (Appendix II) addresses a research question on the spatiotemporal variability of climatic control on Dyfi basin precipitation/discharge that arose in Chapter 4. The research in Chapter 5 on hydroclimatological linkages across Great Britain was published in the *Journal of Hydrology* (Appendix III). Work in Chapter 7 on seasonal climate model forecast skill was published in *Geophysical Research Letters* (Appendix IV). Research in Chapters 4, 6 and 7 have also been presented at workshops and conferences.

# 2. LITERATURE REVIEW AND RESEARCH OBJECTIVES

## 2.1 Introduction

This chapter undertakes a literature review to identify research gaps for investigation. The review is split into three parts. Firstly, a summary is given on the premise for seasonal climate prediction. Secondly, hydroclimatological relationships across Great Britain are reviewed. Thirdly, seasonal hydrological prediction around the world is discussed. The chapter ends by presenting the research gaps identified and the corresponding objectives to be addressed in the thesis.

## 2.2 Definition of a Forecast versus a Prediction

In hydrology there is a subtle difference between a *forecast* and a *prediction*. The estimation of future conditions at a specific time or during a specific time interval is known as a *forecast*, while a *prediction* is the estimation of future conditions without referring to a specific time (Lettenmaier and Wood, 1993). Despite the distinction made between a *forecast* and a *prediction* these definitions are not strictly adhered to throughout this thesis, and herein the terms *prediction* or *predictive* are occasionally used as synonyms for *forecast* (for both climate and hydrological purposes).

The aim of a prediction is to foretell a target variable (predictand) by means of applying a technique or function *f* to one or more predictor variables (2.1).

$$predictand = f(predictor) \tag{2.1}$$

The function $f$ employed can be either (1) a statistical or empirical approach or (2) a dynamical approach. Statistical techniques use historical observations to build a predictive model between a predictor variable and a predictand, whereas a dynamical method uses a

General Circulation Model (GCM) to integrate in time the physical equations that describe the ALO system processes to determine future states of the system. For hydrological prediction the GCM output is used to drive a hydrological model.

### 2.3 Seasonal climate prediction

This section only provides an overview of seasonal climate prediction, as many previous papers have given comprehensive reviews of the topic. For these reviews, see Palmer and Anderson (1994), Carson (1998), Goddard *et al.* (2001), Harrison (2005) and Troccoli (2010).

The atmosphere is an example of a chaotic system – that is if a small perturbation is imparted on the initial atmospheric state, the atmosphere will evolve into a different state than the realisation without a perturbation (Harrison, 2005). In the ALO system, the atmosphere, if uncoupled from the lower boundary of the land and oceans will display fluctuations on the fastest time scales. Conversely, the land surface (soil moisture and snow cover) and most notably the oceans (SST and sea-ice cover) have greater persistence and evolve on a slower time scale than that of the atmosphere (Toth *et al.*, 2007). Slowly evolving anomalies of the lower boundary conditions (especially SST) are the basic premise for seasonal climate predictability because they can influence atmospheric development and predestine the future state of the climate (Palmer and Anderson, 1994, Kumar and Hoerling, 1995).

The El Niño Southern Oscillation (ENSO) is the key to seasonal prediction (Troccoli, 2010). Gradual development of ocean temperature anomalies in the tropical Pacific redistribute the surface heating, the low level wind fields and hence the tropical convection in the atmosphere. This in turn alters the atmospheric heating that drives the global atmospheric circulation (Goddard *et al*., 2001). In general, high (low) seasonal climate predictability is

found in the tropics (extratropics) because of the relatively weak (high) internal chaotic variability there (Palmer and Anderson, 1994). Although much of the extratropical forecast skill is derived from anomalies in the ENSO-related tropical SST (Barnston *et al.*, 1994), this tropical SST influence can be reduced by the high variability of the extratropical atmosphere (Anderson *et al.*, 1999). Therefore, the potential climate predictability is the degree to which the boundary-forced signal outweighs the essentially unpredictable climate noise (Kumar and Hoerling, 1995). Note that the extratropical climate depends to a greater extent on tropical SSTs when strongly anomalous tropical SST conditions exist (Anderson *et al.*, 1999).

Two approaches have been employed for seasonal climate prediction (as alluded to in section 2.2) and these are statistical and dynamical approaches. In the dynamical technique the equations that describe the ALO system are solved on a coarse GCM grid of approximately $2° \times 2°$ (Goddard *et al*., 2001) at different heights throughout the atmosphere. The coarse GCM resolution means that the ALO processes at the sub-grid scale are unresolved, and instead approximated by parameterisations (Holton, 1992). Hereafter, the dynamical approach to seasonal climate prediction is the focus of this part of the review as it is thought to provide greater scope for describing future climate patterns (Troccoli, 2010).

Climate predictions from GCMs predominately suffer from two sources of error: (1) uncertainties in the initial conditions, and (2) model error due to the inability of GCMs to resolve every process in the climate system (Hagedorn *et al.*, 2005, Doblas-Reyes *et al.*, 2009). To assess the sensitivity of the atmosphere to uncertainties in the initial conditions, an ensemble of GCM forecasts is generated (all with slight perturbations to their atmospheric and ocean initial conditions) and integrated into the future to obtain a range of forecast values (Palmer *et al.*, 2004, Harrison, 2005). To consider model error, a pragmatic approach is to use a multi-model ensemble consisting of GCMs from different meteorological institutes

(Palmer *et al.*, 2004). This approach incorporates GCMs with varying parameterisations and model physics, and thus includes different representations of the processes. The Development of a European Multimodel Ensemble System for Seasonal-to-Interannual Prediction (DEMETER) addressed this issue by producing a multi-model ensemble dataset containing seven GCMs each with nine different ensemble members (see section 3.6; Palmer *et al*., 2004).

As GCMs are unable to resolve sub-grid scale processes, their usefulness for local applications is restricted (Wilby *et al.*, 2002). It is therefore necessary to translate the coarse GCM output to local or regional-scale climate in a process called downscaling (Palmer *et al.*, 2004, Coelho *et al.*, 2006). For a good introduction to climate downscaling see Hewitson and Crane (1996). Two categories of downscaling techniques have emerged, and these are statistical and dynamical methods. Statistical approaches rely on quality historical data to build an empirical model with which to link GCM output and a local predictand such as temperature or precipitation. Dynamical techniques nest a fine resolution Regional Climate Model (RCM) within a coarser resolution GCM (Wilby *et al.*, 2002) to more accurately capture regional atmospheric processes. Palmer *et al.* (2004) expound that dynamical downscaling has the potential to outperform statistical methods in capturing extreme events because of the lack of historical data (of extreme events) to train statistical models.

The literature review of seasonal climate prediction found that although the general pattern of seasonal climate predictability is known (i.e. high predictability in tropics and low predictability in extratropics), no studies have explicitly assessed the ability to which GCMs can realise this monthly or seasonal climate predictability; this fact is also corroborated by Weigel *et al.* (2008). It is however essential to evaluate seasonal climate model predictive skill at different lead times and locations to determine if the predictions can be used to inform decision-making in the climate and hydrology sectors.

## 2.4 Concurrent hydroclimatological relationships across Great Britain

Studies investigating relationships between large-scale climatic circulation and precipitation and river flow most frequently use atmospheric indices, as such indices summarise the main modes of atmospheric variability over a particular region, and many index time-series are freely-downloadable over the internet for research purposes. At seasonal to inter-annual time scales, ENSO is the most pervasive mode of climate variability (Goddard *et al.*, 2001). ENSO is an atmospheric-oceanic phenomenon that occurs in the equatorial Pacific Ocean, with El Niño (La Niña) events having warm (cold) SST anomalies in the eastern and central equatorial Pacific. The Southern Oscillation index (SOI), which is the normalised atmospheric pressure difference between the eastern (Tahiti) and western Pacific (Darwin, Australia), is an indicator of the atmospheric conditions associated with the El Niño and La Niña periods of the equatorial Pacific Ocean. The SOI is significantly correlated with river flow in Australia, the Americas and Europe (Dettinger and Diaz, 2000). The influence of ENSO on global river flows is developed further in section 2.5.1.

The North Atlantic Oscillation (NAO), which refers to the redistribution of atmospheric mass between the subtropical Atlantic and the Arctic (Hurrell *et al.*, 2003), is the leading mode of

atmospheric variability in the Atlantic basin (Marshall *et al*., 2001). The NAO has been shown to be linked with droughts and water availability in Europe (Hurrell *et al.*, 2003). Changes in the NAO phase, as characterised by the NAO index (NAOI), are associated with variations in the frequency and strength of the surface westerly winds over Europe, thus influencing the transport and convergence of atmospheric moisture and hence, regional precipitation occurrence (Marshall *et al*., 2001). Precipitation in the northern British Isles has shown a significant positive correlation with the NAOI during winter (Wilby *et al.*, 1997, Murphy and Washington, 2001, Fowler and Kilsby, 2002); conversely, there is a weaker link between precipitation in northern Britain and the NAOI in summer (Fowler and Kilsby, 2002). In southern Britain weak links are found between the NAOI and precipitation throughout the year (Wilby *et al.*, 1997). In general, the NAOI has a stronger link with winter precipitation in coastal European countries, such as Great Britain (Bouwer *et al.*, 2008), compared to regions more remote from the Atlantic Ocean (Wibig, 1999). Previous research has therefore shown that the influence of the large-scale climatic circulation on precipitation, in terms of the NAOI, varies spatially and temporally in Britain.

Most previous analyses have focused on the winter season because the atmosphere is most dynamically active during winter (Folland *et al*., 2009). In turn, less attention has been given to summer large-scale climatic control on European climate (Zveryaev, 2004). In summer, there is a leading pattern of climatic variability with different characteristics to the traditional NAO atmospheric pattern that has been recognised as the summer North Atlantic Oscillation (SNAO) pattern (Barnston and Livezey, 1987, Zveryaev, 2004). The SNAO is spatially smaller and located further north than the well-known NAO. In a positive SNAO phase, high pressure is present over Northwest Europe and low pressure is present over Greenland and the Mediterranean (Zveryaev, 2004). Under this circulation pattern, warm and dry conditions

occur over Northwest Europe (e.g. British Isles) and cool wet conditions occur over southern Europe and the Mediterranean. As such, precipitation has significant negative (positive) correlation with the SNAO in Northwest (southern) Europe (Folland *et al.*, 2009).

River flow variability is affected by regional climate and basin physiography as first and second order controls respectively (Bower *et al.*, 2004). Positive relationships generally exist between the NAOI and river flow in Northwest Europe (Kingston *et al.*, 2006a), as shown for northern and western British basins, where high flow indices have positive correlation with the NAOI (Hannaford and Marsh, 2008). This may reflect the gradient in precipitation receipt in Britain in which western and northern districts receive the highest totals due to the effect of upland areas (Smith, 1972) and their closeness to the westerly airflow. For example, significant concurrent positive correlation is found between the NAOI and River Ewe discharge in Northwest Britain with strongest relationships in winter; however, for the River Itchen in southern Britain, river flow shows limited significant correlation with the NAOI (Phillips *et al.*, 2003). This geographical variation in the hydroclimatological links may be due to either the difference in the rainfall-runoff transformation (basin characteristics, and in particular the Itchen basin's permeable geology that attenuates the climate-precipitation-discharge signal), or to the difference in the regional climate that affects the basins; the River Itchen in Southeast Britain is more sheltered from the westerly airflows and has lower precipitation than the River Ewe.

The literature reviewed indicates that the relationships between the large-scale climatic circulation and British river basin precipitation/discharge have spatiotemporal variability, but no studies have evaluated this hydroclimatological variation in a systematic way.

## 2.5 Seasonal hydrological prediction

Seasonal hydrological prediction is a growing research area possibly because of the societal benefits it could spawn. Skilful predictions can affect decision making for land and water resources management (Kirono *et al.*, 2010) and provide more appropriate assignment of water for hydroelectric power generation (Cardoso and Silva Dias, 2006, Coelho *et al.*, 2006) and irrigation (Dutta *et al.*, 2006). In turn, there is potential to reduce economic losses associated with floods and droughts (Wood and Lettenmaier, 2006) and increase human preparedness for extreme conditions (Wedgbrow *et al.*, 2002). As with seasonal climate prediction, statistical and dynamical methodologies have been used to predict seasonal river flow. Studies that have used statistical prediction approaches are firstly reviewed followed secondly by dynamical prediction approaches.

### 2.5.1 Seasonal hydrological prediction with statistical approaches

Statistical models exploit empirical (typically lagged) relationships between a target variable of interest (predictand, e.g. precipitation or river flow) and one or more predictor variable (e.g. SST). They are developed from historical data, and such models depend on the availability, quantity and quality of the historical oceanic, atmospheric and hydrological data (Anderson *et al.*, 1999). Statistical models are usually less costly to develop and run than dynamical models, and can be seen as setting a benchmark skill level against which the more computationally intensive dynamical models can be compared (Barnston *et al.*, 1994). Table 2.1 lists and summarises papers that have used a statistical approach for river flow prediction; linear regression and correlation analyses are shown to be amongst the most commonly implemented techniques. In the western US, a regression of seasonal river flow volume on predictor variables is the dominant operational approach for seasonal river flow prediction (Wood and Lettenmaier, 2006).

Table 2.1: Summary of studies using statistical methods for seasonal river flow prediction. Note that linear regression refers to methods that used one or more predictor variables. Studies marked with * denote the use of an ENSO predictor.

| *Authors* | *Geographical Region* | *Method Used* |
|---|---|---|
| (Eldaw *et al.*, 2003) | Africa (Nile) | Correlation/linear regression |
| (Wang and Eltahir, 1999) | Africa (Nile) | Bayesian theorem * |
| (Barlow and Tippett, 2008) | Asia | Correlation/CCA |
| (Chiew *et al.*, 1998, Chiew *et al.*, 2003) | Australia | Serial streamflow/ENSO-streamflow correlation * |
| (Chowdhury and Sharma, 2009) | Australia | Combination of three statistical models * |
| (Kiem and Franks, 2001) | Australia | Classification approach * |
| (Ruiz *et al.*, 2007) | Australia | Linear regression * |
| (Kirono *et al.*, 2010) | Australia | Correlation * |
| (Wang *et al.*, 2009) | Australia | Bayesian approach * |
| (Whitaker *et al.*, 2001) | Bangladesh/India (Ganges) | Linear regression * |
| (Bierkens and Van Beek, 2009) | Europe | Lagged SVD NAO forecast (Rodwell and Folland, 2002) |
| (Gámiz-Fortis *et al.*, 2008, Gámiz-Fortis *et al.*, 2010) | Europe (Douro – Iberia) | ARMA/linear regression |
| (Ionita *et al.*, 2008) | Europe (River Elbe) | Correlation * |
| (Mckerchar *et al.*, 1998) | New Zealand | Classification approach * |
| (Purdie and Bardsley, 2010) | New Zealand | Linear regression * |
| (Archer and Fowler, 2008) | Pakistan | Linear regression |
| (Cardoso and Silva Dias, 2006) | South America (Paraná basin) | Linear regression * |
| (Gutiérrez and Dracup, 2001) | South America (Colombia) | Correlation * |
| (Hastenrath, 1990) | South America | Correlation/linear regression * |
| (Chandimala and Zubair, 2007) | Sri Lanka | Principal component regression scheme * |
| (Zubair, 2003) | Sri Lanka | Correlation * |
| (Kuo *et al.*, 2010) | Taiwan | Wavelet-based ANN-GM model |
| (Wedgbrow *et al.*, 2002) | UK | Correlation |
| (Wedgbrow *et al.*, 2005) | UK | Expert systems |
| (Wilby, 2001, Wilby *et al.*, 2004, Svensson and Prudhomme, 2005) | UK | Linear regression |
| (Devineni *et al.*, 2008) | USA (Eastern) | Regression approach |
| (Grantz *et al.*, 2005, Opitz-Stapleton *et al.*, 2007, Bracken *et al.*, 2010) | USA (Western) | K-nearest neighbour (KNN) locally weighted polynomial (LWP) regression |

River flow variability in many parts of the world is affected by ENSO, with Kahya and Dracup (1994) suggesting the seasonal SOI as a useful predictor of stream flow. In general, El Niño events are correlated with low stream flows in South America (Gutiérrez and Dracup, 2001, Tootle *et al.*, 2008), tropical Central America, in north-western and easternmost North America, in the Nile basin and Australia; conversely, during El Niño high stream flows are found in south-western North America (Barlow *et al.*, 2001), in subtropical South America, and in Europe (Dettinger and Diaz, 2000). During La Niña years opposite geographical patterns of high and low flow generally occur (Dettinger and Diaz, 2000). Due to the ENSO-river flow relationships throughout the world, many studies have used a measure of ENSO typically in correlation or regression to attempt seasonal river flow prediction. In Table 2.1 over half of the studies (17 out of 33) have used a measure of ENSO as a predictor variable (these were mainly located in the low latitudes).

There are many indices available to classify the state of ENSO. Kiem and Franks (2001) used different measures of ENSO in a classification approach and found that the Multivariate Index (MEI), an index based on six variables over the tropical Pacific Ocean (sea-level pressure, SST, zonal and meridional components of the surface wind, surface air temperature and total cloudiness fraction of the sky), outperformed other indices that only consider one variable (e.g. NINO3 SST, SOI). They argued that the single variable based indices are inferior because they are more susceptible to non-ENSO related variability. Using correlation analysis, Gutiérrez and Dracup (2001) uncovered strong correlations between discharge in Columbia and ENSO indicators for lags of between four and six months demonstrating the feasibility of long-range river flow prediction. Wang and Eltahir (1999) used a discriminant approach and showed that at time scales longer than the hydrological response time (2 – 3 months), ENSO information is most important for prediction of the Nile flood. A recent

approach has been to use locally weighted polynomial (LWP) regression to link predictors and discharge instead of fitting a linear (regression) relationship to all data values. In the western USA, LWP has been implemented with some success by relating large-scale climate and snow-water equivalent predictors with discharge (Grantz *et al.*, 2005, Bracken *et al.*, 2010).

In Great Britain five studies were found to have attempted statistical seasonal hydrological prediction (Table 2.1), with linear regression being the most common technique implemented. Wilby (2001) developed a lagged NAOI-river flow regression relationship that explained up to 40% of the variance of August river flow in three English rivers by using the January-February NAOI. Research by Wilby *et al.* (2004) used stepwise regression to build a predictive model between winter predictor variables (SST, sea-ice and atmospheric circulation patterns) and River Thames discharge in summer. Their seasonal models had greater skill than using climatology, with between 13 and 79 % explained variance. Svensson and Prudhomme (2005) used linear regression to skilfully predict British regional river flows in summer using previous winter predictors, with 55% and 61% explained variance of river flows in northwest and southeast regions respectively. Correlation was used by Wedgbrow *et al.* (2002) to link summer/autumn river flow anomalies in Northwest, Southwest and Southeast England with preceding winter values of the Polar-Eurasian (POL) teleconnection, North Atlantic SST anomalies and the NAOI. In particular, in 64 to 93% of summers, below-average flows were found after negative NAO winter phases. It was suggested that in England and Wales the seasonal prediction of river flow anomalies requires flow regimes with an intermediate hydrological memory so that lagged climate responses may be manifested in the groundwater component of river flow (Wedgbrow *et al.,* 2002). Finally, expert systems (ES) were used by Wedgbrow *et al.* (2005) to create a set of rules for

prediction of a predictand in the form of a decision tree comprising 'IF…THEN' statements. The predictor which explains the most variance in river flow (predictand) forms the basis for the first rule of the set. Using this approach River Thames flow anomalies in august were correctly forecasted up to 77% of the time, and the models successfully forecasted the below-average flows for numerous British droughts (e.g. 1976, 1984 and 1995).

Most empirical techniques in Table 2.1 simply have a statistical predictive relationship built on historical observations. However, two recent studies have used a more "process-oriented" or hybrid approach that used both a statistical model and a hydrological model. The work of Bierkens and Van Beek (2009) firstly forecast the NAOI based on lagged singular value decomposition (SVD) method between May North Atlantic SST and average December, January and February (DJF) 500 hPa geopotential height (Rodwell and Folland, 2002). Note that the first component of the geopotential field is similar to a positive NAO phase. Secondly, daily ERA-40 fields of precipitation, evaporation and temperature are taken from the three historical years with NAO indices closest to the NAOI forecast (analogue method); subsequently the three years of ERA-40 data are run through a global hydrological model. The average discharge from the three runs then forms the seasonal discharge prediction. Results suggest that the predictive skill in Europe can be reasonably large, but this is primarily due to having correct initial hydrological system conditions and not because of the NAO seasonal forecast (Bierkens and Van Beek, 2009). The second study by Kuo *et al.* (2010) used a wavelet-based Artificial Neural Network (calibrated by Genetic Algorithm; ANN-GM) model to predict seasonal rainfall based on SST predictors. The seasonal rainfall was disaggregated to a finer temporal scale and then run through a rainfall-runoff model. The authors concluded that the resultant discharge predictions would be useful for water resources management.

As the literature review showed that statistical seasonal hydrological prediction has previously been undertaken in Great Britain, this thesis does not conduct another statistical hydrological prediction study.

### 2.5.2 Seasonal hydrological prediction with dynamical approaches

A dynamical approach entails using seasonal climate model (or GCM) predictions as the basis for seasonal hydrological prediction, and by comparing Tables 2.1 and 2.2 it is noticeable that fewer studies have used a dynamical method for prediction. To use these GCM predictions for hydrological purposes, however, they have to be corrected or downscaled (see section 2.3) so that they are relevant to local or regional scale climate/hydrology. Both statistical and dynamical downscaling methods have been implemented; studies that have used statistical downscaling techniques are first reviewed, followed by studies that used dynamical techniques.

One statistical downscaling approach is the perfect-prognosis technique (Wilks, 2006). This entails developing a simultaneous statistical relationship (based on observations) between a predictor (e.g. mean sea level pressure MSLP) and a predictand (e.g. river flow) and then substituting in a GCM prediction of the predictor (e.g. MSLP) into the statistical equation to provide a future river flow prediction. Landman *et al.* (2001) used (bias-corrected) GCM predictions in a canonical correlation analysis (CCA) model to predict South African river flow in 12 basins. Skilful categorical prediction potential was discovered for five out of 12 basins. Another approach has been to use a Bayesian downscaling technique (Coelho *et al.*, 2006, Luo *et al.*, 2007, Luo and Wood, 2008). The Bayesian approach merges the observed climatology (e.g. precipitation or river flow) with seasonal climate predictions from multiple GCMs to form the best prediction at a more appropriate scale for hydrological applications. Luo and Wood (2008) ran Bayesian-downscaled multi-model forecasts of CFS and

DEMETER (see section 3.6) precipitation and temperature through the Variable Infiltration Capacity (VIC) hydrologic model and found that it performed significantly better for the first two months of the forecast than the traditional Extended Streamflow Prediction (EPS) methodology. Although Coelho *et al.* (2006) had some success in their research, they produced less skilful predictions for river flow than rainfall, which was in part due to river flow being affected by human practices (reservoir management). In conclusion, a Bayesian approach has been found to improve seasonal river flow predictive skill over using climatology.

As already mentioned in section 2.3, GCM output can be dynamically downscaled using a RCM. However, few studies have attempted a GCM-RCM-hydrologic model dynamical prediction system (Leung *et al.*, 1999, Block *et al.*, 2009). Leung *et al.* (1999) used a RCM to downscale the National Centers for Environmental Prediction (NCEP) Medium-Range Forecast (MRF) model to in turn drive the VIC hydrologic model to simulate river flow in the Columbia River basin, western North America. They showed that the RCM performed better than the GCM in modelling regional climate and found that simulated Columbia basin river flow from downscaled climate fields resembled the simulations driven by observed climate, thus indicating the potential for reliable seasonal predictions. Wood *et al.* (2002, 2005) conducted seasonal hydrological prediction for the eastern and western United States by bias correcting and downscaling (spatially and temporally) NCEP Global Spectral Model (GSM) ensemble climate predictions for input into the VIC hydrologic model. Wood *et al.* (2002) found that the initial hydrologic conditions need to be accurately determined, so that the influence of the land surface can be captured in the prediction. Also, Li *et al.* (2009) concluded that obtaining the appropriate initial conditions is one of the most crucial and difficult tasks in forecast system development.

Table 2.2: Summary of the dynamical approaches used for seasonal river flow prediction.

| *Authors* | *Geographical Region* | *GCM* | *Downscaling Approach* |
|---|---|---|---|
| (Céron *et al.*, 2010) | France | DEMETER | Two-step method (Regimbeau *et al.*, 2007) |
| (Nakaegawa *et al.*, 2007) | Global (P – E) | Japan Met. Agency (JMA) Global Spectral Model (GSM) | None used |
| (Sankarasubramanian *et al.*, 2008, Sankarasubramanian *et al.*, 2009) | Philippines | European Centre/Hamburg Model (ECHAM4.5) | Principal components regression (PCR) |
| (Landman *et al.*, 2001) | South Africa | Centre for Ocean-Land-Atmosphere (COLA) Studies T30 | CCA-based perfect prognosis approach |
| (Block *et al.*, 2009) | South America (Brazil) | ECHAM4.5/NCEP Medium-Range Forecast (MRF) 9 | RCM |
| (Coelho *et al.*, 2006) | South America (Paraná/Tocantins basins) | DEMETER (ECMWF, UKMO and Météo-France) | Bayesian approach |
| (Kim *et al.*, 2000) | USA (California) | University of California, Los Angeles (UCLA) GCM | Regional Climate System Model (RCSM) |
| (Leung *et al.*, 1999) | USA (Northwest/ Columbia basin) | NCEP MRF model T40 | Pacific Northwest National Laboratory RCM |
| (Luo *et al.*, 2007, Luo and Wood, 2008) | USA (Eastern/Ohio basin) | CFS/DEMETER | Bayesian approach |
| (Wood *et al.*, 2002) | USA (Eastern) | NCEP GSM | Bias correction and statistical downscaling |
| (Wood *et al.*, 2005) | USA (Western) | NCEP GSM | Bias correction and statistical downscaling |
| (Wood and Lettenmaier, 2006) | USA 'West-wide system' | NASA NSIPP and NOAA/NCEP | Bias correction and statistical downscaling |

The review has found that no study in Great Britain has used seasonal climate model output to drive a rainfall-runoff model for seasonal hydrological prediction. It is important to undertake such a study to ascertain the current level of achievable predictive skill using an "end-to-end" cascade of dynamical models.

## 2.6 Summary of key research gaps

The literature review has identified three research gaps for investigation. These gaps were first introduced in section 1.2 and are summarised below again.

### 2.6.1 River flow prediction using seasonal climate models and a rainfall-runoff model

No published literature was found (as of October 2010) that attempted to use seasonal climate model output to force a rainfall-runoff model for seasonal river flow prediction in Great Britain. This gap is important because it will show how feasible it is to directly use GCM precipitation predictions (near a river basin) for river flow simulation without undertaking exploratory data analyses to find climatic-oceanic predictors of precipitation/river flow.

### 2.6.2 Hydroclimatological relationships across Great Britain

No studies have undertaken a systematic analysis of the spatiotemporal variability of hydroclimatological relationships across Great Britain implying that the linkages between the large-scale climatic circulation and British precipitation and river flow are not completely known.

### 2.6.3 Seasonal climate model predictive skill

The literature review of seasonal climate prediction found that there is a paucity of published papers that have assessed monthly or seasonal climate model predictive skill; this fact is also corroborated by Weigel *et al.* (2008). It is essential to evaluate seasonal climate model

predictive skill at different lead times and locations to determine if the predictions can be incorporated into the decision-making processes for users.

## 2.7 Research objectives

This thesis focuses on three research objectives designed to address the identified knowledge gaps (sections 1.2 and 2.6). A conceptual model of the relationships and feedbacks in the ALO system is shown to highlight what factors the research addresses (Figure 2.1).

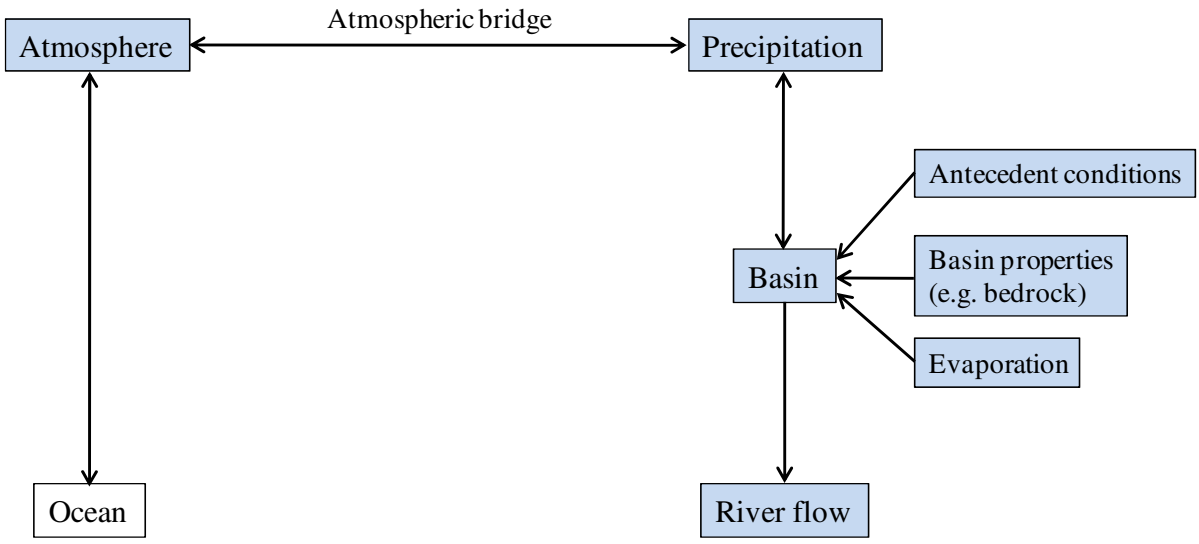


Figure 2.1: Conceptual model showing the links between different components of the ALO system. The direction of the arrows show which parts of the ALO system affect other parts of the system and the blue boxes highlight the factors considered in this research.

### 2.7.1 Assessment of river flow predictive skill using a chain of dynamical models in Great Britain

The first objective of this thesis is to attempt seasonal hydrological prediction in Great Britain with climate model data and a rainfall-runoff model to uncover the realisable level of river flow predictive skill using a cascade of dynamical models. The use of GCM precipitation and downscaled GCM precipitation will show the improvement in predictive

skill when using downscaled precipitation time series. This research objective considers all the blue boxes in Figure 2.1 and is presented in Chapter 4.

### 2.7.2 Identification of hydroclimatological relationships across Great Britain

The second objective of this research is to identify the "hot spots" of climatic control on British river basin precipitation/discharge (by using a systematic approach for multiple river basins) and on European precipitation. This work uses large-scale gridded atmospheric fields to uncover the detailed spatiotemporal variability of climatic drivers of basin precipitation/discharge.

This objective investigates the connections in Figure 2.1 between the atmosphere and river basin precipitation/discharge. As well as improving hydroclimatological process understanding, the identification and quantification of statistical relationships between the atmosphere and basin precipitation/discharge can inform the development of downscaling models and could be used in a "perfect-prognosis" approach with seasonal climate model output for seasonal precipitation/river flow prediction. This research is presented in Chapter 5.

### 2.7.3 Assessment of seasonal climate model predictive skill across the World

The third objective of this thesis is to undertake an assessment of the predictive skill of 2-metre temperature, precipitation and mean sea level pressure (MSLP) in the DEMETER and CFS climate models for applications. In this research a users' statistic evaluates predictive skill, so that the results are understandable to potential forecast users (*pers. com.*, John Schaake, NOAA). Further justification for the use of a users' statistic is given in a study by Steinemann (2006), which found that water managers encountered difficulties understanding, applying, evaluating, and trusting the climate predictions, thus precluding them from using

such predictions in their decision making. The predictive skill assessment of MSLP will also show if large-scale atmospheric circulation variables can be skilfully predicted by seasonal climate models for use in the empirical hydroclimatological relationships uncovered in Chapter 5. This research is presented in Chapter 7.

## 2.8 Chapter summary

This chapter has performed a literature review of the previous research undertaken on seasonal climate prediction, the space-time variation of hydroclimatological relationships across Great Britain and seasonal hydrological prediction. The identified knowledge gaps and the objectives of this thesis to address these research gaps have been documented. The next chapter presents the research design and describes the data and overarching methods used in the thesis.

# 3. RESEARCH DESIGN, DATA AND METHODS

## 3.1 Introduction

This chapter (1) details the research design of the thesis by showing how all aspects of the research fit together, (2) describes the data employed in the analyses, and (3) introduces the generic statistical methods used. Each research chapter gives further information on specific methods used.

## 3.2 Research design

The research undertaken primarily constitutes four chapters of the thesis. Chapter 4 evaluates the skill of seasonal hydrological prediction in the River Dyfi Great Britain (local-scale analysis) when using climate model output to force a rainfall-runoff model, thus addressing one of the identified research gaps (section 2.6.1). Following this work, Chapter 5 identifies the geographical areas with strongest climatic control ("hot spots") on river basin precipitation/discharge across Britain (regional/national scale analysis). This was conducted to (1) improve hydroclimatological process understanding across Great Britain, hence addressing a knowledge gap (section 2.6.2), and (2) determine whether the most appropriate GCM grid point was used in the precipitation downscaling process in Chapter 4. In Chapter 6 the associations between large-scale mean sea level pressure (MSLP) and European precipitation (continental scale analysis) are investigated to further the research of Chapter 5. Chapter 7 assesses the level of predictive skill of 2-metre air temperature, precipitation and MSLP in seasonal climate models, thus addressing the final knowledge gap in section 2.6.3 (global scale analysis). The thesis is concluded in Chapter 8 by drawing the main conclusions of the research and suggesting pertinent areas for further work.

### 3.3 Study areas

Research is conducted at a number of scales throughout the thesis from local-to-regional-to-continental-to-global scales i.e. from basin-scale to Great Britain to Europe to the World.

The focus area for local and regional scales is Great Britain, which is the main island in the British Isles located between 50°N and 60°N and 6°W and 2°E on the western edge of the European continental land mass. Many different air masses travel over Great Britain including arctic, polar and tropical types and depending on the source of the air mass and hence the route taken to reach Britain, the air mass can be either humid (maritime route) or dry (continental route). Westerly winds, which are the most common in Britain (Mayes and Wheeler, 1997), bring moisture-laden air off the North Atlantic Ocean creating an east-to-west and south-to-north precipitation gradient across Britain. The western and northern districts receive more precipitation due to their closeness to the westerly airflow and the effect of upland areas (Smith, 1972).

Hydrological response depends on a combination of precipitation, evapotranspiration, basin permeability and basin steepness. In western Britain precipitation is dominant in the balance between precipitation and evapotranspiration throughout the year, which together with basin impermeability and steepness create a rapid hydrological response to precipitation. In southern and eastern Britain precipitation and evapotranspiration are in closer balance, with the evapotranspiration demand generally exceeding precipitation receipt in the summer. This greater evapotranspiration demand in this region together with generally higher basin permeability and shallower basin slopes cause a slower hydrological response to precipitation. Land use and human activity also affect basin hydrology, but this thesis only uses near-natural basins where human influences are limited.

The focus for the regional scale is the European continent. The length of the north-western edge of the European continent (e.g. Northwest Scotland to Scandinavia) is influenced by moisture-laden westerly winds (especially in winter) that travel over the North Atlantic Ocean, while the more continental European areas are less affected by westerly winds (Wibig, 1999) and hence they have a more continental climate (Berg *et al*., 2009). Consequently, high winter precipitation is found over western Britain and Western Europe. In summer convective precipitation events are more prevalent (Berg *et al*., 2009), with high intensity precipitation found over Central and southern Europe. Hydrological response of course also varies across Europe, but this is not analysed in this thesis.

Finally, the global scale is used in Chapter 7 for the assessment of seasonal climate model predictive skill to determine whether seasonal climate predictions can be incorporated into the decision making process for users' applications.

## 3.4 River basin data

### 3.4.1 Criteria for river basin selection

River basins were chosen to investigate the spatiotemporal variability of hydroclimatological relationships in Britain and to assess the feasibility of seasonal river flow prediction. The basins have a wide geographic coverage, hence capturing most of the different precipitation and river flow drivers across Britain. Basins were selected according to the following five criteria:

1. The river basin must be on the benchmark list of natural catchments of the National River Flow Archive (NRFA). Benchmark catchments are near-natural, and thus have relatively small human influences (Bradford and Marsh, 2003).

2. If available, a low-medium grade of Artificial Influence (AI) on low flows from the NRFA. Grades span from 1 to 8, and a grade ≤ 4 was recommended for a basin to be included in selection. For the Scottish catchments the AI was not available, but, generally it is possible to assume that the benchmark catchments in Scotland have small artificial influences (*pers. com.*, Jamie Hannaford, NRFA).

3. The basins should cover a large geographic coverage across Britain to capture the east-to-west and south-to-north precipitation gradient (as shown by the Standard Annual Average Rainfall (SAAR) in Table 3.1). The SAAR represents the average annual rainfall over a basin from 1961-90 and allows inference on the different water balance characteristics in Britain.

4. A wide range of values of basin 'average altitude' against 'area', and basin 'Base Flow Index (BFI)' against 'SAAR'. The BFI is associated with the basin geology and indicates the amount of river discharge derived from stored sources (Gustard *et al.*, 1992). High (low) BFI denotes a high (low) groundwater component and is seen in permeable (impermeable) basins (Svensson and Prudhomme, 2005).

5. A continuous and long as possible record of river flows for the identification of stable statistical hydroclimatological relationships.

After imposing the basin selection criteria, there were only a limited number of basins available for study and the 10 basins chosen are shown in Figure 3.1. Their characteristics and monthly descriptive statistics are given in Tables 3.1 and 3.2 respectively, which show a broad range of basin areas, altitudes, annual rainfalls and BFIs. The common data period is January 1976 to December 2001. The main research undertaken on these basins is presented in Chapter 5.

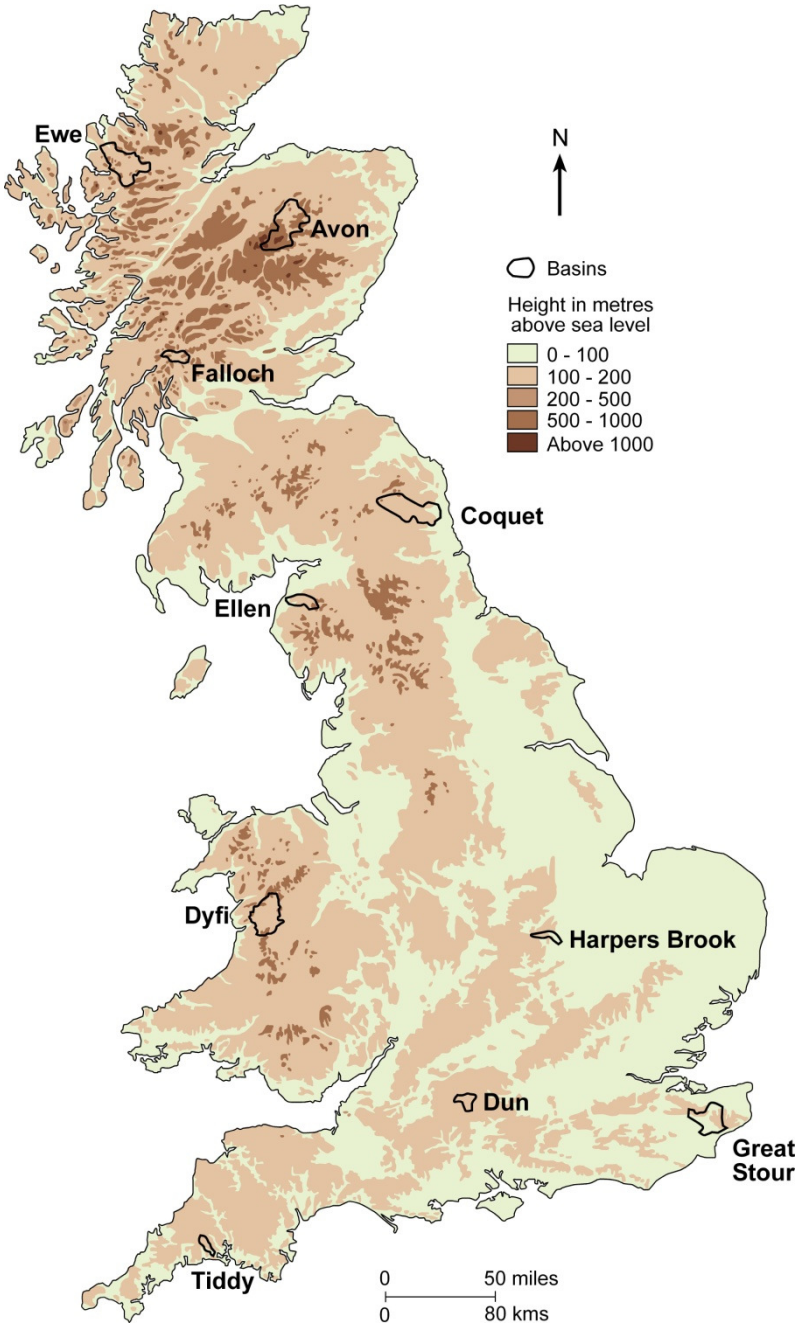


Figure 3.1: Map of Great Britain with the 10 selected river basins.

Table 3.1: The 10 selected river basins (Key: NA means that an AI value was not available).

| Station Name | Latitude | Longitude | Area ($km^2$) | Average Altitude (m) | SAAR (mm/year) | BFI | AI | Min. Rain Gauges | Max. Rain Gauges | Basin description |
|---|---|---|---|---|---|---|---|---|---|---|
| Avon at Delnashaugh | 57.40°N | 3.35°W | 542.8 | 525 | 1111 | 0.56 | NA | 3 | 14 | Gneisses and metamorphosed limestones with some igneous, some sandstones. Mountain catchment draining N side of highest Cairngorm peaks with moorland and rough grazing; a little arable farming in valley bottom. |
| Coquet at Morwick | 55.33°N | 1.63°W | 569.8 | 225 | 850 | 0.44 | 1 | 10 | 21 | Predominantly upland catchment draining from Cheviots. Largely Carboniferous Limestone and low permeability Devonian Igneous series, with 60% superficial deposits. 50% grassland, some upland afforestation and arable in low-lying areas |
| Dun at Hungerford | 51.41°N | 1.54°W | 101.3 | 157 | 786 | 0.95 | 1 | 3 | 7 | A mainly pervious (Chalk) catchment but with appreciable Clay-with-Flints cover in the northern part of the catchment. Rural character (chiefly agricultural but the Dun drains part of Savernake Forest). |
| Dyfi at Dyfi Bridge | 52.60°N | 3.85°W | 471.3 | 281 | 1834 | 0.39 | 1 | 6 | 19 | Geology: impermeable Silurian formations, minor Boulder Clay and alluvium deposits. Catchment is 60% grassland and 30% forested, with patches of upland heath |
| Ellen at Bullgill | 54.73°N | 3.40°W | 102.6 | 165 | 1110 | 0.50 | 3 | 1 | 8 | Steep headwaters drain Uldale Fells and flow westward. Lower reaches follow the E-W trend of the Coal Measures with Carboniferous Limestone to the south. Extensively overlain by Boulder Clay with alluvium within the main river valley. |
| Ewe at Poolewe | 57.76°N | 5.60°W | 441.0 | 311 | 2273 | 0.64 | NA | 4 | 9 | Very wet, mountainous catchment developed largely on ancient metamorphic formations (Lewisian Gneiss and Torridonian Sandstone). Impermeable bedrock catchment with about a third overlain by superficial deposits. Rough pasture and moorland; some forestry. |
| Falloch at Glen Falloch | 56.34°N | 4.72°W | 80.3 | 447 | 2842 | 0.16 | NA | 1 | 9 | Very wet, mountainous, catchment draining southern slopes of Benn Oss and northern slopes of Beinn a Chroin and Beinn Chabair. Developed on ancient metamorphic formations with isolated outcrops of igneous intrusions (impermeable). Small lochans in some headwaters, but have little affect on flows. Land use mainly moorland and rough grazing with small amounts of forestry. |
| Great Stour at Horton | 51.25°N | 1.00°E | 341.9 | 84 | 747 | 0.70 | 2 | 3 | 26 | The east and west branches of the Stour flow over Weald Clay; below the confluence (at Ashford - the only significant urban area). Geology: Chalk dominates - but with appreciable Drift cover. A rural catchment with mixed land use. |
| Harpers Brook at Old Mill Bridge | 52.40°N | 0.55°W | 74.3 | 90 | 623 | 0.49 | 1 | 1 | 5 | Low-lying impervious catchment, >70% cover of Boulder Clay. predominantly agricultural, with 20% forest. Some ironstone mines working until early 1980s. |
| Tiddy at Tideford | 50.41°N | 4.32°W | 37.2 | 109 | 1277 | 0.61 | 1 | 1 | 6 | Elongated, linear, natural catchment. Headwaters rise from southernmost outcrop of Bodmin granite. Great bulk of the catchment on Devonian shales and slates interspersed with tuffs and lavas. Moderate relief. Land use: agricultural, dairy and mixed farming rough grazing. Some forestry |

Table 3.2: The monthly hydrological descriptive statistics of the 10 basins.

| Station Name | Missing Daily Flows (%) | Mean Flow | Max Flow | Min Flow | Standard. deviation of river flow |
|---|---|---|---|---|---|
| Avon at Delnashaugh | 0.011 | 14.489 | 42.203 | 2.867 | 6.927 |
| Coquet at Morwick | 0.042 | 8.652 | 35.753 | 0.800 | 6.991 |
| Dun at Hungerford | 0 | 0.722 | 2.330 | 0.202 | 0.413 |
| Dyfi at Dyfi Bridge | 0 | 23.754 | 79.226 | 0.663 | 17.441 |
| Ellen at Bullgill | 0.168 | 2.310 | 7.584 | 0.194 | 1.737 |
| Ewe at Poolewe | 0 | 30.301 | 97.871 | 3.735 | 19.015 |
| Falloch at Glen Falloch | 0.695 | 6.193 | 21.397 | 0.133 | 4.415 |
| Great Stour at Horton | 0.295 | 3.157 | 15.399 | 0.826 | 2.186 |
| Harpers Brook at Old Mill Bridge | 1.042 | 0.456 | 2.473 | 0.049 | 0.448 |
| Tiddy at Tideford | 0 | 0.969 | 3.639 | 0.078 | 0.792 |

### 3.4.2 River basin precipitation, potential evapotranspiration (PE) and discharge

River basin precipitation, potential evapotranspiration (PE) and river discharge were all obtained from the NRFA. Basin-averaged precipitation was estimated by the triangle method (Jones, 1983) from daily rain gauge records. This entails creating a mesh of points across the basin, and for each mesh point producing a triangle in which to search for local rain gauges. The rain gauges are then weighted according to the inverse-square distance method and the average precipitation calculated for each day. Monthly basin-scale PE data were calculated with the UK Meteorological Office Rainfall and Evaporation Calculation System (MORECS) (Hough and Jones, 1997). Mean daily river flows ($m^3s^{-1}$) were recorded at the gauging stations named in Table 3.2. Six basins had missing river flow data of up to 1% (Table 3.2). The missing river flow values were infilled as follows:

1. Interpolation: add a trend or straight line to the missing data. This was only done for up to two days of missing data. This method was used by the author for the Avon.

2. Inference: similar to adding a "hand-drawn line" to the data series. This was only done for up to 7 days if there was a good comparative site. This method was used for the Coquet by the NRFA.

3. Equi-percentile method: firstly, locate a nearby closely related surrogate river basin. On the days when there are missing values in the selected basin, take the percentile flow of the surrogate basin and use this percentile on the flow duration curve of the selected basin to find the estimated flow on that day. This was applied for a period of missing values of more than 7 days, or when there were more than two periods of missing data. The equi-percentile method was undertaken by the NRFA on the author's behalf for the Ellen, Falloch, Great Stour and the Harpers Brook.

River Dyfi basin-scale precipitation, PE and discharge were used in Chapter 4 for river flow simulation and prediction, and Chapter 5 used all 10 river basins' data to investigate the space-time variability of hydroclimatological relationships across Great Britain.

### 3.5 Gridded Precipitation Datasets

Two different gridded precipitation products were used:

- Gridded (E-OBS) gauge-based precipitation over Europe (Haylock *et al.*, 2008) from the ENSEMBLES project (Hewitt and Griggs, 2004). This dataset was selected because of its long daily record that overlapped with the ECMWF ERA-40 re-analysis (section 3.6) time coverage of September 1957 to August 2002, and because of its relatively fine latitude/longitude resolution of 0.5° × 0.5°. The density of precipitation gauges used in the E-OBS dataset varies across Europe, with the UK, Netherlands and Switzerland having the highest station densities. Uncertainties in daily estimates are shown to be dependent on the number of available observations and the season (Haylock *et al.*, 2008).

Also, note that in general, rain gauge locations are biased towards urban areas and areas of low relief. This E-OBS product was used in the assessment of large-scale climatic control on European precipitation (Chapter 6). The geographical domain used in the analysis was 36.25°N–74.25°N and 10.25°W–24.75°E; note that North African precipitation time series in this spatial domain were not used as some series were incomplete.

- Gridded precipitation from the Global Precipitation Climatology Centre (GPCC; Rudolf *et al.* (2005)). GPCC was selected because of its global land coverage and long monthly record from January 1901 to December 2007. Only observed precipitation from in-situ gauges is used in the GPCC dataset, which means that certain areas, such as Central Africa, have few observations that contribute to the product resulting in increased uncertainty. GPCC is available at a 1.0° × 1.0° latitude/longitude resolution and was used as the reference for verification of monthly DEMETER and Climate Forecast System (CFS; section 3.6) seasonal precipitation forecasts over global land masses (Chapter 7). The GPCC precipitation was regridded by box-averaging to 2.5° resolution to match the DEMETER and CFS climate models' resolution.

### 3.6 Atmospheric Data

Atmospheric data were required (1) for the prediction of river flows with GCM output (Chapter 4), (2) for the identification of hydroclimatological linkages in Britain and Europe (Chapters 5 and 6 respectively) and (3) for the assessment of seasonal climate model predictive skill (Chapter 7).

- Re-analysis datasets are currently the source of the best estimates of the real atmosphere. By assimilating historical observations of the atmospheric state into short-range re-

forecasts of the atmosphere in a process called data assimilation, an atmospheric re-analysis is produced. The ECMWF ERA-40 re-analysis was the source of the atmospheric data (Uppala *et al.*, 2005) and covers the period September 1957 to August 2002 (45 years). Data at a 2.5° × 2.5° grid resolution were retrieved. In Chapter 5 the domain 15°N–70°N and 75°W–35°E was chosen to encompass the atmospheric areas where the Azores High / Icelandic Low pressure systems are usually situated. In Chapter 6, a half-hemispheric area 0°N–90°N and 90°W–90°E was chosen to detect the influences of the Azores High / Icelandic Low / Siberian High pressure systems on European precipitation. A pool of 11 atmospheric variables (Table 3.3) was chosen for exploratory data analysis to uncover the large-scale climatic circulation linkages with precipitation and river flow in the selected British river basins (Chapter 5). The rationale behind the final selection of atmospheric variables is given in Chapter 5. ERA-40 was also used in Chapter 7 as a reference in the assessment of seasonal climate model predictive skill of 2-metre air temperature and MSLP.

Table 3.3: The pool of ERA-40 variables used in the analyses.

| Climate Variable | Level | Units |
|---|---|---|
| Geopotential, Z850 | 850 hPa | $m^2s^{-2}$ |
| Geopotential, Z500 | 500 hPa | $m^2s^{-2}$ |
| MSLP | Surface | hPa |
| Specific Humidity, q850 | 850 hPa | kg $kg^{-1}$ |
| Specific Humidity, q500 | 500 hPa | kg $kg^{-1}$ |
| Temperature, T850 | 850 hPa | K |
| Temperature, T500 | 500 hPa | K |
| Zonal Wind, U850 | 850 hPa | $ms^{-1}$ |
| Zonal Wind, U500 | 500 hPa | $ms^{-1}$ |
| Meridional Wind, V850 | 850 hPa | $ms^{-1}$ |
| Meridional Wind, V500 | 500 hPa | $ms^{-1}$ |

- The NAOI summarises the atmospheric patterns affecting the Euro-Atlantic region and the NAO has been considered the most significant mode of climate variability in the North Atlantic region (Marshall *et al.*, 2001, Murphy and Washington, 2001). It was used to test if the gridded ERA-40 atmospheric data could yield stronger empirical relationships with British river basin precipitation/discharge and European precipitation than an atmospheric index (Chapters 5 and 6 respectively). NAOI time series were obtained from the University of East Anglia's (UEA) Climatic Research Unit (CRU) website (http://www.cru.uea.ac.uk/cru/data/nao/; accessed January 2009) and represents the monthly normalised pressure difference between Gibraltar and Southwest Iceland (Jones *et al.,* 1997).
- DEMETER was a European Union (EU) funded project that generated a multiple seasonal climate model ensemble re-forecast (hindcast) dataset with seven models each containing nine ensemble members. The models are from climate centres around Europe and their acronyms are: CERFACS, ECMWF, INGV, LODYC, METEO-FRANCE, MPI, and UKMO. The DEMETER models were initialised on 1st February, 1st May, 1st August and 1st November to assess the seasonal dependence of the hindcasts, and integrated for 180 days (Palmer *et al.*, 2004). DEMETER models were available on a 2.5° × 2.5° grid resolution over the common period of 1980–2001 (22 years) and were used in Chapters 4 and 7 for driving the Probability-Distributed Model (PDM) rainfall-runoff model and for the assessment of seasonal climate model predictive skill respectively. Chapter 4 used a single model grid point (52.5°N 2.5°W) and Chapter 7 used all grid points over the globe to undertake a comprehensive assessment for applications in all parts of the globe. DEMETER was used as opposed to the ENSEMBLES project (Weisheimer *et al*., 2009) because ENSEMBLES data was not available until too late in the PhD project.

- The CFS has 15 nine-month hindcasts initialised during each calendar month (Saha *et al.*, 2006). CFS was available on a 2.5° × 2.5° grid resolution over the period 1981-2001 (21 years) and was used in Chapter 7 for the assessment of seasonal climate model predictive skill (all grid points over the globe were used).

### 3.7 Overview of statistical methods

This section introduces the format of a statistical (or hypothesis) test, and then serves as a background to the statistical methods used herein. Further details of the methodologies used in this research are given in each of the chapters.

#### 3.7.1 Introduction to statistical testing

The framework for conducting a statistical test follows that of Reimann *et al.* (2008). When conducting a statistical test, it is first necessary to formulate a *hypothesis* about the behaviour of the system under study. This hypothesis statement contains two parts, a null hypothesis ($H_0$) that describes what is supposed to be true about the system, and an alternative hypothesis ($H_1$) that describes the contrary situation (i.e. if the null hypothesis is unlikely). The second step is to choose a *significance level* $\alpha$ for the statistical test, which identifies the probability that $H_0$ is erroneously rejected ($\alpha = 0.05$ is used herein). At this stage, the choice between a parametric or nonparametric (distribution-free) statistical test is made. A parametric test, which uses parameters that summarise the data distribution (e.g. mean and standard deviation), usually assumes that the underlying data distribution is normal (Helsel and Hirsch, 1992). If the statistical assumptions in a parametric test are violated, incorrect conclusions may be drawn; hence, the use of a nonparametric test would be more suitable. Once the appropriate test statistic has been calculated, a *p-value*, or probability, is determined which relates to the chosen test. If the *p-value* is less than the *significance level* $\alpha$ ($p < \alpha$), $H_0$

can be rejected, $H_1$ can be accepted, and the statistic is said to be statistically significant at the *significance level* $\alpha$. If $p > \alpha$, then $H_0$ is not rejected as the data does not provide statistical evidence to reject $H_0$. At the end of the test, the physical reasoning behind any uncovered significant statistical result needs to be explained.

### 3.7.2 Shapiro-Wilk test

The Shapiro-Wilk test is used in testing for univariate normality, as it is recognised as being one of the most powerful tests for detecting non-normality (Helsel and Hirsch, 1992). It is based on computing the linear Pearson correlation coefficient ($r$) between the data and the normal quantiles on a probability plot. The null $H_0$ and alternative $H_1$ hypotheses are:

$H_0$: the data has a normal distribution.

$H_1$: the data does not have a normal distribution.

The Shapiro-Wilk test was used in Chapters 5 and 6 to determine the normality of atmospheric, precipitation and river discharge data.

### 3.7.3 Pearson linear correlation coefficient *r*

The Pearson correlation coefficient $r$ is a parametric measure of linear correlation between two variables. The null $H_0$ and alternative $H_1$ hypotheses are:

$H_0$: no correlation exists between the two variables ($r = 0$).

$H_1$: the two variables are correlated with one another ($r \neq 0$).

The Pearson correlation was used in the assessment of seasonal climate model predictive skill in the DEMETER and CFS models in Chapter 7. The rationale behind forecast quality assessment using the Pearson correlation is also given in Chapter 7.

### 3.7.4 Spearman's rank correlation $\rho$

Spearman's rank correlation $\rho$ is a nonparametric measure of correlation between two variables (Spearman, 1904). It is calculated as the Pearson correlation coefficient on the ranks of the data. The null $H_0$ and alternative $H_1$ hypotheses are:

$H_0$: no correlation exists between the two variables ($\rho = 0$).

$H_1$: the two variables are correlated with one another ($\rho \neq 0$).

In Chapter 4 Spearman rank correlation was used to determine the association between monthly observed and forecasted river flows. In Chapter 5 it was used to identify hydroclimatological relationships between atmospheric data and precipitation and river discharge across Britain, and Chapter 6 used the Spearman rank correlation in the analysis of large-scale atmospheric control on European precipitation.

### 3.7.5 Mann-Kendall trend test

The nonparametric Mann-Kendall trend test is used in testing for the existence of linear trends in a time series (e.g. Helsel and Hirsch (1992)). The null $H_0$ and alternative $H_1$ hypotheses are:

$H_0$: there is no trend in the data.

$H_1$: there is a trend in the data.

The Mann-Kendall test was used in Chapter 6 to determine whether trends existed in atmospheric data and European precipitation.

### 3.7.6 Bootstrapping

Bootstrapping is a procedure to re-sample data. This method involves sampling the original data series with replacement to yield a new series with the same number of values as the original series. The generated series may contain certain values multiple times, while other values may not appear at all. An advantage is that the generated series comes from the same distribution as the observed (empirical) distribution of the original data (Kundzewicz and Robson, 2004). Bootstrapping was used in Chapters 5 and 6 to determine whether trends had an impact on the significance of the correlation between atmospheric data and precipitation and river discharge.

## 3.8 Probability-Distributed Model (PDM)

The PDM is a lumped rainfall-runoff model (based on probability distributed moisture stores) that transforms precipitation and PE to river flow at the basin outlet (Moore, 2007). PDM was used in Chapter 4 for the River Dyfi basin, West Wales, to evaluate the river flow predictive skill using GCM data. Daily basin-averaged precipitation, monthly basin-averaged PE and daily river flow data were used to calibrate the PDM (calibrated for 01/05/1980–30/04/1990, and evaluated for 01/05/1991–30/04/2001). For further details of the PDM see Moore (2007).

## 3.9 Chapter summary

This chapter has presented the research design of the project, which showed how the chapters fit together. The study area of the thesis together with the hydrology and predominant climate that affects Great Britain is discussed; the wider European precipitation climatology is then briefly covered. The data employed in the analyses and the generic statistical methods used

are also introduced and described. The next chapter evaluates seasonal hydrological prediction in the River Dyfi West Wales, thus addressing the first research objective.

# 4. RIVER FLOW PREDICTION USING A HYDROLOGICAL MODEL AND CLIMATE MODEL OUTPUT

Chapter Objective: To uncover the realisable level of river flow predictive skill using climate model output to force a rainfall-runoff model.

## 4.1 Introduction

Hydrological extremes (floods and droughts) are expected to become more commonplace under changing climatic conditions (Kundzewicz *et al.*, 2007). The harmful socioeconomic effects of these extremes could potentially be mitigated through the advanced warning provided by skilful seasonal hydrological predictions. These predictions could aid water management decision making and increase human preparedness for extreme conditions. The need for research on seasonal river flow prediction has been brought to the fore in Great Britain after recent extreme hydrological conditions (e.g. 2004–06 drought (Marsh *et al.*, 2007) and the summer 2007 floods (Marsh, 2008)).

A literature review of seasonal hydrological prediction found (as of October 2010) that no published study had tested its feasibility in Great Britain using GCM output to force a rainfall-runoff model. Therefore, previous investigations have not explored how appropriate seasonal climate predictions are for generating river flows. Research is needed to show whether GCM precipitation can be used for river flow prediction, or if a downscaling process is required for skilful precipitation generation and hence river flow prediction. Also of particular interest is if the sub-monthly temporal structure of simulated river flows matches that of observed river flows.

The aim of this chapter is to drive a hydrological model using (1) precipitation and downscaled precipitation from the ERA-40 re-analysis (as re-analysis data are currently the

best GCM data due to the assimilated observations), and (2) precipitation and downscaled precipitation predictions from the DEMETER multiple seasonal climate model dataset. The generated discharge will be analysed to assess the river flow predictive skill. The work addresses one research gap found in the literature review (section 2.6.1).

### 4.2 Data

The River Dyfi at Dyfi Bridge in West Wales, Great Britain (Figure 4.1; see Tables 3.1 and 3.2 for the basin characteristics), was chosen for the study as it is near-natural, and hence the climate-flow signal should be clear. The Dyfi river flows were simulated using the PDM, which is a lumped rainfall-runoff model that converts rainfall and PE to river flow at the basin outlet (Moore, 2007). Daily basin-averaged precipitation (Jones, 1983) and MORECS PE (Hough and Jones, 1997) and daily river flow data were used to calibrate (01/05/1980 to 30/04/1990) and evaluate (01/05/1991 to 30/04/2001) the PDM.

The climate model output used to drive the PDM hydrological model came from two sources: (1) the ECMWF ERA-40 re-analysis of meteorological observations (Uppala *et al.,* (2005); section 3.6) and (2) the DEMETER seasonal climate model dataset, which consists of seven GCMs (CERFACS, ECMWF, INGV, LODYC, METEO-FRANCE, MPI, and UKMO) each with nine ensemble members i.e. total of 63 members (Palmer *et al.,* (2004); section 3.6). The ensemble of nine members per model represents the uncertainty in the initial GCM conditions, while the multiple climate models take into account the error due to the model setup (Hagedorn *et al.*, 2005, Doblas-Reyes *et al.*, 2009). ERA-40 and DEMETER were available at a 2.5° × 2.5° grid resolution and model output at the closest land-based grid point to the River Dyfi basin (52.5°N 2.5°W) were used. DEMETER models cover a six month hindcast period and were available from 1st February, 1st May, 1st August and 1st November

initial conditions. Most results are presented for 01/05/1980–30/04/2001, as this period is common to ERA-40 and the DEMETER models.

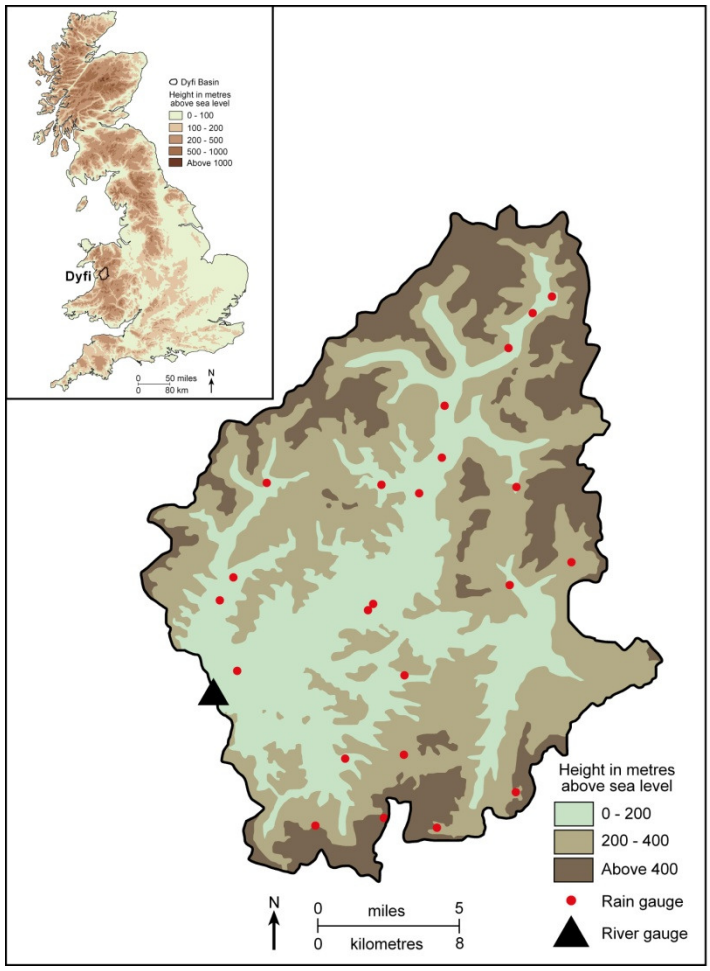


Figure 4.1: A map of the River Dyfi at Dyfi Bridge basin.

### 4.3 Methods: river flow generation

#### 4.3.1 Direct input from GCMs

The ERA-40 stratiform precipitation, convective precipitation and snowfall were summed daily at 52.5°N 2.5°W to produce a total precipitation time series. This precipitation time series together with the MORECS PE data were run through the PDM to forecast river flow. In this work simulated PE is not used because river flow in Wales is first conditioned by

precipitation and this study in part wants to determine if only considering the major climate factor (precipitation) is sufficient.

For DEMETER models precipitation, each model ensemble member (i.e. 63 members) from the four initial conditions (February, May, August and November) in each year was split into the first three (0–3) and last three (4–6) months. The 0–3 and 4–6 months split hindcasts from each start date were then concatenated to produce two continuous time series, one series consisting of the first three (0–3) months lead time and the other series consisting of the second three (4–6) months lead time (Figure 4.2). These concatenated time series of daily precipitation and the monthly MORECS PE were used to drive the PDM to forecast river flow.

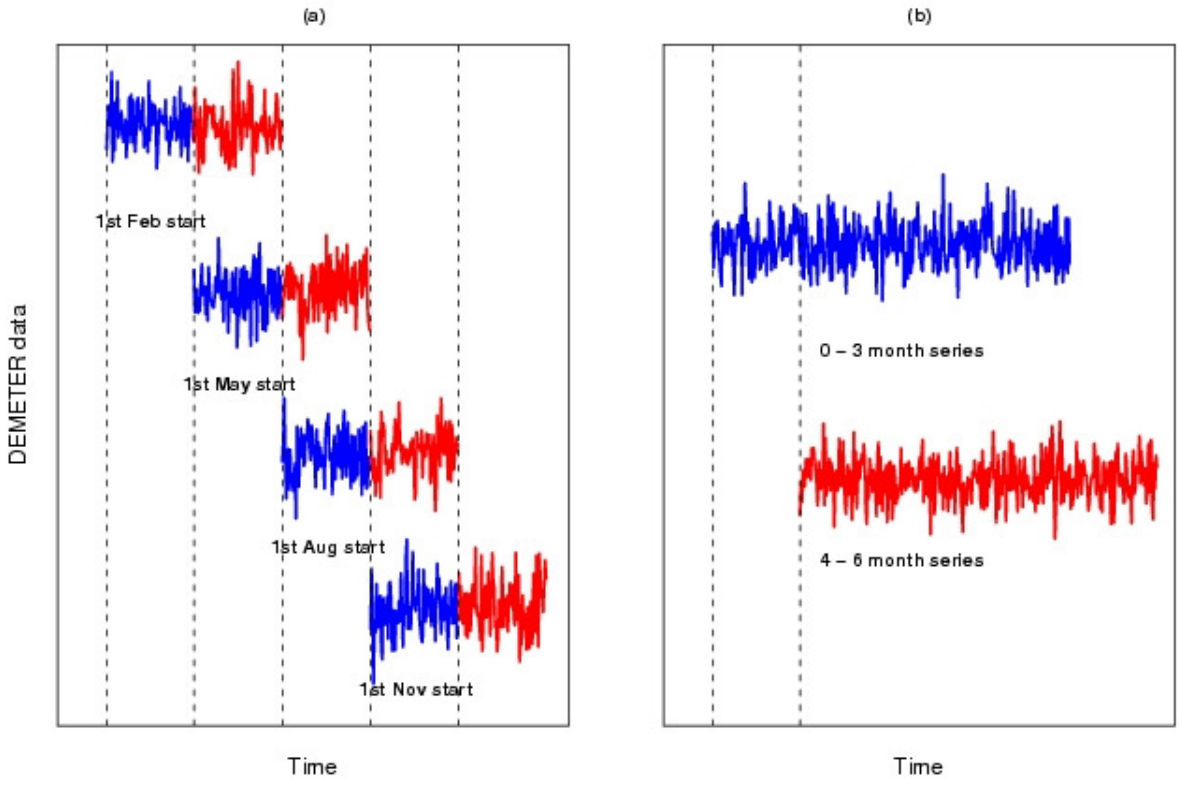


Figure 4.2: Schematic of the generation of the 0–3 and 4–6 months DEMETER models' time series from (a) the original hindcasts to (b) the continuous DEMETER time series.

### 4.3.2 Downscaled input from GCMs

Because of the coarser resolution of the ERA-40 and DEMETER data compared with the spatial scale of the Dyfi river basin (471.3 $km^2$), the Statistical Downscaling Model SDSM (Wilby *et al.*, 2002) Version 4.1 was utilised to evaluate if by using atmospheric variables as a proxy of precipitation more reliable precipitation time series could be obtained. This is because precipitation generating mechanisms are very complex and perhaps not well resolved in the GCMs, while large-scale atmospheric flow might be better simulated at the GCM grid scale. SDSM uses multiple linear regression models to link large-scale atmospheric (ERA-40) predictors with observed basin-scale precipitation, and a stochastic weather generator to produce downscaled daily precipitation series based on the regression equations. The regression models were built for each month to allow for different precipitation generating mechanisms to be considered throughout the year. The predictors in the regression equations were carefully selected by analysing the correlation matrix of ERA-40 atmospheric variables and Dyfi basin precipitation. Three predictors best explained the basin-scale precipitation: zonal wind (U) at 500 hPa, meridional wind (V) at 850 hPa and geopotential (Z) at 500 hPa. The SDSM regression equations were built and calibrated from 01/05/1976 to 30/04/1991 and validated from 01/05/1991–30/04/2001; the regression equations are given in Table 1 in Appendix I. For the downscaling of the ERA-40 data, 10 precipitation time series were generated over the 1991–2001 validation period (downscaled ERA-40 precipitation series were not generated over 1980–2001 as artificial skill would be added because the SDSM was built using ERA-40 data over 1976–1991). For the DEMETER concatenated predictor time series (over 01/05/1980–30/04/2001), each original ensemble member was used to generate 10 downscaled precipitation time series over the period 01/05/1980–30/04/2001 (90 members per model; total of 630 members). The 10 downscaled ERA-40 time series (over 1991–2001)

and the 630 downscaled DEMETER (over 1980–2001) time series of daily precipitation and the MORECS PE were used to drive the PDM.

In this analysis the *"observed"* river flow is the PDM simulated flow from observed precipitation and the *"forecast"* river flow is the river flow forecasted by ERA-40 and DEMETER data. This means that both observed and forecasted river flows contain PDM model errors, which are assumed to be of the same magnitude. Comparison of these two time series provides information on the property of the input data to reproduce realistic flow characteristics.

### 4.4 Evaluation Methodology

In weather forecasting, the benefit of using the ensemble mean is that it tends to average out differences between ensemble members, while highlighting characteristics that are shared by the forecast ensemble members (Wilks, 2006). Following this same reasoning, the assessment of river flow predictive skill herein uses the ensemble mean river flow prediction generated from an ensemble of precipitation predictions.

The river flow driven by the ERA-40 precipitation and the ensemble mean river flow generated by the 10 downscaled ERA-40 precipitation time series were used in the assessment. For DEMETER the ensemble mean river flow prediction from each of the DEMETER models, and the equal-weighted (averaged) multi-model ensemble mean river flow prediction using all DEMETER models' members were calculated. For individual DEMETER models precipitation (downscaled precipitation) this is the ensemble mean river flow prediction of nine (90) members, and for the DEMETER multi-model precipitation (downscaled precipitation) this is the ensemble mean river flow prediction of 63 (630) members.

River flow predictions were assessed using the Nash-Sutcliffe coefficient (NS; Nash and Sutcliffe, 1970) on daily (NS-1) and 30 day moving averaged (NS-30) flows (4.1). NS values range from -∞ to 1 (1 is a perfect forecast), with positive (negative) values indicating a prediction better (worse) than that obtained using a reference river flow.

$$NS = 1 - \frac{\sum_i (x_i - \hat{x}_i)^2}{\sum_i \left(x_i - \hat{x}_{ref,i}\right)^2} \qquad (4.1)$$

where $x$ is the observed flow, $\hat{x}$ is the forecast and $\hat{x}_{ref}$ is the reference forecast.

Two reference flows $\hat{x}_{ref}$ were used in the NS calculation: (1) the mean annual river flow over the period studied (grey horizontal lines in Figure 4.3), which is the conventional NS calculation, and (2) the daily mean historical river flows (red lines in Figure 4.3). By using the daily mean historical river flow as a reference, the seasonality of the Dyfi river flow is considered. For a given day, this daily mean flow could be a forecast, which is the equivalent to using the climatology for precipitation forecasts.

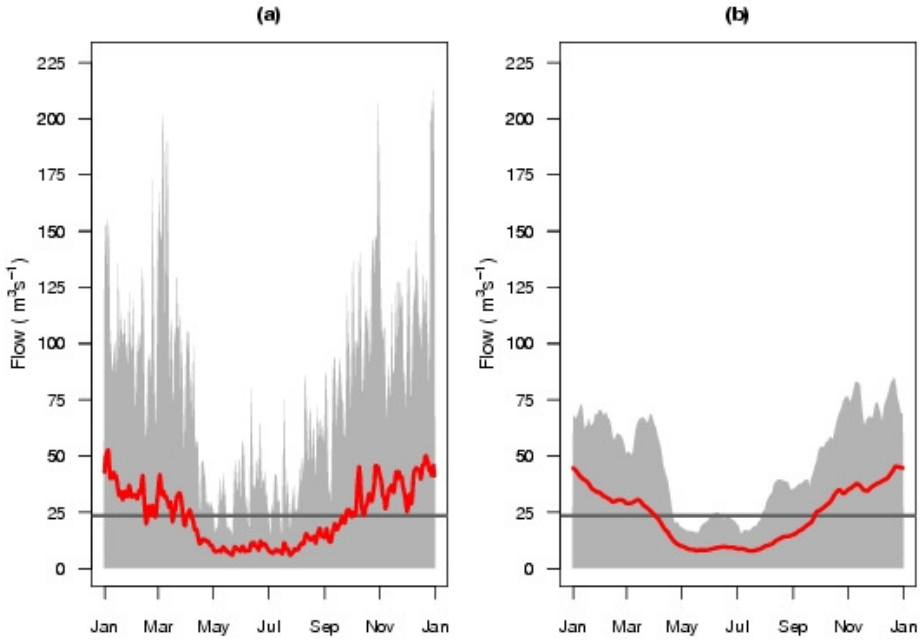


Figure 4.3: Historical River Dyfi flows for (a) daily flows and (b) 30 day moving average flows over 01/05/1980 to 30/04/2001. The grey background is the envelope of observed flows and the red line is the mean daily observed river flow.

On a monthly basis from May 1980 to April 2001 two further statistics were employed. Firstly, Spearman rank correlation $\rho$ was used to show the association between monthly observed and predicted river flows. Secondly the mean relative bias in percent (4.2) was calculated to discern whether the predicted river flows overestimated or underestimated the observed flows.

$$bias = 100 \times \frac{1}{n}\sum_{i=1}^{n}\left(\frac{\hat{x}_i - x_i}{x_i}\right) \qquad (4.2)$$

where $n$ is the number of pairs of forecasts and observations.

Two extreme hydrological events in the River Dyfi basin, a low flow period (01/07/1984–31/08/1984) and a high flow period (01/10/2000–30/11/2000), were chosen to assess how the forecasted river flow driven by the downscaled 0–3 months precipitation series captured

extreme events. Forecast skill during these events was evaluated with contingency tables (Mason, 2003), which showed the number of days when forecasted and observed daily river flow were above or below the median observed river flow over the analysed period. An example contingency table is shown in Table 4.1. From the contingency table the percent correct rate (4.3) can be calculated, which highlights the forecast performance.

Table 4.1: An example of a contingency table. The green boxes A and D show the occurrences when the river flow forecast and observed river flow lie simultaneously above or below the set threshold (correct forecasts). Conversely, the light red boxes B and C show the occurrences when the river flow forecast and observed river flow lie on opposite sides of the set threshold (incorrect forecasts).

| | | Forecasts | | % |
|---|---|---|---|---|
| | **Model** | >med | <med | Totals |
| Observed | >med | **A** | B | A+B |
| | <med | C | **D** | C+D |
| | Totals | A+C | B+D | A+B+C+D |

$$percent\ correct\ rate = \left(\frac{A + D}{A + B + C + D}\right) \times 100 \qquad (4.3)$$

## 4.5 Results

### 4.5.1 River flow forecasting with ERA-40 and downscaled ERA-40 precipitation

The forecasted river flows driven by ERA-40 precipitation are less skilful than using the mean annual flow as a forecast of observed flows, as shown by the negative NS values (NS-1=-0.196 and NS-30=-0.670). When using the daily historical mean flow as a reference, $NS\text{-}1_{HIST}$ and $NS\text{-}30_{HIST}$ decrease to -0.567 and -2.14 respectively. This poor estimation of

river flow with ERA-40 precipitation is to be linked with the incorrect daily precipitation intensity by the ERA-40 GCM assimilating model. When precipitation was downscaled (with SDSM) prior to its input in the PDM, a marked improvement in river flow forecast skill was found over 01/05/1991–30/04/2001 (NS-1=0.520 and NS-30=0.683; $NS\text{-}1_{HIST}$=0.373 and $NS\text{-}30_{HIST}$=0.468). Note that it was not possible to produce river flow with downscaled ERA-40 over 1980–2001, as the SDSM models were built using ERA-40 over 1976–1991, which would have added artificial skill to the river flow forecasts.

### 4.5.2 River flow forecasting with DEMETER and downscaled DEMETER precipitation

The forecasted river flows using the DEMETER models' precipitation are poor (Table 4.2). The ensemble mean river flow driven by the METEO FRANCE model 0–3 months precipitation produces the best forecasts, but the negative NS values imply that these forecasts are not as skilful as using the mean annual flow or the daily historical mean river flow as a forecast (NS-1=-0.122 and NS-30=-0.282 when the mean annual flow is the reference). For the 4–6 months precipitation series, the METEO FRANCE model also produces the most skilful forecast (NS-1=-0.090 and NS-30=-0.199 for mean annual flow reference; Table 4.3). As all of the precipitation forecasts from the DEMETER models generate river flow forecasts worse than the mean annual flow (negative NS values; Tables 4.2 and 4.3), the results obtained from direct GCM precipitation inputs are not discussed in detail hereafter.

Table 4.2: Nash-Sutcliffe values for the 0–3 months series of DEMETER models' ensemble mean of daily and 30 day moving average river flow forecasts. The first NS value in each box uses the mean annual flow as a reference, while values in brackets use the historical mean daily and mean daily 30 day moving average river flow as a reference. Bold values are the forecasts with the highest skill in each category.

| Model | 0–3 months precipitation | | 0–3 months downscaled precipitation | |
|---|---|---|---|---|
| | NS-1 | NS-30 | NS-1 | NS-30 |
| CERFACS | -0.143 (-0.499) | -0.323 (-1.491) | 0.062 (-0.229) | 0.232 (-0.446) |
| ECMWF | -0.286 (-0.686) | -0.645 (-2.098) | 0.024 (-0.280) | 0.186 (-0.533) |
| INGV | -0.335 (-0.749) | -0.727 (-2.253) | 0.029 (-0.273) | 0.218 (-0.472) |
| LODYC | -0.295 (-0.697) | -0.660 (-2.126) | 0.068 (-0.221) | 0.252 (-0.408) |
| METEO FRANCE | **-0.122** (**-0.471**) | **-0.282** (**-1.414**) | 0.046 (-0.250) | 0.177 (-0.549) |
| MPI | -0.264 (-0.657) | -0.592 (-1.997) | 0.068 (-0.221) | 0.193 (-0.520) |
| UKMO | -0.303 (-0.707) | -0.679 (-2.161) | 0.052 (-0.242) | 0.216 (-0.476) |
| DEMETER | -0.238 (-0.623) | -0.542 (-1.903) | **0.128** (**-0.143**) | **0.289** (**-0.339**) |

Table 4.3: Nash-Sutcliffe values for the 4–6 months series of DEMETER models' ensemble mean of daily and 30 day moving average river flow forecasts (Key as Table 4.2).

| Model | 4–6 months' precipitation | | 4–6 months' downscaled precipitation | |
|---|---|---|---|---|
| | NS-1 | NS-30 | NS-1 | NS-30 |
| CERFACS | -0.109 (-0.454) | -0.250 (-1.354) | 0.061 (-0.230) | 0.174 (-0.556) |
| ECMWF | -0.271 (-0.665) | -0.600 (-2.014) | 0.063 (-0.228) | 0.196 (-0.514) |
| INGV | -0.321 (-0.731) | -0.722 (-2.242) | **0.121** (**-0.152**) | **0.283** (**-0.349**) |
| LODYC | -0.295 (-0.697) | -0.654 (-2.115) | 0.056 (-0.237) | 0.190 (-0.526) |
| METEO FRANCE | **-0.090** (**-0.429**) | **-0.199** (**-1.258**) | 0.021 (-0.284) | 0.105 (-0.685) |
| MPI | -0.239 (-0.624) | -0.527 (-1.875) | 0.070 (-0.219) | 0.212 (-0.484) |
| UKMO | -0.311 (-0.719) | -0.702 (-2.206) | 0.062 (-0.229) | 0.194 (-0.517) |
| DEMETER | -0.223 (-0.603) | -0.504 (-1.833) | 0.111 (-0.166) | 0.248 (-0.417) |

River flow forecast skill improves when downscaled precipitation is used to force the PDM rainfall-runoff model, as shown by the positive NS values obtained when the mean annual river flow is used as a reference (Tables 4.2 and 4.3). The ensemble mean river flow from the downscaled DEMETER multi-model precipitation (0–3 months series) has the highest forecast skill, with positive NS values indicating that this river flow forecast is more skilful than using the mean annual river flow as a forecast (NS-1=0.128 and NS-30=0.289 respectively). Positive NS values are also found for the ensemble mean of each DEMETER model (0–3 months series). For the downscaled 4–6 month series, the forecast remains better than that obtained from the mean annual river flow (Table 4.3), with the INGV model associated with the highest forecast skill for the 4–6 months series. This means that there is not a large degradation in forecast skill when using the 4–6 months downscaled time series.

It must be noted that the forecast skill in terms of the NS are not very good, and in general NS values greater than 0.6 would be required to consider a model fit as acceptable. However, the downscaled precipitation series do produce improved flow forecasts compared to using direct GCM precipitation.

The bias and Spearman rank correlation $\rho$ values for the mean monthly flow forecasts from the downscaled DEMETER 0–3 months and 4–6 months multi-model ensemble are shown in Table 4.4 (Table 2 in Appendix I shows the bias and correlation results for the DEMETER 0–3 months and 4–6 months multi-model ensemble precipitation). The monthly mean bias has negative and positive values indicating that the forecast river flows both underestimate and overestimate the observed flows. Note that for DEMETER 0–3 and 4–6 months precipitation all bias values are negative indicating that the flow forecasts always underestimate the observed river flow (see Table 2 in Appendix I). The correlation results are generally poor, with only the downscaled 0–3 months series having two months with significant correlation

at $\alpha$=0.05 level ($\rho$=0.47 and $\rho$=0.71 for June and August respectively). This suggests that there is not strong association between forecasted and observed hydrological events.

Table 4.4: Bias and Spearman rank correlation for the mean monthly river flow forecasts driven by the downscaled DEMETER 0–3 months and 4–6 months multi-model ensemble over May 1980 to April 2001 (n=21). Bold values indicate significant Spearman rank correlation at $\alpha$=0.05 level.

| DEMETER Multi-Model | 0–3 months downscaled precipitation | | 4–6 months downscaled precipitation | |
|---|---|---|---|---|
| | Bias | Correlation | Bias | Correlation |
| January | 42.85 | 0.06 | 43.27 | -0.04 |
| February | 17.77 | 0.42 | 33.19 | 0.04 |
| March | 9.44 | -0.05 | -0.31 | -0.08 |
| April | -2.27 | 0.10 | -9.26 | 0.13 |
| May | -19.49 | 0.27 | -19.91 | 0.24 |
| June | -65.28 | **0.47** | -61.55 | 0.08 |
| July | -55.26 | -0.10 | -53.33 | -0.01 |
| August | -69.71 | **0.71** | -62.63 | 0.28 |
| September | -40.53 | -0.31 | -49.07 | -0.03 |
| October | -29.64 | -0.05 | -37.60 | -0.28 |
| November | 8.62 | 0.28 | 18.99 | 0.27 |
| December | 3.67 | -0.21 | 6.97 | 0.12 |

The improvement of the river flow forecasts obtained from downscaled precipitation as compared with direct precipitation is further shown by plotting Flow Duration Curves (FDC). An FDC represents the river flow cumulative frequency as a function of the percentage of time that the river flow is exceeded (Hisdal *et al*., 2004). On an FDC the percent exceedance flow (QN) can be determined; for example the Q5 value is the river flow which is equalled or exceeded 5 % of the time (high flow index), and the Q95 value is the river flow which is equalled or exceeded 95 % of the time (low flow index). For the daily and 30 day moving average forecasted river flows on the FDCs in Figure 4.4, it is shown that the ensemble mean river flow forecast from the DEMETER multi-model (0–3 months) precipitation ensemble

(dashed black line) substantially underestimates the observed river flow (red line) throughout the flow regime and especially for high flows (e.g. Q5). The FDC of the ensemble mean river flow driven by the downscaled DEMETER multi-model precipitation (solid black line) is closer to the observed river flow in all parts of the Dyfi flow regime highlighting the improvement obtained by the downscaling process. However, the FDCs show that the high river flows are still not well simulated with the downscaled precipitation and this is especially noticeable for the daily river flow forecasts (Figure 4.4a).

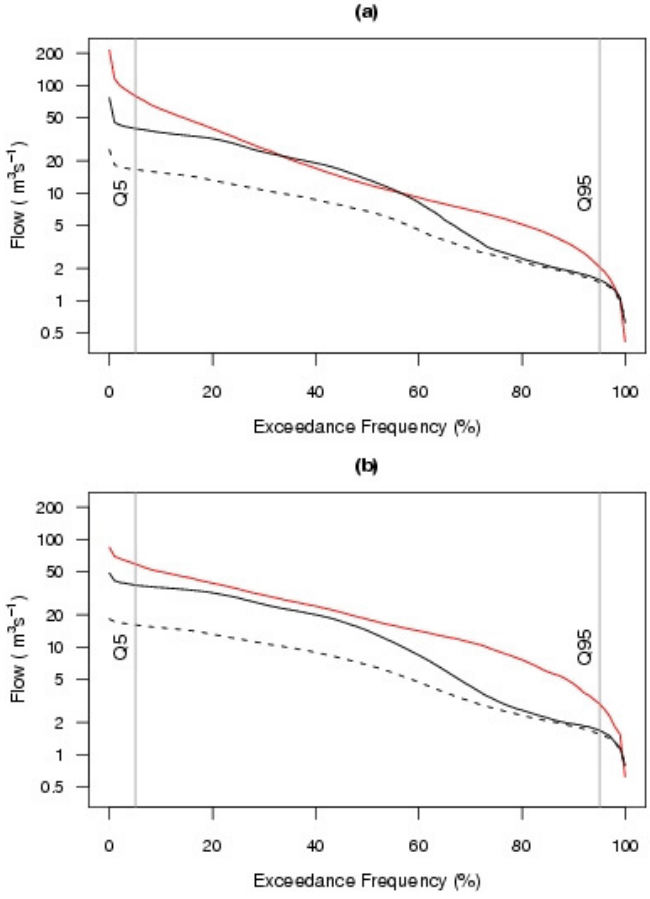


Figure 4.4: Flow duration curves for the River Dyfi at Dyfi Bridge for (a) daily river flows and (b) 30 day moving average river flows over 01/05/1980–30/04/2001. The red line is the observed flow, the solid black line is the ensemble mean river flow forecast from the downscaled DEMETER multi-model precipitation (0–3 months series), and the dashed black line is the ensemble mean river flow forecast from DEMETER multi-model precipitation (0–3 months series).

The NS statistics calculated with the historical mean daily and historical mean daily 30 day moving average river flow as a reference are all negative (Tables 4.2 and 4.3). The downscaled precipitation yields higher river flow forecast skill than directly using DEMETER models' precipitation, with the ensemble mean river flow from downscaled DEMETER (0–3 months) multi-model precipitation having the highest NS value ($NS\text{-}1_{HIST}$=-0.143). As the NS values calculated using the historical flows have no positive values even with the downscaled precipitation as the driving data, it implies that these river flow forecasts are currently not as skilful as those possible from the historical river flow 'climatology'.

Interestingly for the river flows driven by downscaled DEMETER models, the application of the moving average has a different effect on the NS statistic depending on what reference river flow is used. When using the mean annual flow as a reference, the 30 day moving average river flow forecast has higher skill compared to the daily flow forecast (cf. NS-1=0.128 and NS-30=0.289 for 0–3 months DEMETER multi-model ensemble mean flow; Table 4.2). Conversely, when the daily historical mean river flow is used as a reference the moving average leads to a decrease in skill. The hydrographs in Figure 4.5 help to explain the reasoning behind this observation. In Figure 4.5b the 30 day moving average of the observed river flow (red line) smoothes out the large daily flow fluctuations (shown in Figure 4.5a) bringing the observed flow closer to the moving average (0–3 months) DEMETER multi-model ensemble mean river flow (black line; Figure 4.5b), in turn leading to smaller errors compared with the reference mean annual flow (straight blue line) and thus a larger NS-30 value compared to NS-1. When the daily historical mean flow is used as the reference, the application of the moving average produces the opposite effect. In this case the observed and historical moving average river flows tend to be more closely aligned than with the (0–3

months) DEMETER multi-model ensemble mean river flow leading to lower NS-30 values compared to NS-1 (Figure 4.5d).

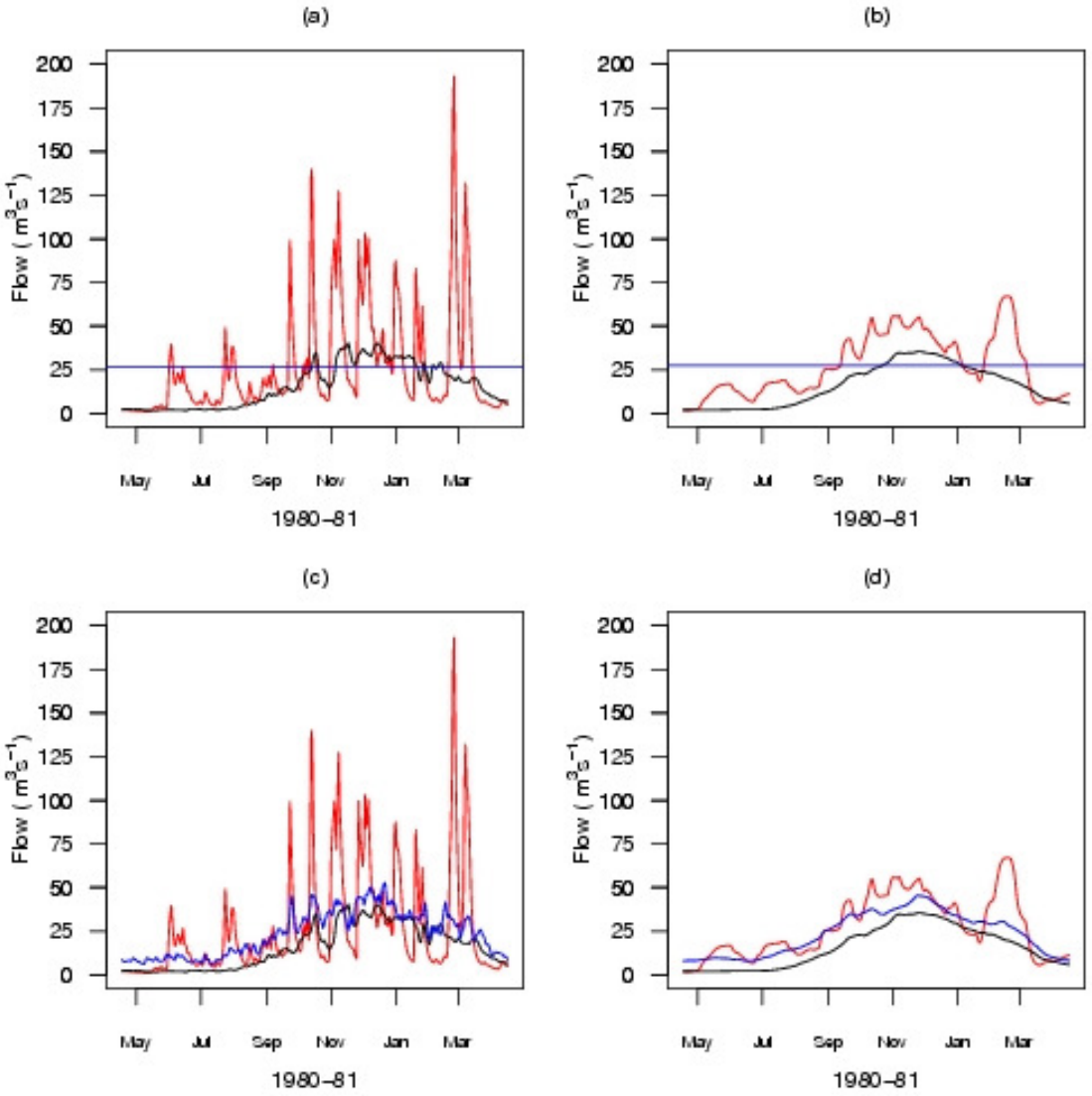


Figure 4.5: Observed river flows (red line), downscaled 0–3 months DEMETER multi-model ensemble mean river flows (black line), and historical river flows (blue line) over 01/05/1980 to 30/04/1981. In (a) the daily flows and (b) the 30 day moving average flows are shown with the mean annual flow as a reference; in (c) the daily river flows and (d) the 30 day moving average river flows are shown with the historical river flows as a reference.

### 4.5.3 River flow forecasts during two extreme hydrological events

Hydrographs for two extreme hydrological events in the Dyfi basin, a low flow period (01/07/1984–31/08/1984) and a high flow period (01/10/2000–30/11/2000), are shown in Figure 4.6. The hydrographs show the daily ensemble mean river flow driven by the downscaled 0–3 months DEMETER models precipitation series. The percent correct rate of the forecasts (Table 4.5) highlights the information contained in the contingency tables (see Tables 3 and 4 in Appendix I). Note that as the downscaled 0–3 months DEMETER multi-model ensemble mean river flow forecast had the highest NS values over 1980–2001 (cf. Tables 4.2 and 4.3), only river flow forecasts of the extreme events forced with 0–3 months downscaled precipitation are shown and discussed.

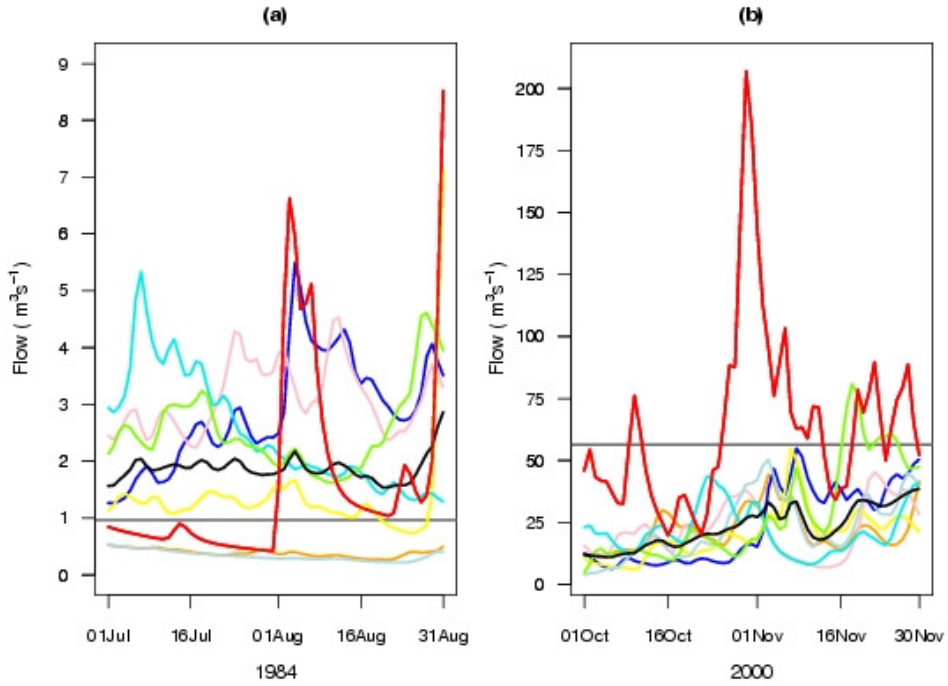


Figure 4.6: Hydrographs of the downscaled (0–3 months series) DEMETER models daily ensemble mean river flows for (a) July and August 1984 and (b) October and November 2000. The model forecasts and their colours are: CERFACS (orange), ECMWF (blue), INGV (pink), LODYC (yellow), METEO FRANCE (light blue), MPI (cyan), UKMO (light green), DEMETER multi-model (black), and observed (red) river flows. The grey horizontal line is the median observed flow over each period.

For the low flow event in 1984, the best percent correct rate was 50% which was obtained by all models except LODYC (Table 4.5). Generally the forecasts can not reproduce the low observed flows, which can be seen in Figure 4.6a. The CERFACS and METEO FRANCE forecasts are closely aligned with the observed river flows in July 1984, but these models could not capture the higher flows in August 1984. For the high flow event in 2000, no model could forecast the extremely high flow (> 200 $m^3s^{-1}$) at the end of October 2000. The UKMO ensemble mean flow forecast had the best percent correct rate of 57 % during this high flow period (Table 4.5) and all other river flow forecasts forced by DEMETER models had a 50 % correct rate. These results imply that poor sub-monthly forecast skill exists in these river flow forecasts.

Table 4.5: The percent correct rate % for the low (01/07/1984–31/08/1984) and high (01/10/2000–30/11/2000) river flow events using the ensemble mean river flow forecast from each DEMETER model and the DEMETER multi-model (0–3 months series).

| Model | Percent Correct Rate (%) | |
|---|---|---|
| | July-August 1984 | October-November 2000 |
| CERFACS | 50 | 50 |
| ECMWF | 50 | 50 |
| INGV | 50 | 50 |
| LODYC | 35 | 50 |
| METEO FRANCE | 50 | 50 |
| MPI | 50 | 50 |
| UKMO | 50 | 57 |
| DEMETER | 50 | 50 |

## 4.6 Conclusions

The aim of this chapter was to drive a rainfall-runoff model using (1) GCM and downscaled GCM (ERA-40 re-analysis) precipitation, and using (2) precipitation and downscaled precipitation forecasts from seasonal climate models (DEMETER) to assess the skill of river

flow forecasting. Results highlight that ERA-40 GCM precipitation, which has observed precipitation assimilated into it, can not skilfully simulate river flow in the PDM rainfall-runoff model. DEMETER seasonal precipitation forecasts are also unable to reliably force the rainfall-runoff model for the Dyfi basin. The GCM precipitation (ERA-40 and DEMETER) used to drive the PDM rainfall-runoff model generate river flow forecasts that underestimate the observed river flows. This is likely to be due to the inability of the ERA-40 assimilating model and DEMETER seasonal climate models to resolve basin-scale (or GCM sub-grid scale) atmospheric processes such as orographic enhancement of precipitation over the Welsh Mountains, thus precluding a direct operational use of current GCM precipitation output.

With the aid of the SDSM statistical downscaling technique, river flow forecast skill was improved. The river flows simulated using downscaled ERA-40 data generated the highest NS values (for both mean annual and daily historical mean reference flows), which is thought to be due to the fact that ERA-40 atmospheric predictors (close to observations) were used to produce the downscaled precipitation and because the river flow forecasts were only verified over a 10 year period (1991–2001). The downscaled DEMETER driven ensemble mean river flow forecasts were more skilful than using the mean annual river flow. However, when the ensemble mean river flow forecasts generated by downscaled DEMETER precipitation were compared with the daily historical mean river flow (or "climatology"), the flow forecasts were less skilful than the historical flow. Considering that the use of the ERA-40 predictors in the downscaling process over 1991–2001 produced skilful river flow forecasts, the relatively poor downscaled DEMETER driven river flow forecasts may result from inaccurate forecasts of the large-scale climatic circulation in the DEMETER models. A promising result to note is that the downscaled DEMETER driven river flow forecasts only

had a small degradation in skill when using the 4–6 months downscaled precipitation time series compared to the 0–3 months time series, potentially indicating that this type of forecast could be utilised at this longer lead time.

There are a few reasons why the methodology used could have had lower forecast skill compared to the historical river flows. Firstly, only precipitation and atmospheric downscaling predictors at the closest GCM grid cell to the River Dyfi basin (52.5°N 2.5°W) were used. This may not have been the most appropriate as the atmospheric predictors with the strongest relationship with Dyfi basin precipitation may be located at some distance from the basin. Research in Chapter 5 investigates and identifies the geographical locations where the large-scale atmospheric predictors have the strongest control on British river basin precipitation and discharge in part to determine whether the ideal predictor regions were selected in this chapter. Secondly, the direct use of GCM precipitation might not have been suitable if the seasonal climate model predictive skill of precipitation is low. Furthermore, the predictive skill of DEMETER atmospheric predictors may also be poor. These research questions are addressed in Chapter 7. Finally, it is possible that insufficient historical climate data (atmospheric circulation and basin precipitation) were available to train the multiple linear regression SDSM downscaling models; this will only be rectified with the availability of longer historical time series.

### 4.7 Chapter summary

This chapter has evaluated a physically realistic end-to-end seasonal river flow forecast system for the River Dyfi in West Wales (Great Britain) and found that GCM precipitation is unable to skilfully force the PDM rainfall-runoff model. Precipitation downscaled from DEMETER seasonal climate model predictors performs better in forcing the rainfall-runoff

model, but is not as accurate as using daily historical mean river flows as a forecast. Reasons for the lower river flow forecast skill (compared to daily historical river flows) are considered to be the use of an inappropriate GCM grid point for the atmospheric downscaling predictors, and the seasonal climate model predictive skill of precipitation and downscaling predictors. These factors form the research in Chapters 5 and 7 respectively.

# 5. LARGE-SCALE CLIMATE, PRECIPITATION AND BRITISH RIVER FLOWS: IDENTIFYING HYDROCLIMATOLOGICAL CONNECTIONS AND DYNAMICS

Chapter Objective: to characterise the spatiotemporal variability of hydroclimatological relationships across Great Britain.

## 5.1 Introduction

Identifying relationships between large-scale climatic circulation, and river basin-scale precipitation and discharge provides insight into understanding the hydroclimatological process chain (Kingston *et al.,* 2009). Statistically significant empirical climate linkages could be exploited for predicting precipitation and river flow anomalies at seasonal time-scales, if combined with accurate seasonal predictions of the driving large-scale climatic circulation. Such long-term hydrological predictions are important to help improve advanced planning of water resources and increase human preparedness for hydrological extremes, including floods and droughts (Wedgbrow *et al.,* 2002). This is an important challenge because hydrological extremes are expected to become more commonplace in a changing climate (Kundzewicz *et al.,* 2007).

Indices that summarise the main modes of atmospheric variability over a particular region are most frequently used for investigating relationships between the large-scale climatic circulation and precipitation and river flow. Over the Euro-Atlantic region different phases of the NAO, as measured by the NAOI, are known to be associated with variations in the surface westerly winds and precipitation occurrence over Europe (Uvo, 2003). At the regional scale across Great Britain, previous research suggests that relationships between the NAOI and precipitation and river flow exhibit spatiotemporal variation (for more details see section 2.4).

Through consideration of atmospheric dynamics, a physical process informed approach can be adopted to select explanatory climate variables that control precipitation and river flow. For extratropical synoptic-scale weather systems, horizontal wind velocities are approximately *geostrophic* (or *quasi-geostrophic*), which means that the horizontal pressure gradient and Coriolis force balance, producing a constant horizontal wind parallel to the isobars or contours. Using *quasi-geostrophic* theory, the *omega equation* can be formulated that provides a method of diagnosing the vertical velocity of air from a distribution of geopotential (Holton, 1992). Sapiano *et al.* (2006) used the *quasi-geostrophic* theory to determine the primary factors affecting extratropical large-scale precipitation. In particular, they identified that low MSLP and the meridional temperature gradient affects extratropical precipitation amount. MSLP is collocated with vertical velocity in the midtroposphere, and is thus indicative of cyclonic development and precipitation. A strong meridional temperature gradient in the extratropics is related to vertical zonal wind shear by the *thermal wind relation*, and through further manipulation the zonal (west-east) wind can be written in terms of the meridional gradient of MSLP (or geopotential) (Sapiano *et al.,* 2006). A strong westerly wind increases moisture transport across the Atlantic, and leads to above average precipitation and river flow in Northwest Europe (Kingston *et al.,* 2006b). Based on our extension of *quasi-geostrophic* theory to hydrological variables, MSLP and zonal wind variables are included in this study, along with the NAOI, to determine their relation with precipitation and river flow in Britain.

The aim of this chapter is to investigate how the hydroclimatological relationships between large-scale climatic circulation and precipitation and river flow vary in time and space for ten near-natural river basins across Great Britain. In addressing this aim, the following three hypotheses are tested: (H1) the hydroclimatological relationships across Britain vary spatially

and seasonally reflecting climatic gradients that are influenced by topography (i.e. mountains), and proximity to the moisture-laden westerly flow from the North Atlantic; (H2) the use of gridded atmospheric data uncovers the detailed spatial and temporal variability of atmospheric control on precipitation/river flow, and leads to an improvement in statistical associations and process understanding over using an index, such as the NAOI; and (H3) the rainfall-to-runoff transformation varies in space and time because different river basin properties, such as permeability of geologies, attenuate the climatic signal on river flow to varying degrees.

## 5.2 Data and Methods

Ten near-natural basins (Tables 3.1 and 3.2) were selected from the UK NRFA's benchmark catchment list (Bradford and Marsh, 2003), as these basins are not significantly impacted by human activity. This means that climate-precipitation-flow links are not modified strongly by water management. The geographic coverage of the 10 catchments across Britain (Figure 3.1) captures the east-to-west and south-to-north precipitation gradient (as shown by SAAR in Table 3.1). The catchments were selected to sample a range of hydrological response times, as measured by the BFI. The BFI is indicative of the proportion of river flow derived from longer residence time water sources (e.g. groundwater, lakes, wetlands, snow, and ice). Typically, high (low) BFI denotes a high (low) storage component; basins with high BFI tend to have a longer 'hydrological memory' and greater buffering of climatic inputs (Fleig *et al.,* in press).

The river basin precipitation and discharge were provided by the UK NRFA, which ensured a strict quality control of all the data. Daily river basin precipitation time series were calculated by averaging across all available rain gauges in the river basin (number of gauges used in

Table 3.1), and daily river flow was measured at the gauging stations in Table 3.1. Six basins had some missing river flow values, but data gaps were very limited at most being 1 % of daily river flows for the Great Stour. For periods of missing flows larger than seven days, the equi-percentile method was used to infill missing values (Hannaford, 2004). Daily precipitation and river flow from January 1976 to December 2001 (26 year period) were aggregated to monthly values for the analyses herein.

Five atmospheric variables (on a 2.5° × 2.5° grid from 15°N–70°N and 75°W–35°E; 1035 points) were extracted from the ECMWF ERA-40 reanalysis dataset (Uppala *et al.,* 2005) from January 1976 to December 2001. Following the *quasi-geostrophic* theory (Sapiano *et al.,* 2006), MSLP and the Zonal Wind U are included (by convention U is positive when there is a westerly wind). In addition to U, the Meridional Wind (V) was chosen to determine the influence of north-south airflow on precipitation and discharge occurrence (V is positive when there is a southerly wind). Two atmospheric levels (500 and 850 hPa) were also considered to determine if correlation strength varied significantly with height in the troposphere, and to identify the level containing the most useful information for understanding precipitation and river flow generation dynamics. The spatial disparity between the basins' areas (ranging from 0.1° to 0.25°) and the 2.5° atmospheric grid is not an issue because of the relatively smooth change in space of the selected atmospheric variables. Moreover, as this study is concerned with the effect of large-scale atmospheric control on basin hydrology, it is necessary to analyse atmospheric variables on the coarser 2.5° grid.

As the NAOI has been widely used in previous research (section 2.4), it was used in this study as a benchmark against which to compare the links with gridded variables. NAOI time series were obtained from the UEA CRU website (http://www.cru.uea.ac.uk/cru/data/nao/;

accessed January 2009) and represents the monthly normalised pressure difference between Gibraltar and Southwest Iceland (Jones *et al.,* 1997).

Normality of the atmospheric variables, precipitation and river flow was tested with the Shapiro-Wilks test (Reimann *et al.,* 2008), and as normality could not be accepted, the Spearman rank correlation coefficient ($\rho$) was used as a measure of links between concurrent monthly time-series of atmospheric variables and precipitation/river flow. To investigate seasonal variability in detail, correlation analysis was undertaken on a monthly basis (i.e. analysing time-series of each month individually) between the gridded ERA-40 atmospheric data and NAOI, and basin precipitation and river flow data over the period 1976 –2001.

Note that correlation on daily data was also tested for a hydrologically-responsive sample basin (i.e. Ewe); but daily analysis yielded lower absolute correlation values than monthly analysis. This could be due to noise in the data at a daily timescale, but could also reflect the complex mechanisms of precipitation generation. Although low pressure systems are often associated with precipitation occurrence because of the large-scale lifting, precipitation is not consistent throughout a low pressure system. This means that there is a disconnection in space and time at the daily level between the large-scale atmosphere and precipitation receipt (i.e. it might or might not rain when MSLP is low) resulting in correlations lower at the daily timescale than at the monthly timescale. No daily correlation analyses are reported in this chapter.

Monthly field significance was examined using Monte Carlo simulations for the ERA-40 variables against precipitation and discharge in each river basin to assess if the observed significant correlation areas were greater than those expected by chance alone. Here, 200 simulations were used as suggested by Livezey and Chen (1983) and Phillips and McGregor

(2002), so that the probability density function of the number of significant grid points observed in each simulation could be estimated accurately. For each simulation, a series of 26 values (i.e. same length as the monthly time series over 1976–2001) was generated randomly from the empirical distribution of the precipitation or discharge time series, and then correlated with the 1035 grid points of each ERA-40 atmospheric variable field. The number of grid points with significant ranked correlation at the 0.05 level in each simulation was recorded. The 200 simulations provided an associated empirical probability distribution. A correlation pattern is considered field significant (at the 0.05 level) if the area of observed significant correlation is larger than that expected by chance, as given by the 95% percentile of the constructed empirical probability distribution. Correlation patterns that are field significant will be considered as possible centres ('hot spots') of atmospheric circulation related to precipitation and river flow.

The estimation of the correlation between time-series of precipitation (and discharge) and atmospheric variables could be affected by the presence of linear trends in any of these variables; this was tested using a bootstrap procedure (Efron and Tibshirani, 1998). The atmospheric data and precipitation / discharge time-series were re-sampled with replacement $B$=200 times (keeping the concurrent pairs of the variables of interest), obtaining $B$ samples of the same size as the observed series ($n$=26). For each bootstrap sample, Spearman's $\rho$ was computed giving its bootstrap empirical distribution. This procedure was repeated in each basin for each month and variable at all 1035 grid points in the domain for precipitation and discharge. Results suggest that the presence of possible linear trends in these variables has negligible influence on the correlation results, and hence data were not de-trended.

## 5.3 Results and Discussion

As an organisational framework, the field significance results are presented followed by a discussion and interpretation of the large-scale circulation correlation results: firstly for precipitation and secondly for river flow.

### 5.3.1 Field significance of large-scale circulation and precipitation / river flow

Two observations emerge from the monthly field significance analysis of the correlation patterns for precipitation and discharge (Figure 5.1). First, field significant correlation patterns are found generally in more months for precipitation than river flow, as particularly highlighted for the Dun (Figure 5.1h). The weaker patterns for river flow are probably due to the role the catchment plays in transforming the climate signal into discharge. For the Dun (BFI=0.95), such differences are likely to result from the large groundwater component of river flow where the geology acts as a buffer between precipitation and river flow, thus reducing the direct influence of climate on river flow. The differences are less marked for more responsive catchments (lower BFI), such as the Dyfi (BFI=0.39; Figure 5.1g). Although the Ewe has a moderate-high BFI of 0.64, field significance results for precipitation and discharge are almost identical because this basin has sub-monthly water storage (water storage in the Ewe basin is discussed further in section 5.3.3).

Second, basins located in western Britain (and not associated with major aquifers) tend to have more months with field significant results (both for precipitation and river flow; e.g. Falloch basin, Figure 5.1c), which may reflect a stronger connection between large-scale climatic circulation and precipitation and river flow due to exposure to westerly winds and moisture fluxes in the west. The mountains of Scotland and Wales and the English Pennines act as a barrier to the westerly winds resulting in fewer significant patterns in the east. In

general, Figure 5.1 shows that variables at 850 hPa have more field significant months than at 500 hPa, implying that the lower level (850 hPa) has a larger control on the basin precipitation and discharge. Owing to this fact, only the months with field significant correlations at 850 hPa (and MSLP) are the focus of discussion hereafter.

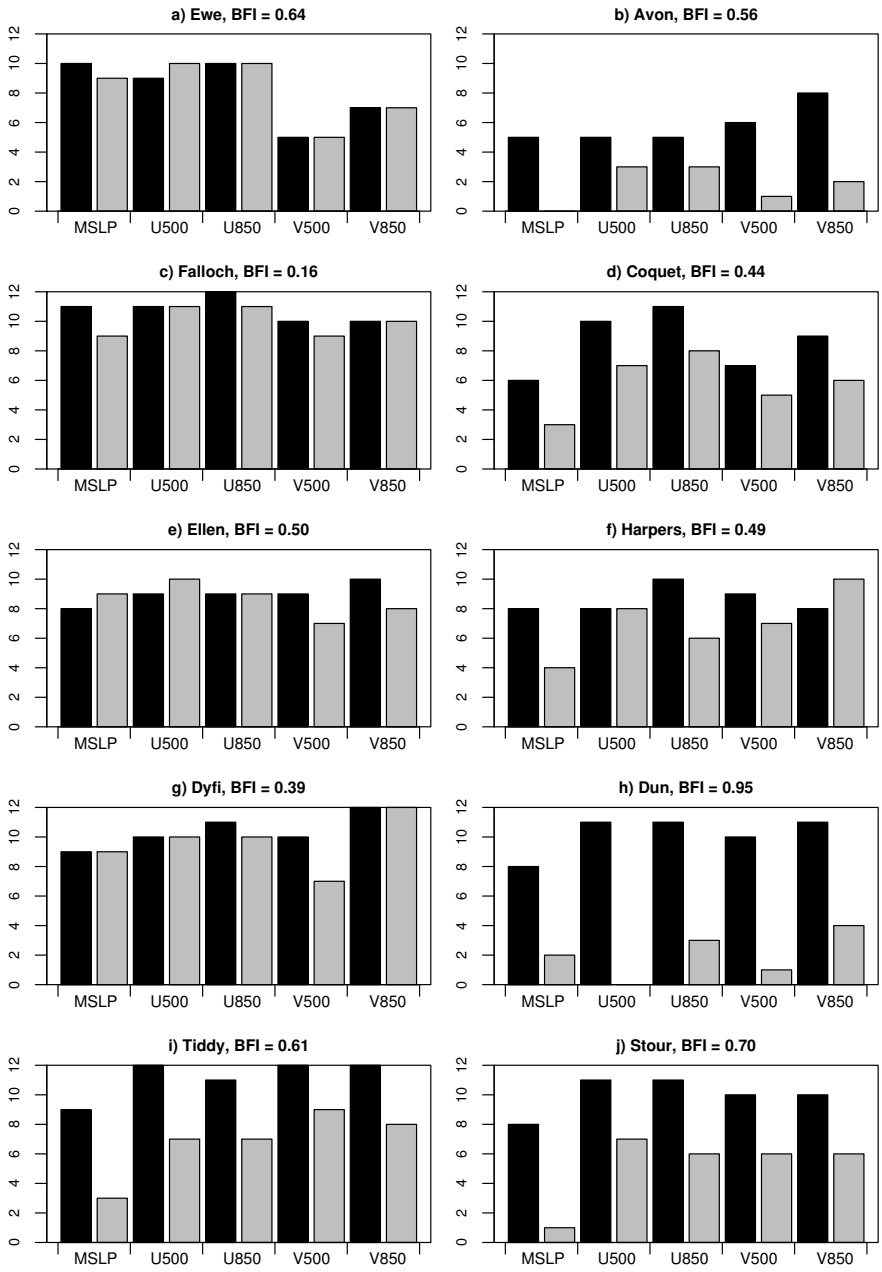


Figure 5.1: Number of field significant months (at the 0.05 level) for ERA-40 atmospheric variables against precipitation (black) and river flow (grey) for each basin.

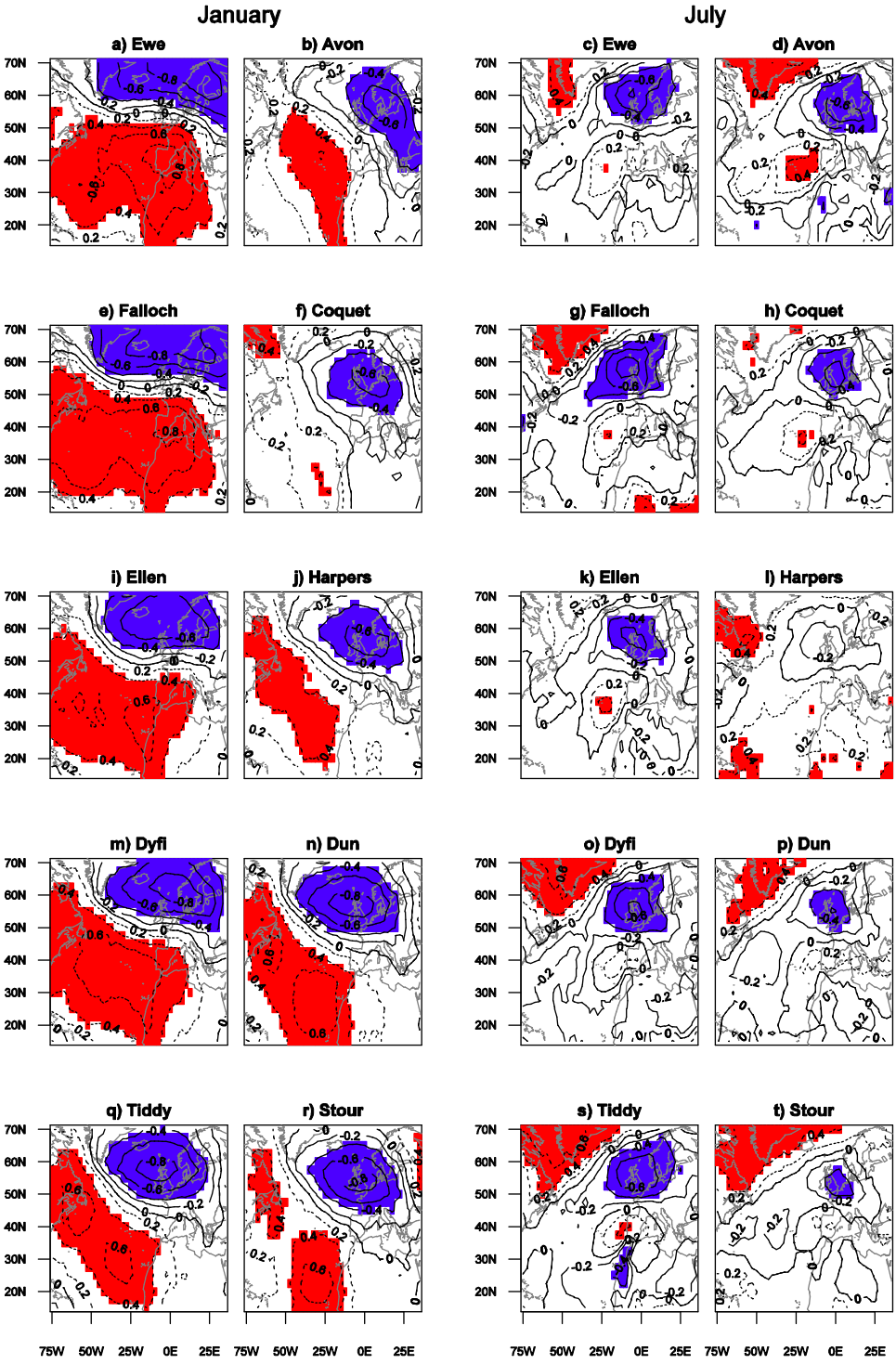


Figure 5.2 (a-t): Spearman rank correlation between basin precipitation and MSLP for all basins for January (left plots) and July (right plots) over 1976–2001. Solid (dashed) contour lines at a 0.2 interval show negative (positive) correlation, with blue (red) colour signifying significant negative (positive) correlation (*significance level* $\alpha = 0.05$).

### 5.3.2 Correlation between large-scale circulation and precipitation

Significant rank correlation between large-scale climatic circulation and river basin precipitation show gradients in strengths and patterns primarily reflecting the location of the basin and its position relative to the topography of Britain. In western Britain (Dyfi, Ellen, Ewe and Falloch), precipitation is connected with a strong MSLP correlation dipole pattern particularly in winter. A correlation dipole is characterised by significant positive and negative correlations in two different geographical regions. For these catchments, positive (negative) correlation is located across the southern (northern) part of the study domain (Figure 5.2a, 5.2e, 5.2i and 5.2m for January). These centres of correlation are located to the south/ southwest (Azores High) and north/ northwest of Britain (Icelandic Low), which are located near the reference measures of the NAOI. The season of the strongest pattern is winter, when the temperature gradient between the Equator and the North Pole is largest. The significant correlation pattern suggests that when MSLP falls in the Icelandic Low region and increases in the Azores High region, precipitation occurs over the four basins. The situation corresponds to a MSLP field associated with westerly winds over Britain, bringing extratropical weather systems and precipitation. Strong westerly winds increase precipitation receipt, as also reflected by the significant positive U correlation at 850 hPa ($\rho > 0.8$) (Figure 5.3a, 5.3e, 5.3i and 5.3m). The area of strongest positive U correlation is situated on the southern edge of the strongest negative MSLP correlation (Figure 5.2a, 5.2e, 5.2i and 5.2m), as a result of the anti-clockwise circulation that occurs around low pressure systems in the Northern Hemisphere. This is consistent with links between high winter precipitation over northern Europe and a more frequent western atmospheric flow, as highlighted by Bouwer *et al.* (2006), and such circulation patterns can be related to the Westerly weather type of the Lamb Classification (Lamb, 1972). The relationship of the westerly flow with precipitation is

further corroborated by the positive NAOI correlation with basin precipitation during the winter half-year (Table 5.1). The Dyfi and Ellen only have significant positive NAOI correlation during the winter half-year, whereas the Ewe and Falloch have positive NAOI correlations that are, for the most part, significant throughout the year (highest value of 0.87 in February for the Falloch) possibly because of orographic enhancement of precipitation by the western Scottish mountains. V correlation at 850 hPa for these four western basins show a great deal of variability, although in general negative (positive) V correlation is noticeable to the west (east) of Britain, which relates to the northerly (southerly) wind (Figure 5.4a, 5.4e, 5.4i and 5.4m) in the anti-clockwise circulation around a low pressure system.

Table 5.1: Monthly NAOI-precipitation correlations (correlation significant at the 0.05 level is in bold).

| | Jan | Feb | Mar | Apr | May | Jun | Jul | Aug | Sep | Oct | Nov | Dec |
|---|---|---|---|---|---|---|---|---|---|---|---|---|
| Avon | 0.33 | 0.17 | 0.04 | -0.06 | 0.06 | -0.20 | 0.06 | 0.19 | -0.22 | -0.14 | -0.13 | 0.37 |
| Coquet | 0.01 | 0.03 | **-0.47** | 0.06 | 0.09 | -0.27 | 0.26 | -0.27 | -0.26 | -0.25 | -0.11 | 0.00 |
| Dun | **0.44** | 0.32 | -0.18 | 0.14 | -0.14 | -0.34 | 0.13 | -0.06 | -0.32 | 0.13 | 0.23 | 0.06 |
| Dyfi | **0.68** | **0.56** | 0.21 | **0.48** | 0.08 | -0.15 | 0.05 | 0.27 | 0.12 | **0.41** | **0.55** | **0.71** |
| Ellen | **0.64** | **0.75** | 0.19 | **0.47** | 0.15 | 0.07 | 0.17 | 0.22 | 0.34 | **0.54** | **0.65** | **0.79** |
| Ewe | **0.83** | **0.81** | **0.67** | **0.57** | **0.54** | **0.60** | 0.27 | **0.39** | **0.78** | **0.70** | **0.66** | **0.73** |
| Falloch | **0.84** | **0.87** | **0.83** | **0.66** | 0.33 | **0.52** | 0.30 | 0.29 | **0.89** | **0.75** | **0.73** | **0.82** |
| Great Stour | 0.19 | 0.13 | -0.30 | 0.08 | -0.14 | -0.16 | -0.11 | -0.18 | **-0.55** | 0.03 | 0.19 | 0.17 |
| Harpers Brook | 0.30 | 0.16 | -0.20 | -0.02 | 0.22 | -0.29 | 0.26 | -0.25 | **-0.41** | -0.13 | -0.05 | 0.07 |
| Tiddy | **0.42** | 0.36 | -0.13 | 0.31 | -0.23 | -0.20 | 0.11 | 0.03 | -0.30 | 0.21 | 0.17 | **0.43** |

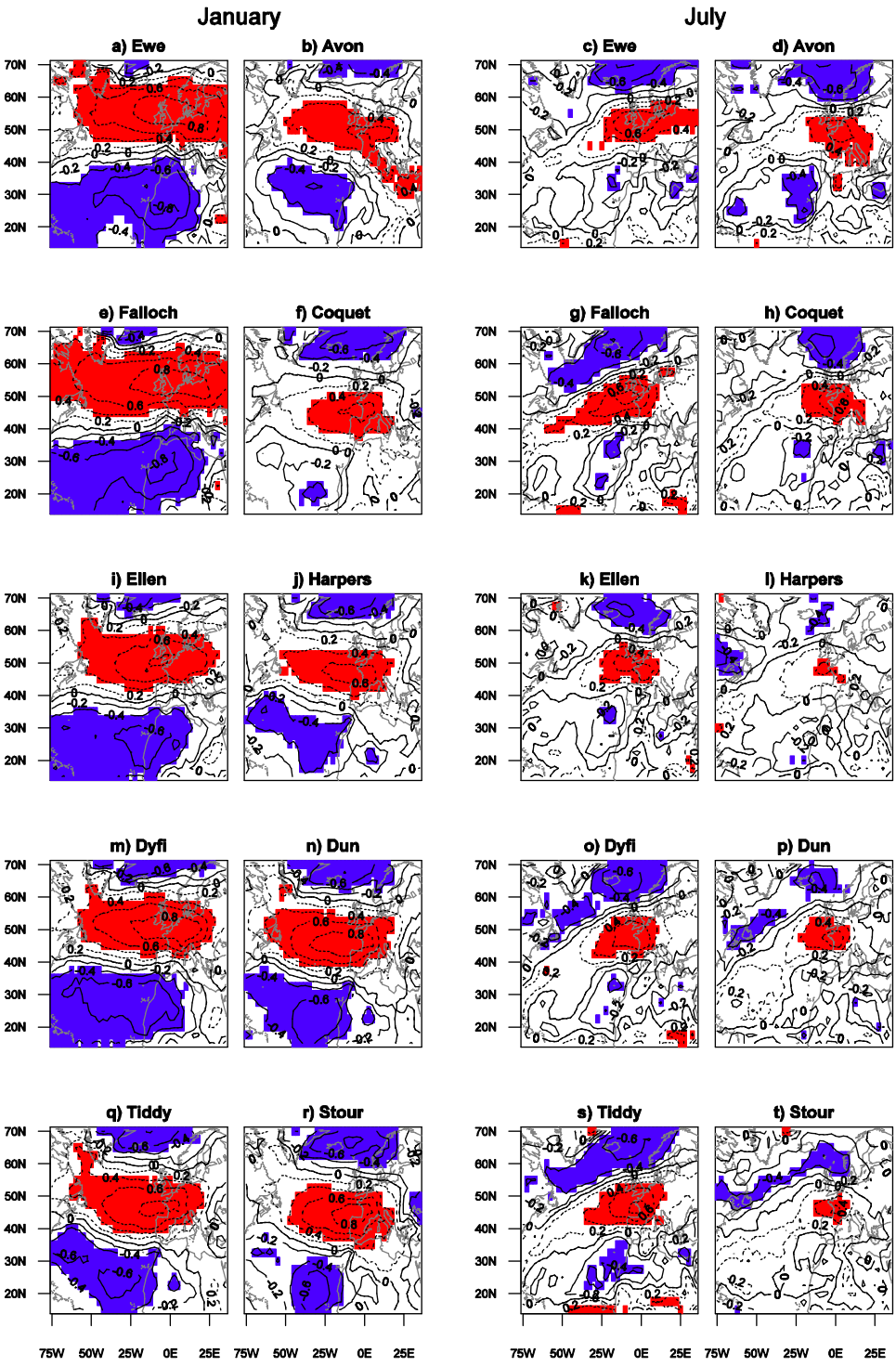


Figure 5.3 (a-t): Spearman rank correlation between basin precipitation and U at 850 hPa for all basins for January (left plots) and July (right plots) over 1976–2001 [Key as Figure 5.2].

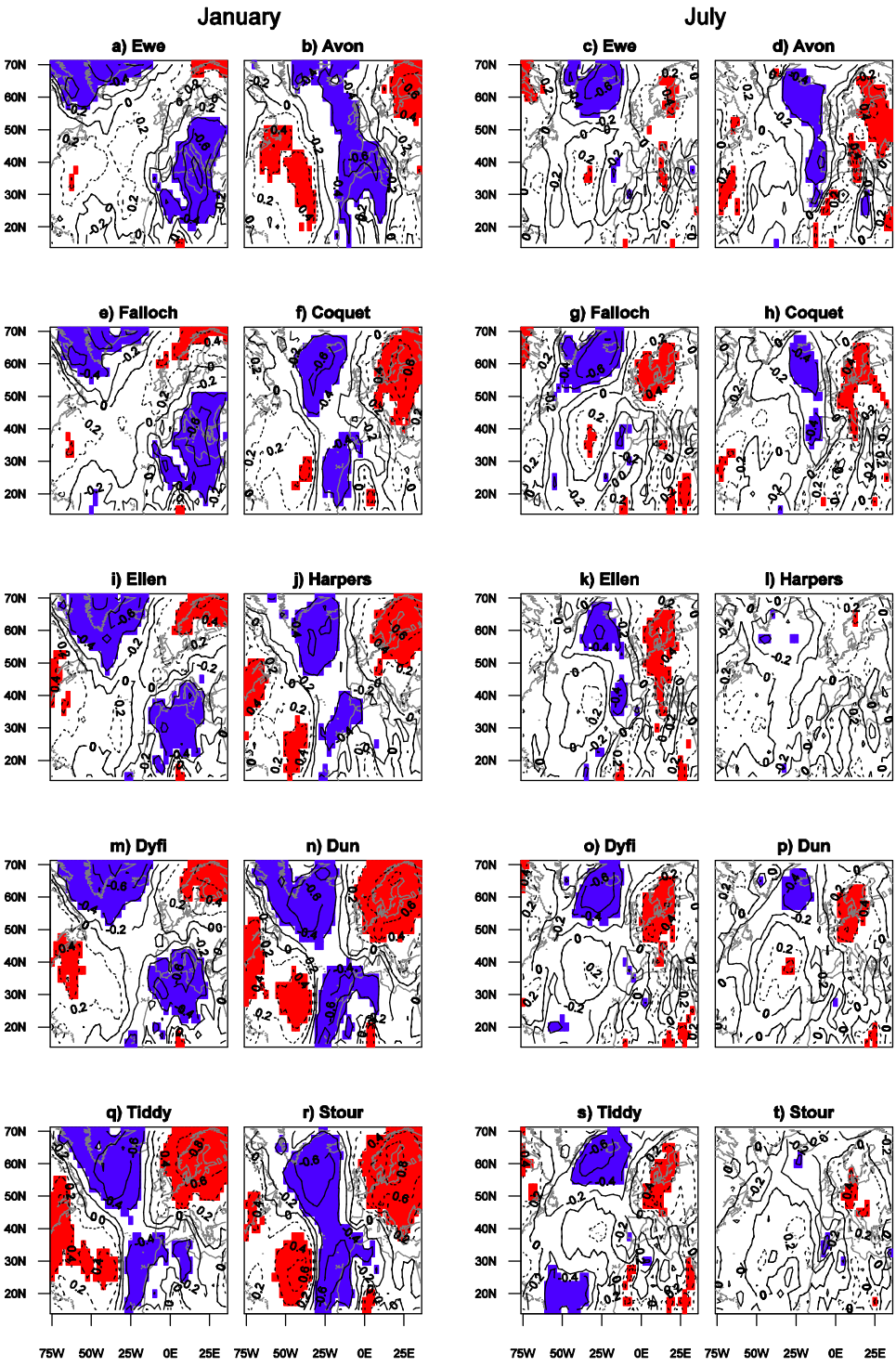


Figure 5.4 (a-t): Spearman rank correlation between basin precipitation and V at 850 hPa for all basins for January (left plots) and July (right plots) over 1976–2001 [Key as Figure 5.2].

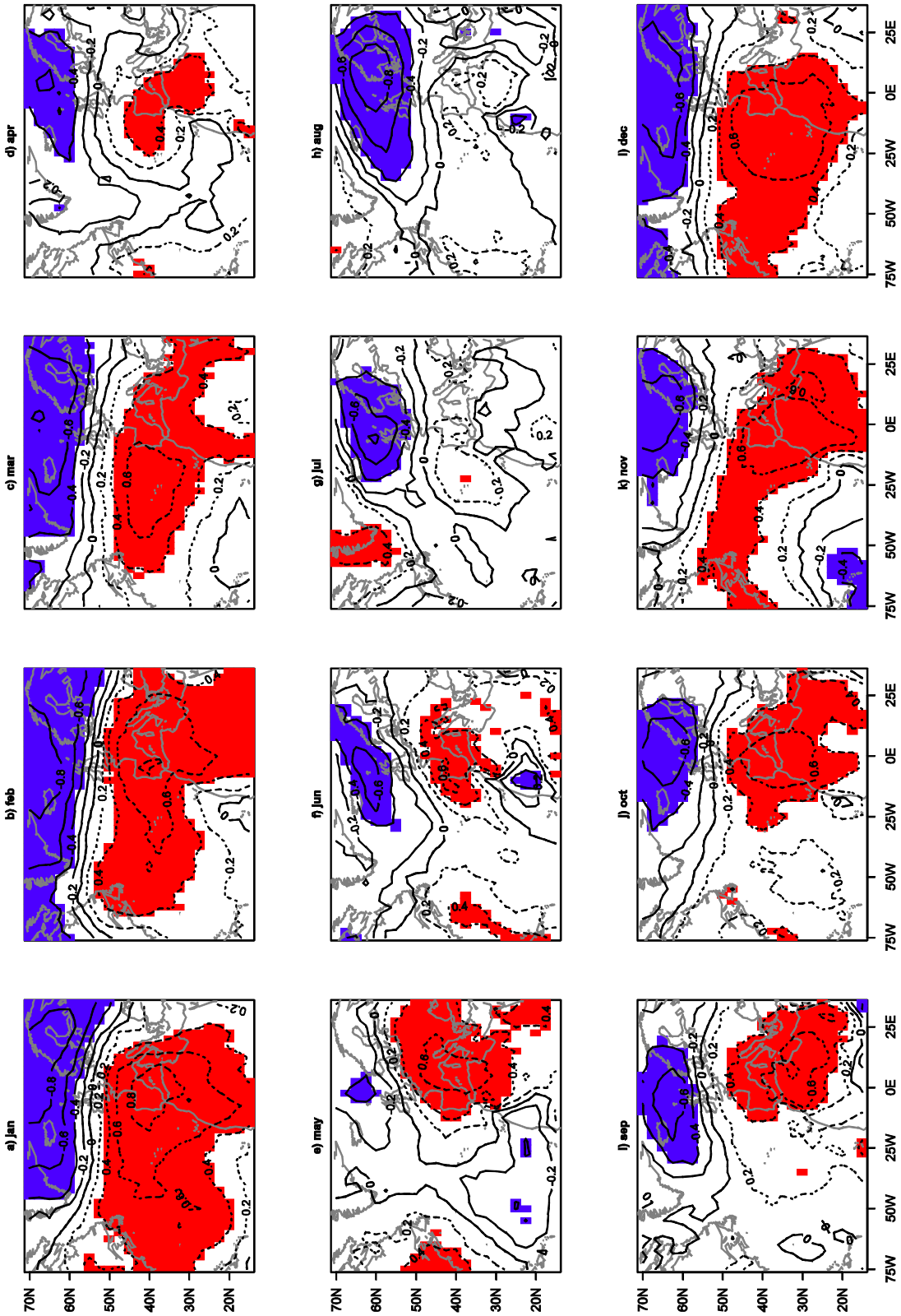


Figure 5.5 (a-l): Spearman rank correlation between Ewe basin precipitation and MSLP for all calendar months for 1976–2001 [Key as Figure 5.2].

Toward summer, the Equator-North Pole temperature gradient lessens, weakening the westerly air flow and reducing the occurrence of the Westerly weather type (Lamb, 1972). From late spring to early summer, the frequency of Westerly weather types is the lowest of the year (Roy, 1997), resulting in lower precipitation amounts and lower correlation between precipitation and MSLP over the Northern Atlantic for April, May and June (Ewe basin; Figures 5.5d, 5.5e, 5.5f); the areas of positive correlation shrink in size and disappear in the summer (Ewe basin; Figure 5.5g and 5.5h). Summer precipitation in the western basins is linked typically with negative MSLP correlation situated across, and north of, Britain (Figure 5.2c, 5.2g, 5.2k and 5.2o for July). The negative correlation areas shift southwards during summer, with their spatial extent also reaching a minimum at this time (Ewe basin; Figure 5.5). This suggests that summer precipitation producing systems are associated with a Cyclonic weather type for which depressions usually stagnate or pass over Britain. Convective storms, particularly prevalent in the summer, have a shorter lifespan than the baroclinic waves that produce the extratropical depressions (Wallace and Hobbs, 2006) and contribute to precipitation receipt in the summer (Berg *et al.,* 2009). Such small-scale weather systems and associated precipitation are masked by the monthly analysis, thus such linkages are not identified here.

In the south and southeast of Britain, the Dun, Great Stour, Harpers Brook and Tiddy basins have similar climate-precipitation relationships. Correlation analysis suggests winter precipitation is produced predominately by low pressure situated over central Britain, which is typical of a Cyclonic weather type (Lamb, 1972). Significant negative correlation exhibits latitudinal variation shifting southwards during summer. Only January has a MSLP correlation dipole with precipitation, exhibiting positive values over the Azores and negative values over Britain (Figure 5.2j, 5.2n, 5.2q and 5.2r), thus not exactly over the NAOI

reference points. The extent of this positive correlation area is smaller than that observed in the western catchments (Figure 5.2). This indicates a weaker influence of westerly weather types on precipitation occurrence in southern Britain. In turn, NAOI correlations are generally not significant for these basins (Table 5.1); this may be because the basins are located in the rain shadow of western mountain chains. Tiddy precipitation has low correlation with the NAOI, despite its western location, which may suggest that the macro-scale NAOI can not resolve the local-scale Tiddy precipitation (basin area is 37.2 $km^2$; McGregor and Phillips, 2004). Zonal wind U has significant positive correlation in all months to the south of the British Isles as shown for 850 hPa (Figure 5.3 for January and July). These westerly winds are to the south of the low MSLP centre (negative correlation; see Figure 5.2) reflecting the anti-clockwise circulation around a low pressure system. Meridional wind V patterns exhibit variability between the four basins, but dominant structures relate to clockwise (anti-clockwise) circulations around high (low) pressure areas (Figure 5.4).

Precipitation in the Coquet basin (Northeast England) is associated with low pressure over Britain, as given by significant negative MSLP correlation, and is characterised by a Cyclonic weather type (Figure 5.2f and 5.2h). However, there is a subtle difference from the patterns for the four southern basins, and this is that the location of the low pressure system would cause an onshore flow (easterly wind or retrograde motion) off the North Sea, thus bringing precipitation to the Coquet. This result corroborates previous research (Wheeler, 1997). NAOI correlations are predominantly not significant, except for March ($\rho$=-0.47). There is an absence of positive MSLP correlation with Coquet precipitation, and hence westerly weather types have weak influence, possibly due to the Pennines mountain chain in England.

Precipitation in the Avon in northern Scotland has significant negative MSLP correlation to the east of Britain (Figure 5.2b and 5.2d). This indicates that low pressure to the east (and sometimes high pressure to the west) of Britain generates precipitation, as north-westerly winds bring moisture and troughs of low pressure. Similarly to the Coquet, previous research has shown that precipitation may be associated with slow moving depressions (Cyclonic weather type) to the south of the basin that lead to easterly winds on the northern edge of the depression (Roy, 1997); this is supported by the U and V patterns in Figures 5.3b and 5.4b respectively. As the Avon is located to the east of the Western Scottish Highlands, the influence of a westerly weather type on the basin is small, as most of the atmospheric moisture is precipitated-out over these mountains before reaching the basin. This is also shown by the non-significant NAOI correlations throughout the year.

### 5.3.3 Correlation between large-scale circulation and river flow

The Dyfi, Ellen, Ewe and Falloch basins in western Britain have similar precipitation and discharge correlation patterns (cf. Figure 5.6 with Figure 5.2 for MSLP). This is consistent with the responsiveness of the basins as summarised by the BFI, as they all have low BFI (except the Ewe), implying more 'flashy' (rapid) runoff response to precipitation. Spearman rank correlation of 0.79 and 0.81 between the NAOI and Ewe river flow in January and February (Table 5.2) are similar to the Pearson correlations of 0.70 and 0.82 found by Phillips *et al.* (2003), and only marginally different to the correlations of NAOI against Ewe precipitation of 0.83 and 0.81 found here. On top of the underlying impermeable rock in the Ewe catchment, Loch Maree acts as a reservoir and attenuates storm flows at short time-scales (days), resulting in a moderate-high BFI. However, sub-monthly loch storage time means that the climate-discharge connection is not significantly buffered at a monthly time step. Although precipitation may fall as snow in the northerly Ewe and Falloch basins, the

relatively rapid response of river flow to precipitation suggests snow storage and meltwater release are not temporally disconnected over extended (i.e. multi-month) periods. This is confirmed by analysis of the mean monthly river flow over 1976–2001, where the Ewe and Falloch basins show peak monthly river flow in January when precipitation is highest and evapotranspiration is lowest. This suggests no significant snow storage that would delay the monthly precipitation-runoff relationships.

Table 5.2: Monthly NAOI-river flow correlations (Key as for Table 5.1).

| | Jan | Feb | Mar | Apr | May | Jun | Jul | Aug | Sep | Oct | Nov | Dec |
|---|---|---|---|---|---|---|---|---|---|---|---|---|
| Avon | 0.22 | 0.35 | 0.36 | 0.05 | 0.08 | -0.05 | 0.00 | 0.08 | -0.22 | -0.13 | 0.12 | 0.09 |
| Coquet | -0.26 | -0.17 | **-0.42** | 0.09 | 0.02 | -0.13 | 0.11 | -0.27 | -0.20 | -0.14 | 0.07 | 0.14 |
| Dun | 0.13 | -0.14 | -0.01 | -0.19 | 0.08 | 0.04 | -0.06 | -0.33 | **0.52** | -0.12 | 0.37 | 0.34 |
| Dyfi | **0.65** | **0.43** | 0.21 | **0.48** | 0.20 | -0.14 | -0.16 | 0.29 | 0.28 | 0.38 | **0.58** | **0.69** |
| Ellen | **0.59** | **0.68** | 0.26 | **0.42** | 0.04 | 0.19 | -0.12 | 0.04 | **0.44** | 0.35 | **0.62** | **0.80** |
| Ewe | **0.79** | **0.81** | **0.53** | 0.37 | 0.37 | **0.51** | 0.29 | **0.46** | **0.74** | 0.37 | **0.61** | **0.74** |
| Falloch | **0.70** | **0.88** | **0.66** | **0.60** | 0.33 | **0.62** | 0.15 | **0.39** | **0.86** | **0.78** | **0.70** | **0.75** |
| Great Stour | -0.04 | -0.15 | -0.23 | -0.10 | 0.09 | -0.04 | -0.36 | **-0.41** | 0.04 | -0.02 | 0.39 | 0.24 |
| Harpers Brook | -0.01 | -0.31 | **-0.39** | -0.14 | 0.17 | -0.16 | -0.04 | -0.06 | -0.10 | -0.12 | 0.21 | 0.17 |
| Tiddy | 0.27 | 0.03 | 0.00 | 0.28 | 0.03 | 0.09 | 0.05 | 0.15 | -0.06 | -0.19 | 0.32 | **0.39** |

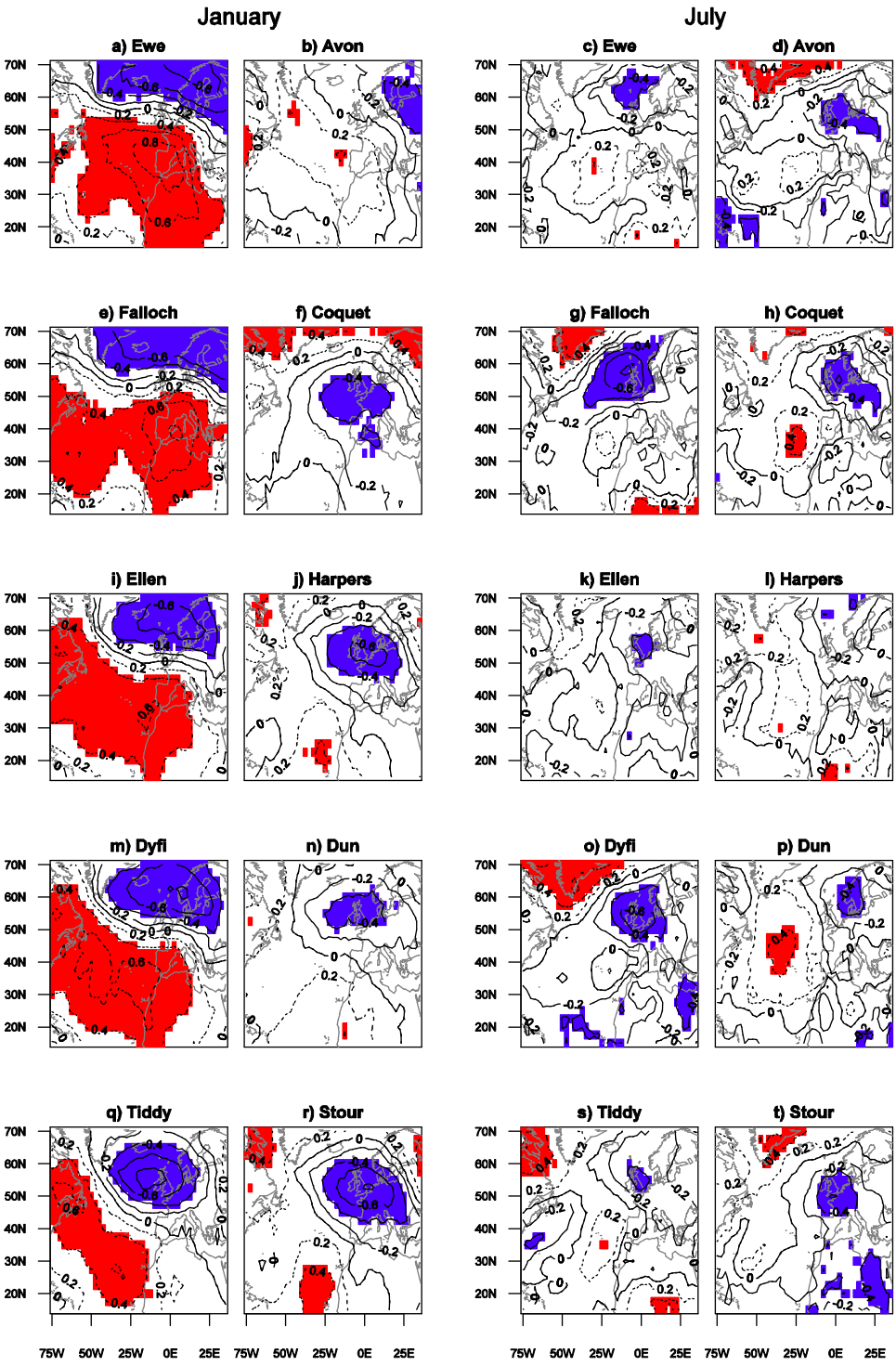


Figure 5.6 (a-t): Spearman rank correlation between basin discharge and MSLP for all basins for January (left plots) and July (right plots) over 1976–2001 [Key as Figure 5.2].

The Dun in southern Britain is underlain predominately by a major chalk aquifer (Marsh and Hannaford, 2008) resulting in long hydrological residence times and very marked basin buffering or hydrological memory, as characterised by a high BFI of 0.95. The role of the river basin in transforming the climate inputs is clearly illustrated by the lack of concurrent correlation between large-scale circulation and river flow (Figure 5.6n and 5.6p), despite existence of significant climate–precipitation associations (Figure 5.2n and 5.2p). The Harpers Brook and Great Stour basins also have weaker climate-discharge relationships than climate-precipitation links suggesting a possible lagged river flow response to the large-scale circulation and precipitation (cf. Figure 5.6 with Figure 5.2 for MSLP). The NAOI has weak insignificant correlations with discharge in Southern Britain (Table 5.2), suggesting that westerly airflows have reduced influence on river flows here; the weak and small centres of positive MSLP correlation in January (Figure 5.6) also testify to the lack of westerly airflow influences. Winter correlation patterns between Tiddy discharge and MSLP have similar structure to those for precipitation (Figure 5.2q and Figure 5.6q for January), with a North Atlantic correlation dipole from November to January. As with precipitation, the Tiddy basin has low NAOI-discharge correlation possibly suggesting that the macro-scale NAOI can not resolve this small basin's discharge (basin area is 37.2 $km^2$).

The Avon has little significant climate-discharge correlation in winter (Figure 5.6b for MSLP) and lacks significant NAOI-discharge correlations (Table 5.2). Due to its relatively northerly location in the Scottish mountains (with average altitude of 525 m), winter precipitation is likely to fall as snow and may be stored before being released as discharge in spring (Kingston *et al.,* 2007). This seasonal storage weakens the direct large-scale climatic impact on flow. Further evidence of snowfall in the Avon's river flow regime is found through analysis of mean monthly river flow over 1976–2001. Peak monthly mean Avon

river flow occurs in April suggesting that warmer spring air temperatures cause snow to melt and, thus the highest river flows to occur then. A reason for snow storage in the Avon in eastern Scotland as compared to low snow storage in the Ewe and Falloch in western Scotland is because the relatively mild westerly air flows that travel over the heat source of the North Atlantic Ocean are blocked from the Avon by the western Scottish mountains. The correlation between Coquet discharge and MSLP is similar, although weaker, to precipitation (cf. Figure 5.6f and 5.6h with Figure 5.2f and 5.2h). As the Coquet has small catchment storage (BFI=0.44), little attenuation of the climatic signal is seen by the basin properties. As for precipitation, NAOI correlations are not significant, except for March ($\rho$=-0.42; Table 5.2). This negative correlation implies that an easterly air stream may cause an onshore flow off the North Sea, generating river flow.

The large-scale climatic circulation against river flow correlation is weaker in summer for all study catchments, even for those with a low BFI. This is possibly because in the summer (especially for the basins in southern and eastern Britain) evapotranspiration has a large role to play in the balance between precipitation and evapotranspiration. This would result in greater evaporation loss in summer than in winter and weaker climate-river flow associations. For all basins, correlations between precipitation and river flow, and the NAOI are systematically lower than for gridded climate variables. For example, MSLP against Tiddy and Great Stour precipitation (Figure 5.2q and 5.2r respectively) yield correlation >|0.8| in January, compared with 0.42 and 0.19 for the NAOI, respectively (Table 5.1). As with the gridded atmospheric data, the NAOI relationship with discharge is weaker than for precipitation (cf. Table 5.1 and Table 5.2), which can be attributed to basin controls.

## 5.4 Conclusions

The aim of this chapter was to investigate in a systematic manner how the hydroclimatological relationships between large-scale climatic circulation and precipitation and river flow varied in time and space for 10 near-natural river basins across Great Britain. To achieve this aim, this study used *quasi-geostrophic* theory to choose appropriate explanatory atmospheric variables, and used correlation analysis to investigate the hydroclimatological links. The methodological approach based on gridded ERA-40 climate data shows that the areas of high climate-precipitation and climate-discharge correlation shift and vary in strength seasonally for all catchments, and these 'hot spots' of high correlation indicate that different weather patterns generate precipitation and, in turn, river flow across Britain.

The location of strongest significant correlation between large-scale climatic circulation and precipitation and discharge varies between the basins and from month-to-month, which validates hypothesis H1. From winter to summer, a southward latitudinal shift is found for MSLP and U, and the significant correlation regions simultaneously shrink in size. Correlation analysis with the NAOI hides these monthly large-scale climatic circulation movements and the NAOI correlations are systematically weaker than with gridded ERA-40 atmospheric data (and in particular the comparable MSLP), which upholds hypothesis H2. This finding means that an index with pre-defined measurement locations is likely to be a less powerful predictor of hydroclimatological response than gridded atmospheric data because of the transient nature of the atmospheric processes, particularly centres of action. Correlation patterns of MSLP, U and V allow inference of the large-scale climatic relationship with precipitation and discharge, and thus aid understanding of the hydroclimatological process chain. Analysis has shown that U and V at 500 hPa had the

weakest correlation of the variables studied, indicating that the lower 850 hPa level has the greatest influence on precipitation and river flow. At the monthly temporal average used herein, the results suggest that the gridded MSLP is sufficient as a proxy for the large-scale atmospheric circulation control on British river basin precipitation and discharge.

The climate-river flow correlation maps have similar structure, although, weaker correlation strengths compared with climate-precipitation maps. Hydrological response depends on a combination of precipitation, evapotranspiration, basin permeability and basin steepness. In western Britain precipitation is dominant in the balance between precipitation and evapotranspiration throughout the year, which together with basin impermeability (low BFI) and steepness create a rapid hydrological response to precipitation and thus strong climate-river flow relationships. In southern and eastern Britain precipitation and evapotranspiration are in closer balance, with the evapotranspiration demand generally exceeding precipitation receipt in the summer. This greater evapotranspiration demand in this region together with higher basin permeability (high BFI) and shallower basin slopes contribute to the weaker climate-river flow relationships uncovered. Our results illustrate clearly that basins with permeable geologies (and other water basin storages) situated in the south and east of Britain have weaker climate-river flow associations than in western regions which confirms hypothesis H3.

Precipitation correlation patterns show inter-basin similarity, as identified for the basins situated in western and southern Britain. Climate-discharge relationships are much harder to generalise than climate-precipitation relationships because of the additional influence of basin water storage, release and transfer processes. Some exceptions can be found, when considering catchments located in similar topographical regions with similar basin properties,

as shown for the four western catchments studied herein. For more permeable basins, lagged correlation could be used to unpick climate-discharge associations by taking hydrological memory into account as suggested by Wilby (2001).

The results found and conclusions drawn on winter precipitation could be applicable across a larger area of Europe because of the large-scale circulation generating winter precipitation in Northwest Europe. However, the precipitation results are likely to be less transferable to other regions of Europe in summer, as this research has shown smaller-scale circulation patterns relate to precipitation in this season. Conclusions for river flow are more basin dependent, as all basins attenuate the rainfall-runoff signal by varying degrees. Consequently, it is likely that the climate-discharge relationships herein will have less transferability to other European regions than for precipitation.

This study has advanced knowledge of the spatially variable hydroclimatological process chain that determines precipitation and river discharge across Britain. These linkages may be used to test the potential skill of precipitation and river flow predictions. Further insight on the rainfall-runoff transformation in the river basins studied may be gained by undertaking hydrological modelling. Also, lagged large-scale climate against discharge correlation analyses are recommended to determine whether stronger statistical relationships could be obtained by exploiting hydrological system memory that occurs in certain basins.

### 5.5 Chapter summary

This chapter has investigated and quantified the spatiotemporal variability of the relationships between the large-scale climatic circulation and 10 river basins' precipitation and discharge across Great Britain. In conclusion, the most appropriate GCM grid point was

not used in the downscaling in Chapter 4, and these results suggest that future downscaling studies must consider this spatiotemporal variability to attain the highest levels of precipitation or river flow predictive skill. As spatial and temporal hydroclimatological variability have been found across Great Britain, Chapter 6 takes the research further by undertaking a continental-scale analysis of the MSLP control on precipitation across Europe.

# 6. EUROPEAN PRECIPITATION CONNECTIONS WITH LARGE-SCALE MEAN SEA LEVEL PRESSURE (MSLP) FIELDS

Chapter Objective: to characterise the spatiotemporal variability of large-scale MSLP control on precipitation across Europe.

## 6.1 Introduction

European precipitation receipt is dynamic seasonally and spatially (Zveryaev, 2004). This variability in precipitation can lead to floods or droughts, which have major socio-economic impacts over Europe (Lorenzo *et al.*, 2008, Zveryaev and Allan, 2010). Agriculture, water resources management and other sectors are reliant on timely and sufficient precipitation supply, with extreme variability potentially causing water shortages and crop failures, or flood inundation in both urban and rural areas. Identification of hydroclimatological relationships between large-scale climatic circulation and precipitation occurrence helps in understanding the climate drivers of precipitation, which may lead to an improvement in skill of climate prediction (Zveryaev and Allan, 2010). With skilful climate prediction, it would be possible to anticipate precipitation and associated hydrological anomalies, which would help mitigate negative impacts and provide societal benefits.

The atmosphere is an example of a chaotic system, that is if a small perturbation is imparted on the initial atmospheric state, the atmosphere will evolve into a different state than the realisation without a perturbation (Harrison, 2005). Predictability of the atmosphere is a property of the climate system that varies in different regions of the world, with the tropics (extratropics) possessing generally higher (lower) predictability due to weak (high) internal chaotic variability there (Palmer and Anderson, 1994). Actual predictive skill is the proportion of this predictability that can be realised; the current climate prediction models

have low actual precipitation predictive skill in the extratropics over Europe (Lavers *et al.*, 2009). This low actual predictive skill may be due to either the random nature of precipitation generation over Europe or because of the inability of the climate models to resolve the extratropical atmospheric dynamics.

The average pole-to-equator temperature gradient in the Northern Hemisphere is larger in winter than summer. According to the *thermal wind relationship*, a horizontal temperature gradient causes vertical zonal (west-east) wind shear resulting in a region of maximum zonal wind near the tropopause that is called the 'jet stream' (Holton, 1992). As the largest temperature gradient occurs in winter, jet streams are also strongest in winter. Over the North Atlantic, they occur just east of North America between 30°N and 35°N in winter and between 40°N and 45°N in summer. Weather systems develop typically in these jet stream regions and travel eastward along storm tracks towards Europe (Holton, 1992). In winter, synoptic weather systems pick up moisture from the North Atlantic and transport the warm moist air and precipitation over Europe. Regions on the western edge of the European continent (e.g. British Isles and Scandinavia) are most affected by these weather systems, while inland areas (e.g. Central Europe) are less affected by systems from the Atlantic Ocean (Wibig, 1999) and so experience a continental climate (Berg *et al.,* 2009). In turn, high winter precipitation is found over Western Europe which is intensified by coastal mountains that force the moisture-laden Atlantic air to rise (i.e. orographic enhancement). In contrast, low winter precipitation occurs over Eastern Europe and Russia. High (low) winter precipitation variability tends to occur in regions of maximum (minimum) precipitation (Zveryaev, 2004). In summer (warm-season), local-scale processes are thought to play a key role in precipitation receipt, in part because European precipitation has a significant statistical relationship with European land surface evaporation (Zveryaev and Allan, 2010). Convective

precipitation events are more prevalent in summer (Berg *et al.,* 2009), with precipitation generally being larger over the central continental parts of Europe and lower near the continental extremities (Zveryaev, 2004). Interestingly summer evaporation from the North Atlantic is not found to relate to European precipitation, which is in stark contrast to the winter (Zveryaev and Allan, 2010). This suggests that the strong winter jet stream and associated synoptic-scale weather systems subside in summer (because of the weaker pole-to-equator temperature gradient), thus limiting this mode of conveyance of North Atlantic moisture and precipitation over Europe.

Climate system diagnostics and indices that describe the state of the large-scale atmospheric circulation (such as the NAOI) have been used previously by several researchers to quantify the connection between the large-scale atmosphere and precipitation. Winter Scandinavian and Baltic precipitation increases with westerly winds, and hence with a positive NAO phase (Hurrell, 1995, Uvo, 2003, Jaagus *et al.*, 2010). Precipitation in northern Britain has also shown a significant positive correlation with the NAO in winter (Wilby *et al.*, 1997, Fowler and Kilsby, 2002). Conversely, over the Iberian Peninsula, winter precipitation is negatively correlated with the NAO (Hurrell, 1995, Lorenzo *et al.*, 2008). In the European Alps, precipitation has shown little relation with the NAO, possibly due to the complex terrain (Bartolini *et al.*, 2009). In general, the NAO has a stronger link with winter precipitation in coastal European countries, such as Greece, Spain, parts of Scandinavia and the UK (Bouwer *et al.*, 2008), and a weaker link with winter precipitation in European regions more remote from the Atlantic Ocean (Wibig, 1999). This suggests that precipitation occurrence at the monthly to seasonal time scale in Europe is not random as the large-scale climatic circulation shows linkages with European precipitation in winter.

As the atmosphere is most dynamically active during winter, most previous analyses have focused on the winter season (Folland *et al.,* 2009) and the NAO, with far less attention given to investigating summer (Zveryaev, 2004, Zveryaev and Allan, 2010). In summer, there is a leading pattern of climatic variability known as the SNAO pattern. In a positive SNAO phase, high pressure occurs over Northwest Europe and low pressure resides over Greenland and the Mediterranean (Zveryaev, 2004). This circulation pattern is associated with warm and dry conditions over Northwest Europe (e.g. British Isles) and cool wet conditions over southern Europe and the Mediterranean, which means that precipitation has significant negative (positive) correlation with the SNAO in Northwest (southern) Europe (Folland *et al.,* 2009). Historical observations have shown there to be significant statistical relationships between the large-scale circulation and precipitation, but only for some European locations and seasons. Few studies have investigated systematically the important large-scale atmospheric influence on summer precipitation variation by month at the continental scale.

The availability of gridded observed precipitation and gridded atmospheric re-analysis MSLP data has made it possible to undertake, for the first time, a consistent and systematic spatiotemporal analysis of the large-scale climatic control on European precipitation. The aim of this chapter is to evaluate the spatiotemporal variability of European precipitation by quantifying the changing connections with large-scale MSLP fields. This will reveal where and when the hydroclimatological links are strongest, and give insight into the different precipitation-generating atmospheric circulations across Europe and precipitation predictability throughout the year (predictability can be inferred if precipitation variability is shown not to be random, i.e. precipitation variation can be linked to another explanatory variable).

## 6.2 Data and Methodology

Two gridded datasets were used: (1) daily observed precipitation (E-OBS dataset) produced by the ENSEMBLES project (Hewitt and Griggs, 2004; Haylock *et al.*, 2008) at a 0.5°×0.5° resolution across central and western Europe (36.25°N–74.25°N and 10.25°W–24.75°E) [North African precipitation time series in the study domain were not used as some series were incomplete]; and (2) daily MSLP from the ECMWF ERA-40 reanalysis dataset (Uppala *et al.*, 2005) on a 2.5°×2.5° grid over half of the Northern Hemisphere (0°N–90°N and 90°W–90°E). MSLP is used as an explanatory variable of European precipitation, as MSLP is collocated with vertical velocity in the mid-troposphere and, therefore, indicative of cyclonic development and precipitation. Monthly precipitation and MSLP time series were derived for the common data period of September 1957 – August 2002. Monthly data were used in our analysis because daily data have been found to be too noisy to detect the fundamental climatic controls on precipitation (see section 5.2). The NAOI from the UEA CRU (http://www.cru.uea.ac.uk/cru/data/nao/nao.dat) acted as a benchmark against which to compare the links with gridded MSLP.

The univariate normality of the MSLP and precipitation time series was tested using the Shapiro-Wilk test (*significance level* $\alpha = 0.05$) as it is one of the most powerful tests for detecting non-normality (Helsel and Hirsch, 1992). Results suggested that some time series were not normally distributed; therefore, the non-parametric Spearman rank correlation method ($\rho$) was used herein (*significance level* $\alpha = 0.05$). Correlation analysis was carried out between MSLP at each grid in the atmospheric domain and each grid of observed precipitation by month (n=45) to assess the detailed spatial variation of MSLP control on European monthly precipitation.

Monthly field significance of the observed MSLP correlation fields (at each precipitation grid) was examined using Monte Carlo simulations to determine whether the observed significant MSLP correlation areas were greater than those expected by chance alone (Livezey and Chen, 1983, Phillips and McGregor, 2002). Livezey and Chen (1983) suggest using 200 simulations to estimate accurately the probability density function of the number of significant MSLP-precipitation correlations observed in each simulation. For each simulation, a series of 45 values (i.e. same as the length of the monthly time series over the period 1957–2002) was generated randomly from the empirical distribution of the precipitation time series, and then correlated with the MSLP time series at each of the 2701 grid points in the MSLP field. The number of MSLP grid points with significant ranked correlation at the 0.05 level was recorded. An observed correlation pattern is considered field significant at the 0.05 level, if the area of observed significant correlation is larger than that expected by chance, as given by the 95% percentile of the empirical probability distribution constructed from the 200 Monte Carlo simulations. Correlation patterns that are field significant are to be considered as possible centres of atmospheric circulation related to precipitation.

The Mann-Kendall trend test (*significance level* $\alpha = 0.05$) was used to determine if trends were present in the monthly MSLP and precipitation time series (e.g. Helsel and Hirsch, 1992) and to assess if spurious MSLP-precipitation correlations could result as a result of any trends. For each month, precipitation time series that had increasing or decreasing linear trends (at $\alpha = 0.05$) underwent a bootstrap procedure to determine if the presence of the trend affected the significance of the correlations with MSLP (following Efron and Tibshirani (1998)).

Note that the bootstrapping process destroys any temporal trends in both the MSLP and precipitation time series. The following bootstrap process was repeated $B$=1000 times. For each bootstrap sample $B$, monthly precipitation (at a particular grid) and MSLP (at all 2701 grid points) were re-sampled with replacement keeping the concurrent pairs to generate time series of the same size as the observed series ($n$=45). At each MSLP grid cell, Spearman's correlation $\rho$ between re-sampled precipitation (at a particular grid) and MSLP time series was computed, providing an empirical bootstrap distribution of 1000 $\rho$ values for each MSLP grid point. If 95% of the constructed empirical bootstrap distribution has a correlation $\rho > 0$ or $\rho < 0$, the trend has no impact on the significance of the correlation at the 0.05 significance level. This significance threshold was used for all MSLP grid points for the relevant precipitation grids. Using this approach, it was possible to assess if the correlations obtained for the observed time series were significant despite a possible presence of trends in these time series.

A spatially nested research design is adopted to facilitate clear presentation of results for different spatial scales and locations. Initially six precipitation grid locations were chosen *a priori* to test the hypothesis that precipitation dynamics are different across the broad climatic zones of Europe. These locations are: (1) western Scotland (57.25°N 5.25°W), (2) Norway (65.25°N 13.75°E), (3) southern Spain (37.75°N 3.75°W), (4) central France (47.25°N 3.25°E), (5) Czech Republic (49.75°N 15.25°E), and (6) the Balkans (42.75°N 20.25°E). Scaling-up from individual grids, results are then presented for all precipitation grids across the British Isles and, at a larger scale still, for all precipitation grids across Europe. The latter provides a novel wider perspective on connections between MSLP and precipitation in Europe.

## 6.3 Precipitation variability, field significance testing and trend analysis

### 6.3.1 European precipitation variability and the NAOI

Figure 6.1 shows the standardised January precipitation anomalies with the NAOI for the six locations selected across Europe [NAOI-precipitation correlation analyses are the focus of section 6.5]. In general, precipitation anomalies (black lines in Figure 6.1) are in phase with the NAOI (grey shading in Figure 6.1) in northern Europe (western Scotland and Norway; Figure 6.1a and 6.1b respectively) and out of phase with the NAOI in southern Europe (southern Spain and the Balkans; Figure 6.1c and 6.1f respectively), which is consistent with the known regional precipitation linkages with the large-scale climatic circulation (Hurrell, 1995). There is less inter-regional agreement between the precipitation time series in July (Figure 6.2), possibly indicating more local-scale convective precipitation generating processes in summer (Berg *et al.*, 2009); an exception is some noticeable co-variability between precipitation time series in western Scotland (Figure 6.2a) and Norway (Figure 6.2b). The lack of precipitation variability in southern Spain (Figure 6.2c) reflects the high number of years with no July rainfall, a climatic feature shared amongst a large area surrounding the Mediterranean.

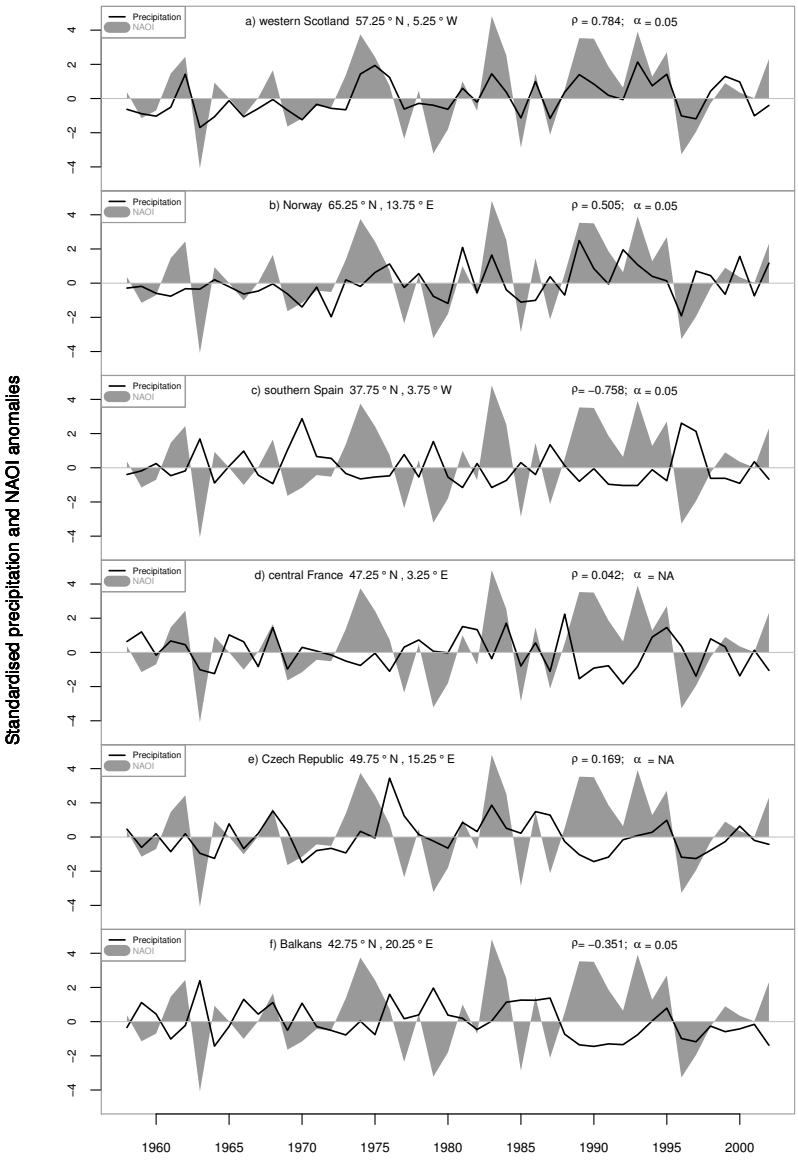


Figure 6.1: Monthly standardised time series of January precipitation anomalies in six grid locations across Europe and the NAOI (1958–2002). The areas shown are: a) western Scotland (57.25°N 5.25°W), b) Norway (65.25°N 13.75°E), c) southern Spain (37.75°N 3.75°W), d) central France (47.25°N 3.25°E), e) Czech Republic (49.75°N 15.25°E), and f) Balkans (42.75°N 20.25°E). The NAOI-precipitation Spearman rank correlations are given for each of the six precipitation grids with the *significance level α* (NA implies the correlation is not significant at the 0.05 level). The precipitation time series are solid black lines and the NAOI time series are shaded solid grey.

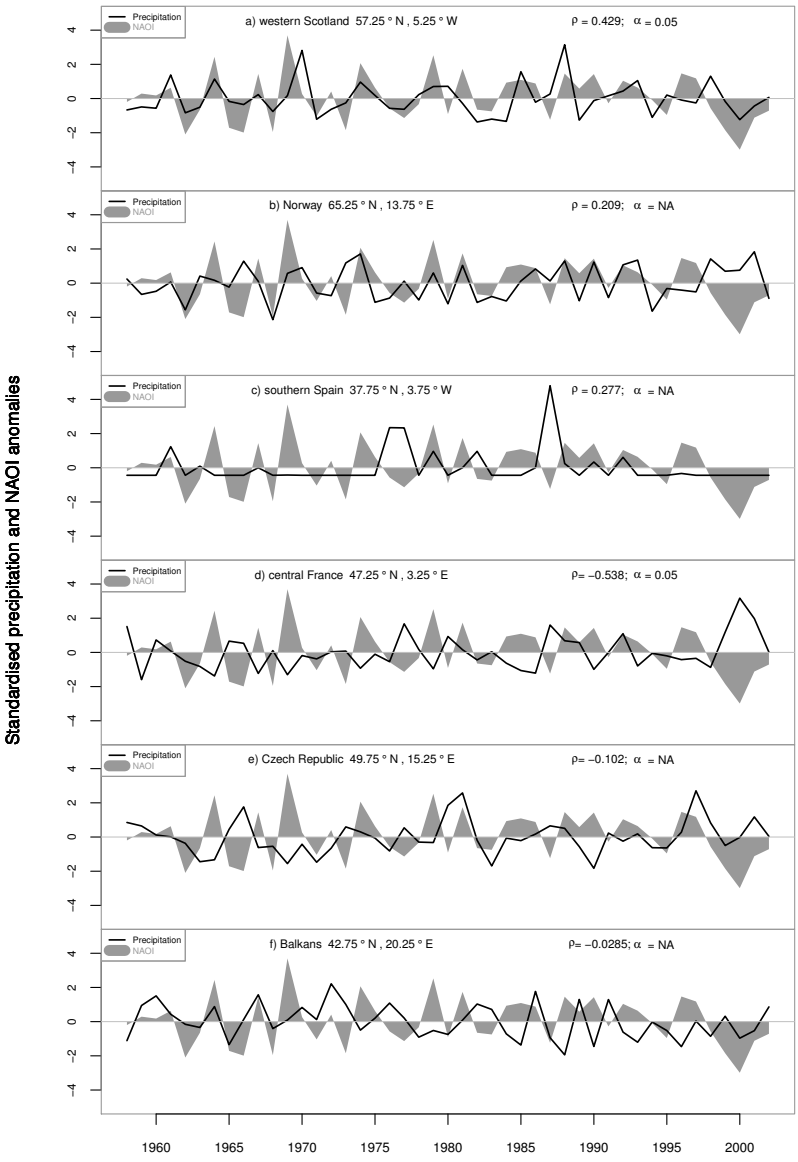


Figure 6.2: Monthly standardised time series of July precipitation anomalies in six grid locations across Europe and the NAOI (1958–2002) [Key as Figure 6.1].

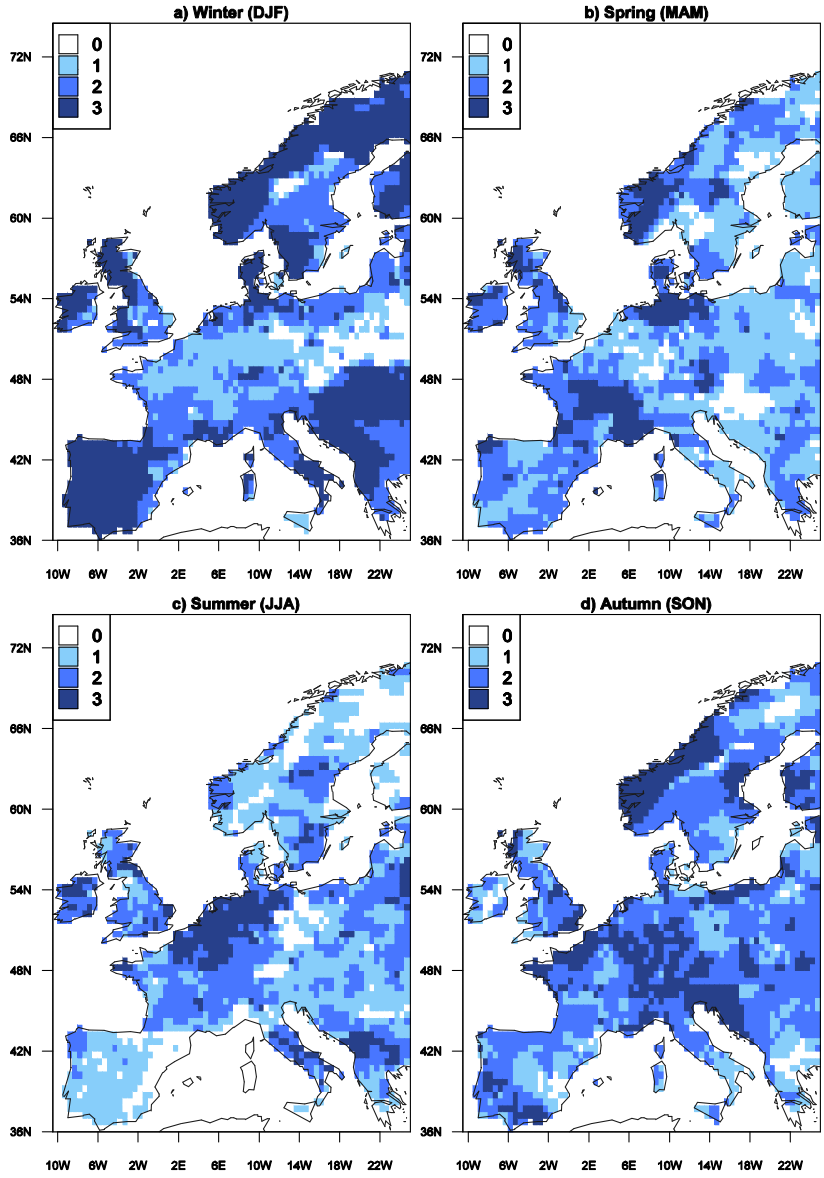


Figure 6.3: Number of field significant months for MSLP for (a) winter (DJF), (b) Spring (MAM), (c) summer (JJA) and (d) autumn (SON) (period of study is September 1957 – August 2002).

### 6.3.2 Field significance

Field significance was assessed to determine if the area (number of MSLP grid points) with observed significant monthly correlation between MSLP and precipitation was larger than what would be expected by chance alone. If this is the case, the correlation pattern associated with this month was described as 'field significant'. The number of months in each season

with field-significant correlations between precipitation and MSLP is shown in Figure 6.3. In winter (December, January and February; DJF) in Figure 6.3a, coastal European regions (except France) have the largest number of field-significant correlation patterns (e.g. Balkans, Iberian Peninsula and western Scandinavia) suggesting that large-scale atmospheric patterns have a significant influence on coastal European precipitation in winter; this corroborates the findings of Wibig (1999). With increasing distance from the Atlantic Ocean and in the lee of mountain ranges (central and East Sweden, central Britain and in the lee of the European Alps), the number of field significant months decreases because of weaker connection between precipitation and the large-scale atmosphere (Figure 6.3a). In spring (March, April and May; MAM) and autumn (September, October and November; SON) in Northwest Britain and western Scandinavia, the many months with field significant precipitation grids may indicate that the winter atmospheric circulation exists for a longer duration (Figure 6.3b and 6.3d respectively). Fewer field significant precipitation grids are found in summer (Figure 6.3c) suggesting that more local-scale weather systems produce the precipitation in summer because the observed significant MSLP-precipitation correlation areas exist across smaller geographical regions. The field significant months over the Low Countries (e.g. Netherlands) and Italy/Balkans in July (Figure 6.3c) indicates a relationship with the SNAO pattern.

### 6.3.3 Influence of trends on the correlation analyses

The precipitation and MSLP time series were tested for trends, which may affect the significance of the correlations. Results of the Mann-Kendall test suggest that trends in precipitation time series occur predominantly in winter (January to March). In Scandinavia (Spain), precipitation has an increasing (a decreasing) trend over 1958–2002. Around 45°N (i.e. the Alps) is the transition zone between increasing and decreasing trends. During winter,

significant increasing (decreasing) MSLP trends are found near the Azores (Iceland), indicating a tightening of the pressure gradient over the North Atlantic and a stronger zonal (westerly) flow, coincident with a stronger positive phase of the NAO. This is consistent with Hurrell and Van Loon (1997); they found that the NAO was often in a positive phase from 1980 until the late 1990s. An increasingly stronger positive NAO could be the cause of the significant increasing (decreasing) precipitation trend observed over Scandinavia (the Iberian Peninsula). Furthermore, the trend towards a strengthening of the NAO influence on European climate during the last part of the Twentieth Century is thought to be due to an eastward movement (i.e. toward Europe) of MSLP anomalies associated with the NAO (Vicente-Serrano and Lopez-Moreno, 2008).

The influence of trends (in both the precipitation and MSLP time series) on the significance of the correlations was assessed using a bootstrap procedure. Figure 6.4 shows the empirical bootstrap distribution of the 1000 correlations produced between the grid cell with precipitation time series with the strongest increasing trend (February, 62.25°N 9.75°E; Norway) and the MSLP grid cell with the strongest observed correlation in February ($\rho$=-0.667; 70°N 7.5°W). The 95% percentile of the empirical bootstrap correlation distribution (black vertical line in Figure 6.4) is less than zero; therefore, the trend does not affect the significance of the observed correlation at this grid point at the 0.05 significance level. Hence, the correlation is significant even without a trend present. Results of the empirical bootstrap distributions at all MSLP grid points for the precipitation grids with significant trends reveals that the significance levels (i.e. 0.05) were almost identical to those obtained through the observed correlation analysis, demonstrating more widely that the presence of trends does not significantly affect the results presented herein.

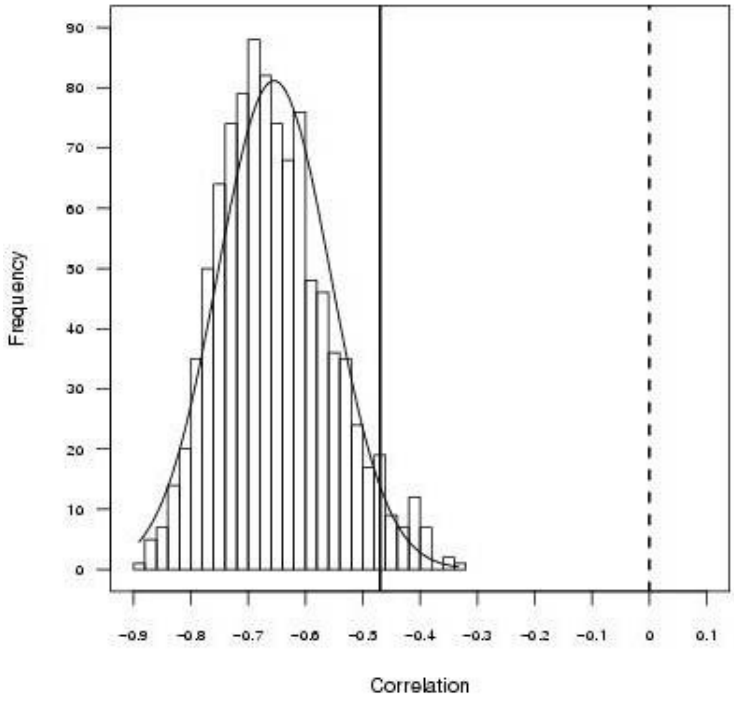


Figure 6.4: The empirical bootstrap distribution of the correlation from the 1000 realisations between the February precipitation time series with the strongest increasing trend (62.25°N 9.75°E; Norway) and the MSLP time series (70°N 7.5°W) with the highest observed correlation with precipitation. Black vertical line is the 95% percentile; dashed line is correlation $\rho$=0.

### 6.4 Correlation between MSLP and precipitation

This section presents the correlation analyses of large-scale MSLP with European precipitation. A precipitation grid in western Scotland (57.25°N 5.25°W) is used to illustrate how the correlation results are presented because of this location's closeness to the westerly flow that results in strong MSLP-precipitation relationships. Figure 6.5 shows the map of correlations in January between the precipitation time series in western Scotland and the gridded MSLP field across the domain 0°N–90°N and 90°W–90°E (i.e. half of the Northern Hemisphere). This map shows a correlation dipole with significant negative correlation (blue colour) centred over the Norwegian Sea and significant positive correlation (red colour) centred near the Azores. This dipole implies that as MSLP falls (rises) to the north

(southwest) of the British Isles, precipitation increases in western Scotland, which relates to the Icelandic Low and Azores high pressure systems respectively. Note that the continuous blue colour at high latitudes (at 90°N) occurs because there is only one MSLP value (i.e. an artefact of the cartographic projection chosen). Following the nested research design adopted, results (with correlation maps similar to Figure 6.5) are firstly presented for precipitation grid cells in the British Isles (Figure 6.6) and secondly presented for Europe (Figures 6.7 – 6.10) for selected months.

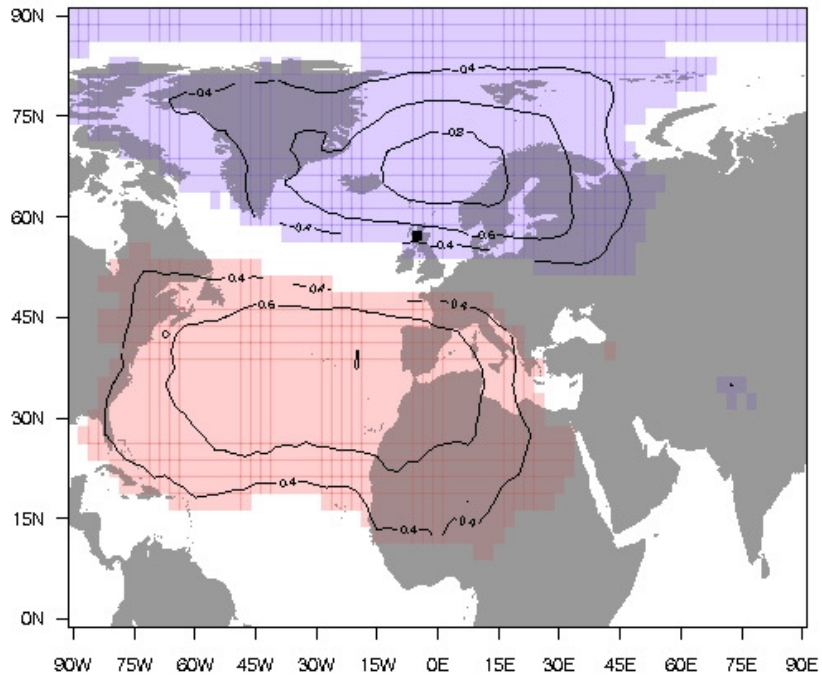


Figure 6.5: Correlation analysis of precipitation in a single grid in western Scotland (57.25°N 5.25°W; location given by black box) with MSLP across 0°N–90°N and 90°W–90°E in January (1958–2002). Red (blue) colour signifies significant positive (negative) Spearman rank correlation (*significance level* $\alpha = 0.05$).

### 6.4.1 Correlation analysis over the British Isles in January

In January across the British Isles, the location of areas with significant correlation between MSLP and precipitation vary both in size and location (coloured areas in Figure 6.6). In western Scotland, the correlation dipole has significant negative (positive) correlation across the northern (southern) part of the geographical domain (as in Figure 6.5); this relates to the Icelandic Low and Azores High pressure centres, respectively. The large areas of significant correlation between MSLP and precipitation in western British districts (including western Scottish Highlands, the Pennines and Welsh mountains) are due partly to the orographic enhancement of rainfall (Roy, 1997, Sumner, 1997, Tufnell, 1997). Notably, as distance increases from the Atlantic Ocean, the correlation dipole shrinks and areas with non-significant correlation become more prominent, probably due to the shelter from the westerly air flow by western mountain chains. Precipitation in eastern Britain has no significant positive correlation with MSLP to the southwest of the British Isles. Instead, positive correlation is seen with MSLP over central Russia, which could relate to the Siberian High pressure system (Figure 6.6). This suggests that precipitation is related to an easterly air flow on the southern edge of the Siberian High. On route to Britain, the easterly flow would be modified becoming moist due to evaporation over the North Sea, which in turn could produce precipitation in northeast England.

Figure 6.6: Correlation analysis of gridded precipitation over the British Isles with MSLP for January 1958–2002. The grey background in each grid box represents the land masses in the study domain [Key as Figure 6.5].

### 6.4.2 Correlation analysis over Europe in winter

The MSLP correlation dipole seen across the western British Isles corresponds with precipitation across northern Norway and Sweden (i.e. across the northwest European boundary with the North Atlantic Ocean; Figure 6.7). This statistically significant MSLP correlation dipole ($\rho > |0.6|$) is strongest in December, January (Figure 6.7), and February; and it implies that, from the western British Isles through to Scandinavia, precipitation occurs when MSLP is low (high) near Iceland (the Azores). This same dipole structure, although smaller in extent (especially for the positive correlation area), is also found across northern continental Europe from northern France to Finland, indicating that precipitation has a

positive relationship with the NAO-like pattern. These results show that a similar large-scale atmospheric circulation generates winter precipitation across northern and western Europe.

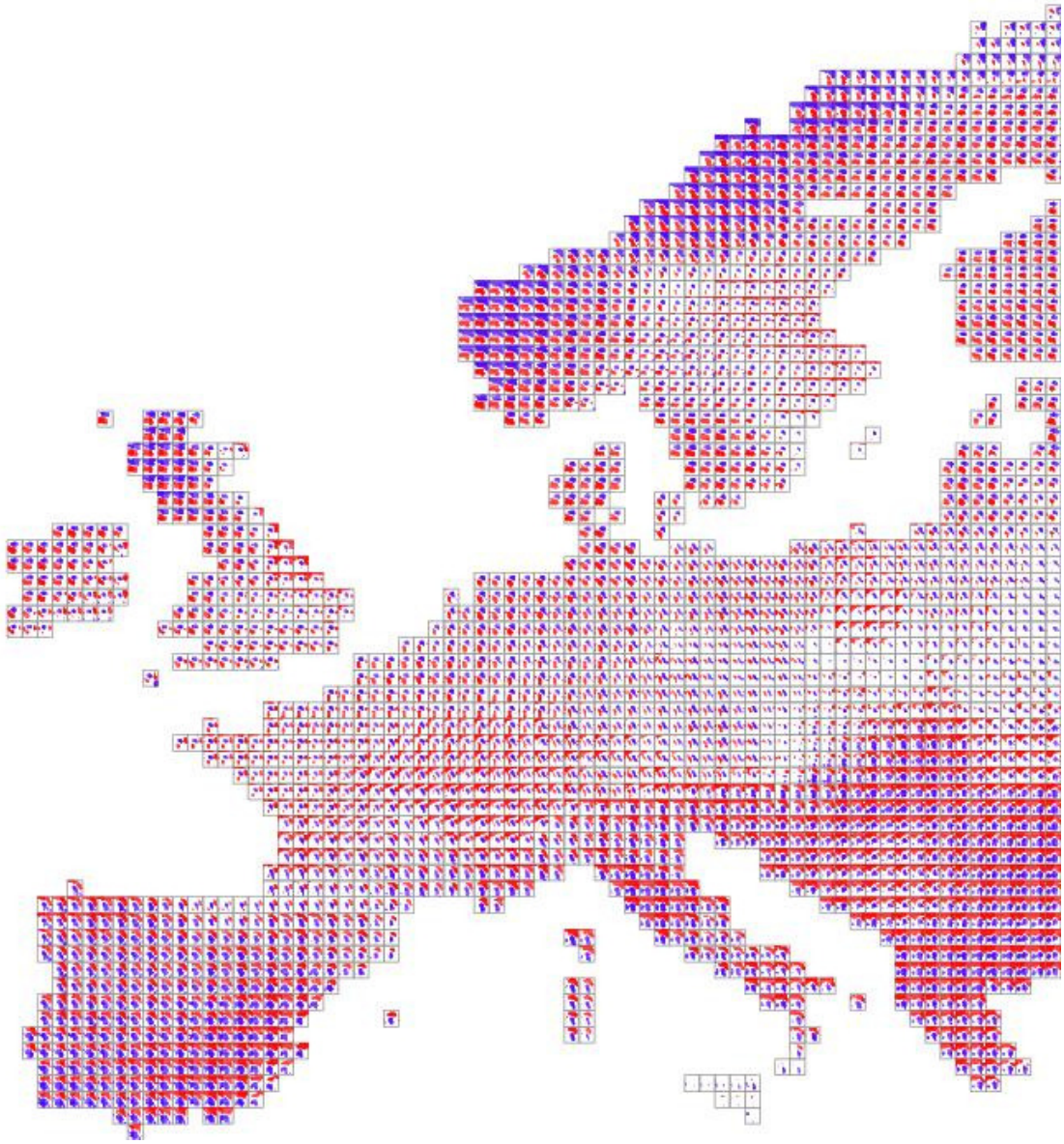

Figure 6.7: Correlation analysis of gridded European precipitation with MSLP for January 1958–2002 [Key as Figure 6.5].

From western to eastern Scandinavia, the size of significant MSLP correlation patterns show a distinct west-east gradient, with stronger and larger MSLP influence on precipitation in the west than in the east. The effect of MSLP on precipitation, as characterised by the correlation

patterns, is less in central and East Sweden than in western Norway which is likely to be due to the Scandes mountains (between Norway and Sweden) reducing the influence of moist westerly winds from the Atlantic on central Sweden (Uvo, 2003, Kingston *et al.*, 2009). In southern Finland, where there is a lesser influence of mountains on the atmospheric flow, westerly winds can penetrate further into the European continent, thus bringing precipitation (Uvo, 2003).

From central France southwards, the winter correlation dipole has a reversed pattern compared to northern Europe (as also identified by Bartolini *et al.,* 2009). From the Iberian Peninsula to the Balkans, large regions of negative and positive correlation are centred over the Azores and northern Europe, respectively (Figure 6.7). This means that as MSLP falls (rises) near the Azores (Iceland), a cyclonic circulation affects southern Europe, thus increasing precipitation. This atmospheric circulation is associated with storm tracks that are located further south than normal that would steer rain-bearing depressions into southern Europe (Marshall *et al.*, 2001). South-eastern European (Balkans) precipitation has positive MSLP correlation over Asia, which indicates a link with the Siberian High pressure system. In central and Eastern Europe downwind of the European Alps, smaller MSLP-precipitation correlation patterns occur indicating that the Alps reduce the influence of westerly winds on precipitation in this region.

### 6.4.3 Correlation analysis over Europe in spring

With the onset of spring, the pole-to-equator temperature gradient across the North Atlantic (hence, the westerly air flow) weakens. The MSLP-precipitation correlation patterns for April (Figure 6.8) show that smaller-scale atmospheric circulation patterns are linked with precipitation and the large-scale winter atmospheric patterns have broken down. However,

note that in northern Scandinavia and in the far northwest of Scotland, a North Atlantic correlation dipole still exists in April suggesting that the winter circulation patterns have a longer duration at higher latitudes.

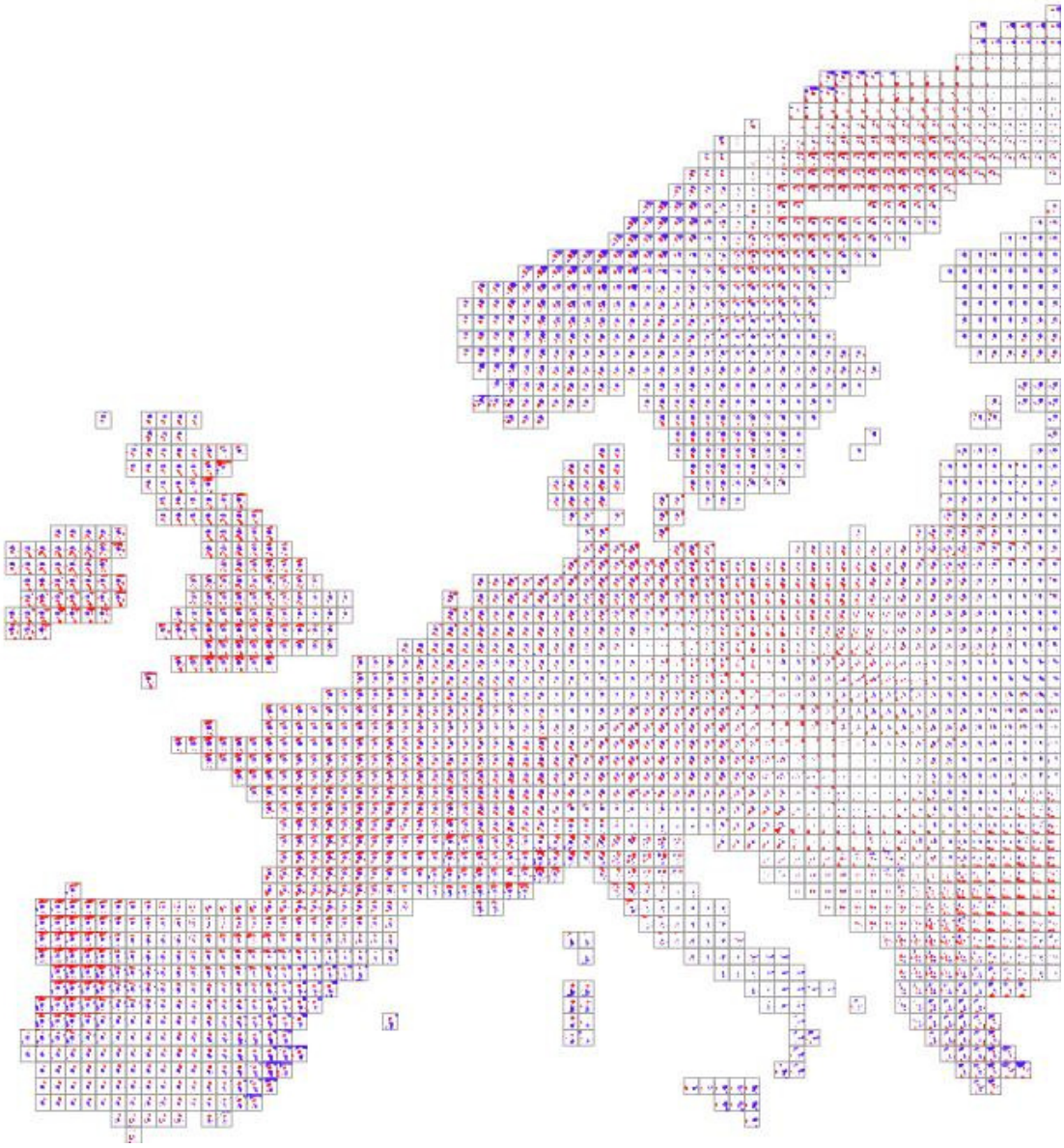

Figure 6.8: Correlation analysis of gridded European precipitation with MSLP for April 1958–2002 [Key as Figure 6.5].

### 6.4.4 Correlation analysis over Europe in summer

As summer approaches, the North Atlantic correlation dipole continues to weaken. During summer (June, July, August; JJA), northern European precipitation has no significant positive correlation over the Azores region. In general, precipitation has fewer significant correlations with the MSLP field (larger white areas in Figure 6.9 in July). During June and July, significant positive (negative) MSLP correlation over Greenland is found with northwest (southern to southeast) European precipitation. This means that as pressure falls over Greenland, pressure rises over northwest Europe resulting in precipitation decrease over northwest Europe; this is shown by the positive (red) correlation in the top-left (northwest) of many precipitation grids in Northwest Europe (Figure 6.9). For southern Europe the negative (blue) correlation areas over Greenland (northwest of each precipitation grid) highlight that as pressure falls over Greenland, pressure falls over the Mediterranean, and precipitation increases over Southeast Europe. Zveryaev (2004) identified summer relationships between precipitation and patterns of high pressure over northwest Europe and low pressure over Greenland and the Mediterranean; this was described as the SNAO. The centres of correlation of MSLP and precipitation shown herein coincide with those of Zveryaev (2004).

The smaller extent of the significant MSLP correlation patterns in summer compared to winter suggests that the large-scale climatic circulation has a lesser influence on summer precipitation. This may be related to the prevalence of convective precipitation events in summer (Berg *et al.,* 2009) that correspond to smaller scale weather systems. Zveryaev and Allan (2010) suggest local processes play a dominant role in summer precipitation occurrence because of an uncovered significant statistical linkage between European precipitation and European land surface evaporation. In our analysis herein, although the temporal (monthly) and spatial (2.5°×2.5°) resolution of the MSLP fields are too coarse to

resolve convective activity, the small size of correlation patterns identified with European precipitation in summer is a sign of smaller scale atmospheric dynamics in operation.

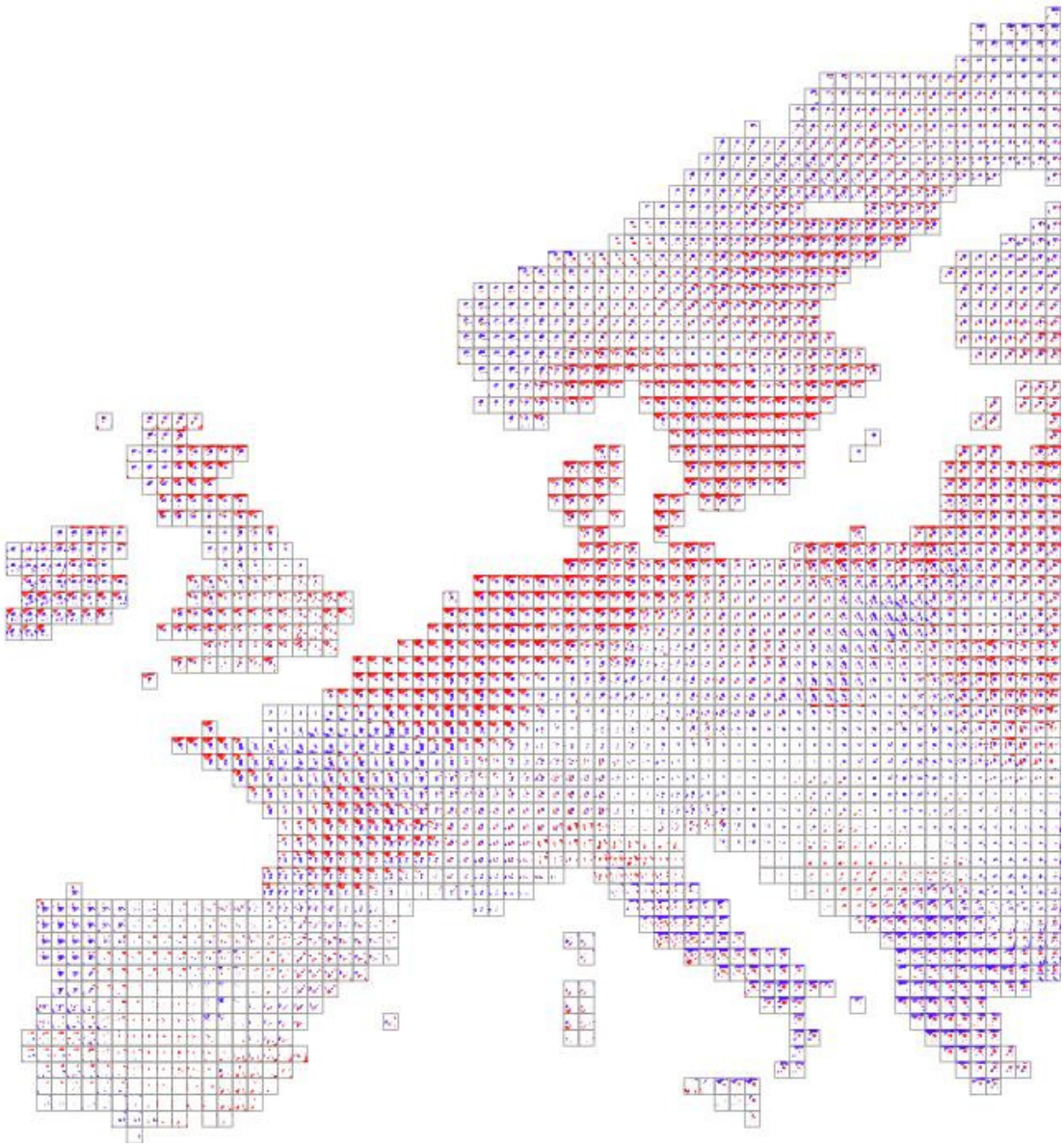

Figure 6.9: Correlation analysis of gridded European precipitation with MSLP for July 1958–2002 [Key as Figure 6.5].

### 6.4.5 Correlation analysis over Europe in autumn

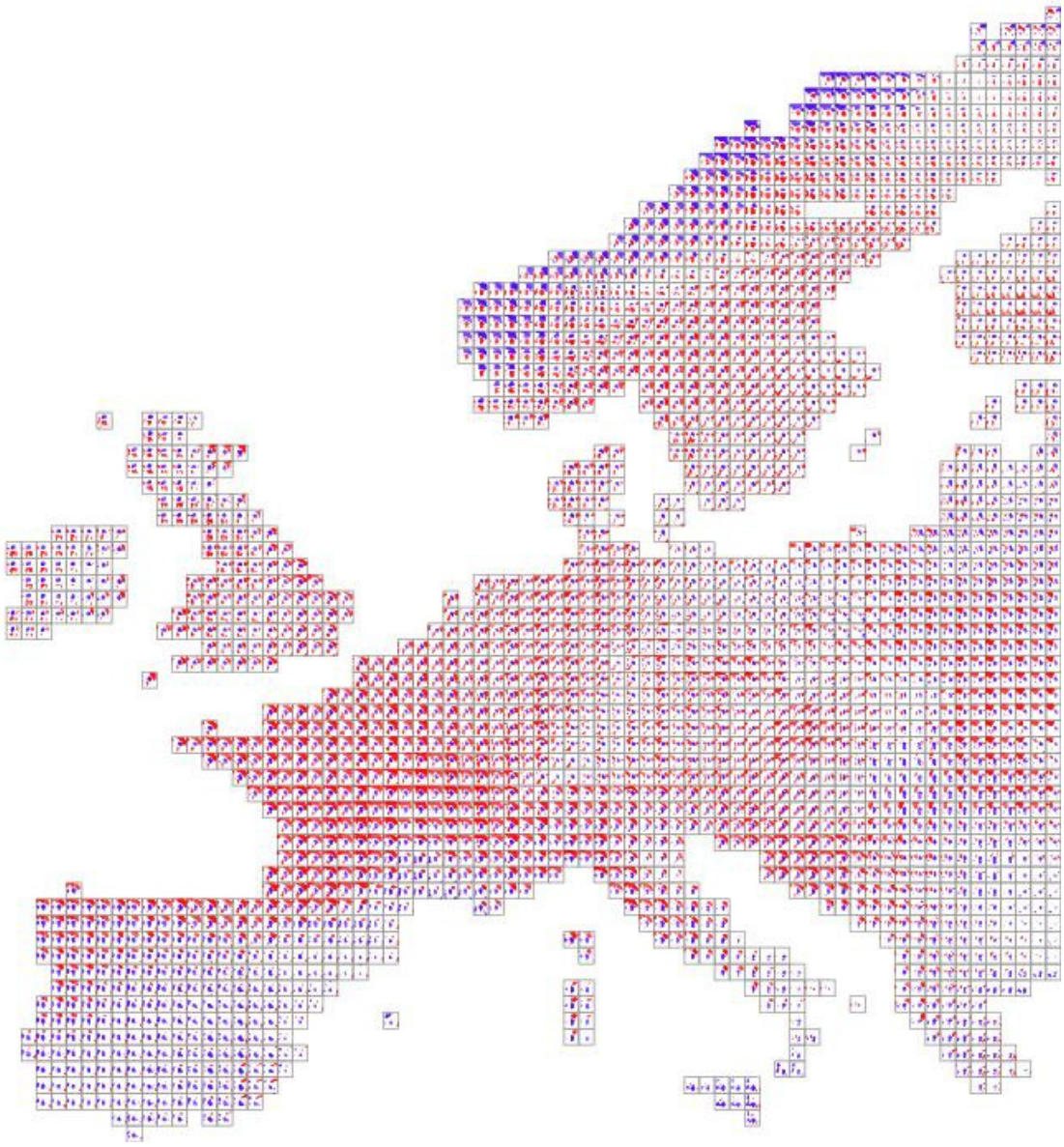

Figure 6.10: Correlation analysis of gridded European precipitation with MSLP for October 1957–2001 [Key as Figure 6.5].

During autumn, the North Atlantic correlation dipole pattern begins to reappear in September in northern Europe; this is visible in October (Figure 6.10) across western British Isles and Scandinavia. Note that over Scandinavia, the MSLP-precipitation correlation patterns have a more easterly location compared to the western British Isles, which suggests a linkage with the Scandinavian climate pattern (Barnston and Livezey, 1987); the Scandinavian pattern is

discussed further in section 6.5. The re-formation of the large-scale North Atlantic atmospheric patterns is not found until December in the southern British Isles and northern France (not shown) suggesting that the winter circulation pattern is in place earlier further north where the winter season is longer.

### 6.5 Correlation between NAOI and precipitation

The maximum and minimum gridded MSLP-precipitation correlations were compared to the NAOI-precipitation correlations for six selected precipitation time series (as in Figures 6.1 and 6.2). Since the NAOI has been used widely as a measure of the strength of the North Atlantic influence on European climate (as reviewed in sections 2.4 and 6.1), our comparative analysis herein serves to benchmark the gridded MSLP-precipitation correlations. For all six locations, precipitation has stronger correlations with the MSLP than with the NAOI, regardless of season (Table 6.1 for January; Table 6.2 for July). This suggests that the NAOI is unable to explain precipitation occurrence as well as MSLP because the centres of strong MSLP correlation do not always coincide with the fixed Azores-Iceland locations defining the NAOI. In January (Table 6.1) northern (southern) European precipitation has a positive (negative) relationship with the NAOI, as shown by the time series plots in Figure 6.1 and as also found by Hurrell (1995). Further east (central France and Czech Republic) the NAOI has lower correlation with precipitation reflecting: (a) a reduced oceanic influence on precipitation and (b) the areas of climatic control on precipitation are not co-located with the NAOI definition. In July, only western Scotland and central France have significant NAOI-precipitation correlations (Table 6.2), possibly reflecting strong maritime influence on western Scottish precipitation due to its close

proximity to the Atlantic Ocean, and French precipitation being influenced by the SNAO pattern (Figure 6.9).

Table 6.1: Spearman rank correlation for the January time series (1958–2002; n=45) of the six precipitation grids of Figure 6.1. Maximum and minimum correlation with the MSLP field and correlation with the NAOI are shown. Correlation at the *significance level* $\alpha = 0.05$ is in bold font.

| Region | Grid | NAOI | Max. MSLP | Min. MSLP |
|---|---|---|---|---|
| western Scotland | 57.25°N 5.25°W | **0.784** | **0.801** | **-0.883** |
| Norway | 65.25°N 13.75°E | **0.505** | **0.806** | **-0.794** |
| southern Spain | 37.75°N 3.75°W | **-0.758** | **0.740** | **-0.902** |
| central France | 47.25°N 3.25°E | 0.042 | **0.566** | **-0.708** |
| Czech Republic | 49.75°N 15.25°E | 0.169 | **0.538** | **-0.630** |
| Balkans | 42.75°N 20.25°E | **-0.351** | **0.627** | **-0.842** |

Table 6.2: Spearman rank correlation for the July time series (1958–2002; n=45) of the six precipitation grids of Figure 6.2 [Key as Table 6.1].

| Region | Grid | NAOI | Max. MSLP | Min. MSLP |
|---|---|---|---|---|
| western Scotland | 57.25°N 5.25°W | **0.429** | **0.413** | **-0.781** |
| Norway | 65.25°N 13.75°E | 0.209 | **0.438** | **-0.680** |
| southern Spain | 37.75°N 3.75°W | 0.277 | **0.432** | -0.287 |
| central France | 47.25°N 3.25°E | **-0.538** | **0.414** | **-0.595** |
| Czech Republic | 49.75°N 15.25°E | -0.102 | **0.653** | **-0.700** |
| Balkans | 42.75°N 20.25°E | -0.023 | **0.477** | **-0.529** |

Other climatic patterns that are characterised by simple indices may also be related to European precipitation. In particular, evidence of the Scandinavian pattern (Barnston and Livezey, 1987) can be found in the MSLP-precipitation correlation maps. A positive phase of

the Scandinavian pattern has an anticyclone over Scandinavia and weaker cyclonic regions over Western Europe and eastern Russia, which results in lower (higher) precipitation totals over Scandinavia (central Europe). For example, precipitation over eastern France in October (Figure 6.10) shows a positive relationship with the Scandinavian pattern with positive (negative) correlations over Scandinavia (Western Europe). In this analysis, however, only the NAOI was used to show that gridded MSLP fields yield stronger statistical relationships with precipitation than this dominant atmospheric mode's index.

## 6.6 Conclusions

This chapter has assessed spatiotemporal variability of European precipitation by quantifying the seasonal and temporal movement of links between large-scale mean sea-level pressure (MSLP) and European precipitation. Correlation analysis between gridded MSLP and precipitation highlighted significant hydroclimatological relationships that improved understanding of precipitation generating mechanisms in Europe, particularly with respect to large-scale atmospheric circulation.

Throughout the year, precipitation is associated with MSLP centres of action located over different areas of the Northern Hemisphere, with the winter yielding generally larger regions of significant correlation than the summer. In winter, precipitation shows links with extensive atmospheric areas reflecting the strong influence of the large-scale atmospheric circulation on European precipitation (especially in the west). In northern (southern) Europe, positive (negative) correlation exists over the Azores and negative (positive) correlation exists near Iceland, implying a positive (negative) relationship with the NAO, as identified by Hurrell (1995). These correlation centres relate to the Azores High and Icelandic Low pressure systems. Over northern Europe, precipitation increases when there is a strong pressure

gradient between the Azores and Iceland, which strengthens the westerly flow (Bouwer *et al.*, 2006). Conversely when a retrograde (easterly) flow occurs, or when the pressure gradient between these two meridional pressure centres is slack, storm tracks have a more southerly trajectory and precipitation increases over southern Europe. The large spatial scale of significant atmospheric patterns over Northwest Britain and Scandinavia is thought to be caused in part by orographic effects on precipitation.

In summer, European precipitation has fewer significant correlations with the large-scale climatic circulation, implying that precipitation is produced by local scale and shorter duration weather systems. As this study used a coarse temporal (monthly) and spatial (2.5°×2.5°) resolution of MSLP, convective systems that are a source of summer European precipitation (Berg *et al.*, 2009) would not have been well captured. The summer MSLP correlation patterns show relationships with the SNAO, a variant of the well-established NAO. A positive phase of the SNAO, relates to lower (higher) precipitation totals over northwest (southern) Europe. In spring and autumn, smaller MSLP patterns are associated with precipitation. Notably, patterns in MSLP reveal an extended winter season in the far north of Europe (e.g. Scandinavia). Also, evidence of the Scandinavian climate pattern is found in the MSLP-precipitation correlation maps over Scandinavia and central Europe.

The gridded MSLP data yield stronger empirical relationships compared to the NAOI because the MSLP can capture the dynamic seasonal movement of the atmospheric areas with strongest control on European precipitation. The fixed-points used in the NAOI definition do not always coincide with the high MSLP-precipitation correlation areas; therefore, the NAOI is a less powerful explanatory variable of precipitation. Although atmospheric indices are useful as a starting point in investigating large-scale climatic control on European precipitation variability, the results herein suggest that finer scale (i.e. gridded)

data yield stronger statistical relationships and improved understanding of this important socially relevant hydroclimatological process.

There is a gradient in the influence of North Atlantic pressure systems over Europe, as shown by larger MSLP-precipitation correlation areas in western districts compared to eastern districts (i.e. from west-to-east Britain, across the European Alps and from Norway to central and East Sweden). This reflects the heterogeneities of the European land mass, in particular the barrier effect of mountain chains such as the Scandes or Alps, which limit penetration of eastward rain-bearing systems resulting in smaller precipitation totals in their lee (i.e. rain shadow) and weaker MSLP-precipitation correlation patterns. As the large-scale atmospheric dynamics are most active in the winter season, this phenomenon is most notable in the winter months.

The availability of gridded precipitation and MSLP has made it possible to undertake, for the first time, a consistent spatiotemporal analysis of the large-scale climatic control on European precipitation. The results presented herein corroborate previous research that considered atmospheric indices (e.g. Hurrell, 1995), but our findings demonstrated that an index with fixed-point definition, such as the NAOI, is not subtle enough to explain precipitation occurrence in certain regions (i.e. central Europe, such as the Czech Republic; Tables 6.1 and 6.2) and seasons (i.e. summer). The strong significant statistical relationships between the large-scale MSLP and precipitation in some areas of Europe and in certain seasons have demonstrated that precipitation variability is not random, but results from variations in the large-scale atmospheric circulation. This suggests that despite high precipitation variability in Europe, there is a certain degree of predictability of precipitation because of its relationship with MSLP, in particular in winter for Western European coastal regions. The identified hydroclimatological relationships could be used to evaluate climate model output to

determine if the location, strength and timing of these hydroclimatological connections can be reproduced faithfully by models. If climate models become capable of reproducing the hydroclimatological correlation patterns, then a portion of European precipitation predictability could be realised yielding scientific and societal benefits.

### 6.7 Chapter summary

This research has shown that there is spatial and temporal variability of the relationships between large-scale MSLP and precipitation across Europe. The fixed-point NAOI is not as powerful in explaining the spatiotemporal hydroclimatological variability in Europe, but note that the NAOI in winter was able to capture precipitation occurrence in European regions closest to the North Atlantic Ocean. Chapter 7 partly assesses seasonal climate model predictive skill of MSLP to determine whether the uncovered significant statistical relationships in this chapter (and in Chapter 5) could be used with seasonal climate model output for monthly or seasonal precipitation predictions.

# 7. ASSESSMENT OF SEASONAL CLIMATE MODEL PREDICTIVE SKILL FOR APPLICATIONS

Chapter Objective: to assess the predictive skill in the CFS and DEMETER seasonal climate models to determine their usefulness for applications.

## 7.1 Introduction

Seasonal climate prediction is based on the premise that the lower-boundary SST forcing, which evolves slowly, imparts predictability on atmospheric development (Palmer and Anderson, 1994). In particular persistent SST anomalies associated with ENSO influence atmospheric circulation, thus producing seasonal climate anomalies (Carson, 1998, Stockdale *et al.*, 2006). Operational climate forecast centres such as the ECMWF and the National Oceanic and Atmospheric Administration's (NOAA) NCEP are now using coupled atmosphere-land-ocean models to produce their seasonal forecasts (Palmer *et al.*, 2004, Saha *et al.*, 2006). Integrating coupled atmosphere-land-ocean models with an ensemble of different initial conditions allows predictions that consider uncertainty in the initial state, resulting in what is referred to as an ensemble forecast. Seasonal climate forecasts can be incorporated into end-user application models for determining crop yield amounts (Cantelaube and Terres, 2005, Challinor *et al.*, 2005) and future epidemic malaria (Thomson *et al.*, 2006). Retrospective forecast (hindcast) datasets, such as those from the DEMETER project, give the opportunity to assess the predictive skill in current seasonal climate forecast models.

Forecast quality in its complete sense can be assessed using a distributions-oriented framework (Murphy, 1993). This approach uses the joint distribution of the forecasts $(f)$ and observations $(o)$ as this contains all of the non-time dependent information necessary for

evaluating the forecast quality (Murphy and Winkler, 1987, Murphy, 1993). For applications, one must determine the following: given a particular seasonal climate forecast, what is the conditional probability distribution of (future) seasonal climate $p(o \mid f)$. The extent to which the conditional seasonal distribution $p(o \mid f)$ varies from the climatological distribution $p(o)$ is an indication of the skill of the forecast. *Murphy and Winkler* (1987) refer to the factorization of the joint distribution into the conditional $p(o \mid f)$ and marginal $p(f)$ distributions as the 'calibration-refinement factorization'. Furthermore, this can also be done within a Bayesian framework that will spatially downscale and bias correct the seasonal climate forecasts, making them relevant for applications (Luo *et al.*, 2007).

The predictability of 2-metre air temperature (hereafter, temperature), precipitation and MSLP is a multidimensional variable that can vary with geographical location (x, y), lead-time (τ), season (t) and with temporal (T) and spatial (L) scales. A thorough literature review of seasonal climate forecast quality assessment suggests a paucity of published papers on evaluation of monthly predictions, a fact also noted by (Weigel *et al.*, 2008). To address this gap, this chapter assesses 1) the actual or realisable predictability of monthly temperature, precipitation and MSLP hindcasts, and 2) the idealised predictability of monthly temperature and precipitation hindcasts from the NCEP CFS (Saha *et al.*, 2006) and seven models from the DEMETER project (Palmer *et al.*, 2004). The analysis shows the current predictive capability in the "actual" and "model" climate systems.

## 7.2 Data and Methodology

DEMETER is a European Union (EU) funded project that created a multi-model ensemble hindcast dataset containing seven models each with nine ensemble members. The models are

from climate centres around Europe and their acronyms are: CERFACS, ECMWF, INGV, LODYC, METEO-FRANCE, MPI, and UKMO. The DEMETER models were initialised on 1st February, 1st May, 1st August and 1st November to assess the seasonal dependence of the hindcasts, and integrated for 180 days (Palmer *et al.*, 2004). For the period being studied, CFS has 15 nine-month hindcasts initialised during each calendar month (Saha *et al.*, 2006). The common period for the DEMETER and CFS models is 1981–2001 (21 years).

Temperature and MSLP at a 2.5° × 2.5° resolution from the ERA-40 re-analysis dataset (Uppala *et al.*, 2005) and monthly observed precipitation at 1.0° × 1.0° from the GPCC (Rudolf *et al.,* 2005) are used as the reference datasets. Precipitation was regridded to 2.5° resolution to match the model hindcasts' resolution.

The joint probability distribution is computed between the model ensemble mean and observations using the operational hindcasts and observed climate outcomes. This joint distribution can be represented by a bivariate-Normal distribution (Wilks, 2006). The conditional mean, $m(o \mid f)$, and variance, $\sigma^2(o \mid f)$, of $p(o \mid f)$ is $m(o \mid f) = m(o) + r\sigma(o)\frac{[f - m(f)]}{\sigma(f)}$ and $\sigma^2(o \mid f) = \sigma^2(o)(1 - r^2)$, where $m(o)$, $m(f)$, $\sigma(o)$ and $\sigma(f)$ are the means and standard deviations of the marginal distributions of $p(o)$ and $p(f)$ respectively, $\sigma^2(o)$ is the variance of the marginal distribution of $p(o)$ and $r$ is the correlation between the forecast and resulting observation. Note that the conditional explained variance due to the forecast is reduced from the unconditional variance (climatology) in the climate variable by $r^2\sigma^2(o)$, which provides a measure of the information content from the seasonal forecast. A variety of skill scores could be used (Wilks, 2006), but the product-moment correlation coefficient $r$ is applied between the observed climate and forecast ensemble mean series at a particular lead time and temporal

average as it is central in determining the usefulness of seasonal forecasts for applications. Correlation represents a traditional summary measure between the forecasts and observations (Murphy *et al.*, 1989), and has been widely used in previous research (Davies *et al.*, 1997, Colman and Davey, 1999, Peng *et al.*, 2000, Folland *et al.*, 2001, Van Oldenborgh *et al.*, 2005, Wu *et al.*, 2009). The methodology is applied for each model separately and for an equally-weighted (averaged) multi-model using all members from the eight models (Hagedorn *et al.*, 2005).

The idealised predictability of a forecasting model is thought to be the upper limit of its predictive capability, where the forecast model and "climate" system have the same physics; that of the forecast model (Koster *et al.*, 2004). This model estimate considers the spread (variance) of the ensemble members, which can be thought of as indicative of the predictive skill. If an ensemble has small (large) spread, then the forecast is likely to be insensitive (sensitive) to initial condition uncertainty, resulting in high (low) predictive skill (Koster *et al.*, 2004, Tang *et al.*, 2008). The methodology used is done for each DEMETER and CFS model (temperature and precipitation only), and assumes that one member of the ensemble is the "truth" and that the remaining ensemble average is the "predictor". As before, $r$ measures the linear association between the observed and predictor series. For DEMETER (CFS) this procedure is repeated nine (fifteen) times with each ensemble member in turn being considered as the truth. The nine (fifteen) values of $r$ are averaged, which forms the final estimate of the system in predicting itself (Koster *et al.*, 2004).

## 7.3 Results

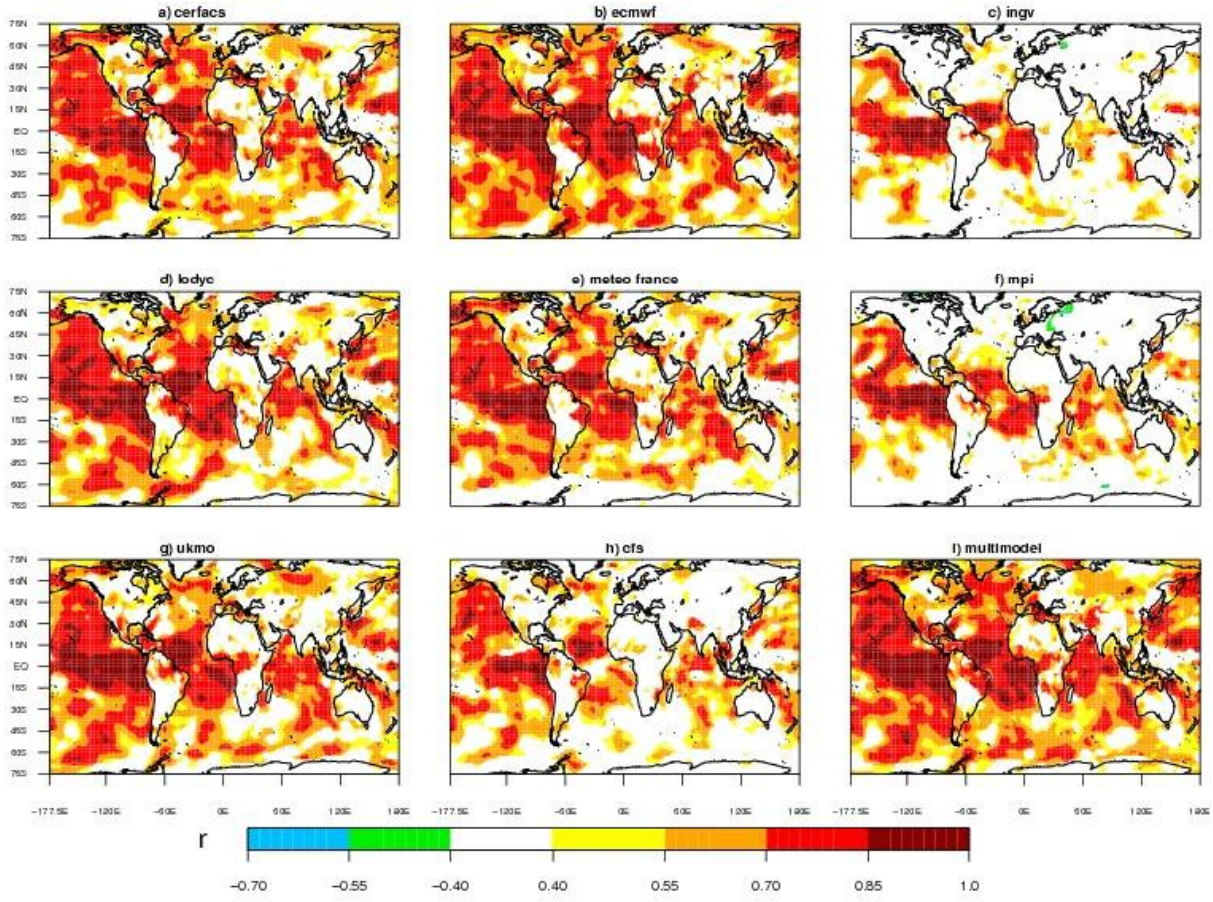


Figure 7.1: Actual predictive skill for each model grid point for 1981–2001 for a 30 day temporal average at a 1 day lead time for May two metre temperature forecasts for a) CERFACS, b) ECMWF, c) INGV, d) LODYC, e) METEO FRANCE, f) MPI, g) UKMO, h) CFS, and i) the MULTI-MODEL. Non-white colours represent significant correlation *r* at the $p < 0.05$ level.

The global actual predictive skill of temperature, precipitation and MSLP for the eight models was calculated at the model grid scale; note that precipitation was only evaluated over the land masses. Figure 7.1 shows the realisable predictive skill of temperature for the eight models and multi-model for the first 30 day period (i.e. a 30 day temporal average at a 1 day lead time, or month-1) from 1$^{st}$ May. High predictive skill of $r>0.70$ is generally confined to the oceans, especially over the equatorial Pacific and subtropical Atlantic. Skilful forecasts

over the equatorial Pacific in the ECMWF (Figure 7.1b) and UKMO (Figure 7.1g) models appear to be largely behind the multi-model skill (Figure 7.1i) in that region. Few models have noteworthy skill over land regions for the first 30 day forecast period.

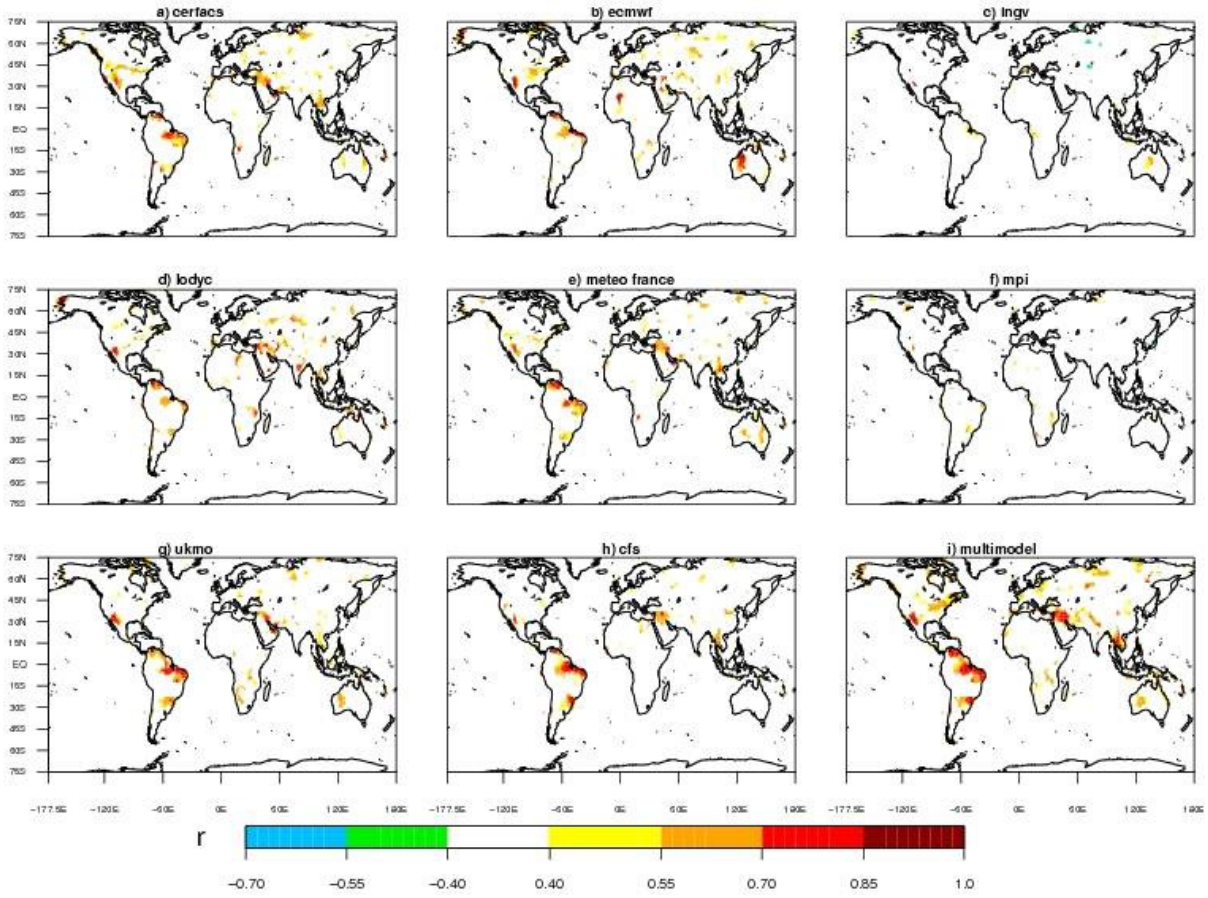


Figure 7.2: Actual predictive skill for each model grid point for 1981–2001 for a 30 day temporal average at a 1 day lead time for May precipitation forecasts for a) CERFACS, b) ECMWF, c) INGV, d) LODYC, e) METEO FRANCE, f) MPI, g) UKMO, h) CFS, and i) the MULTIMODEL [Key as Figure 7.1].

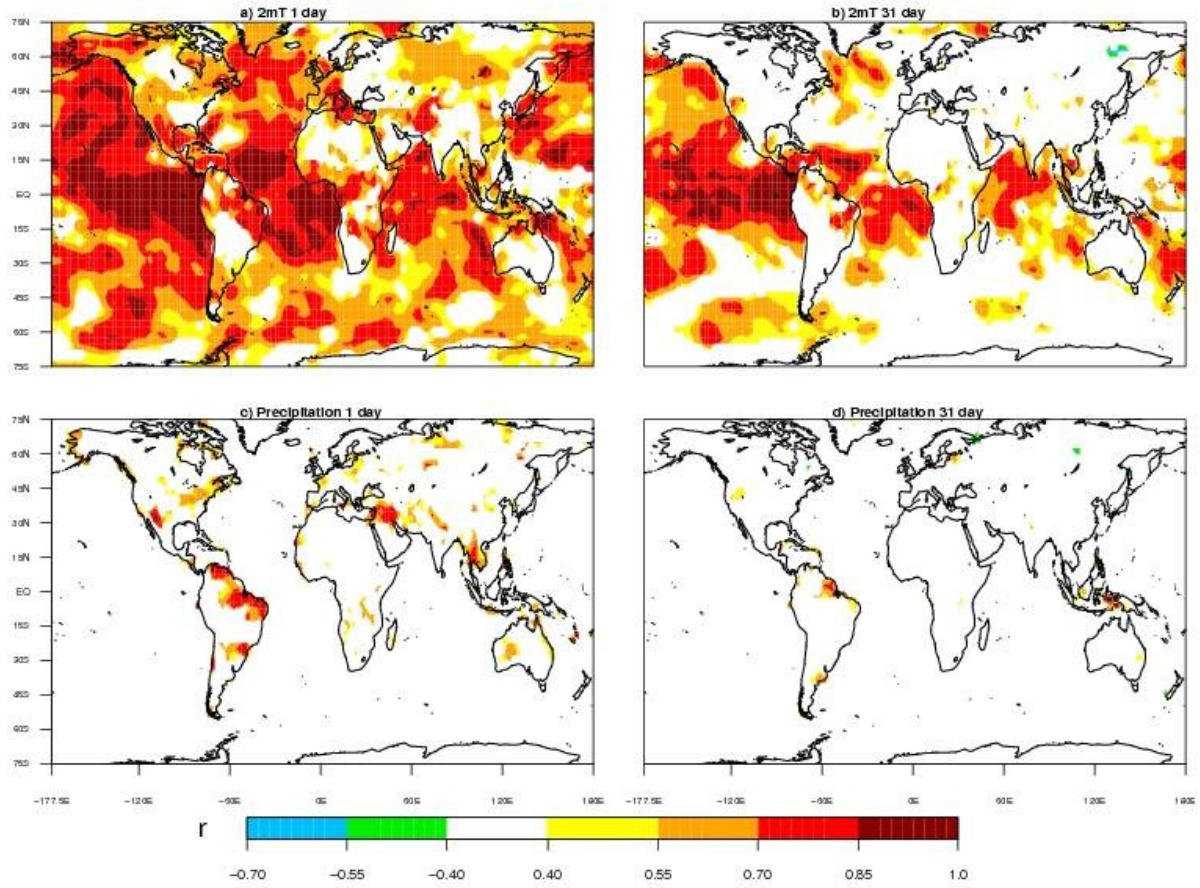


Figure 7.3: Multi-model forecasts for 1981–2001 for a 30 day temporal average at a 1 day lead time for May a) two metre temperature and c) precipitation. Multi-model forecasts for a 30 day temporal average at a 31 day lead time for May b) two metre temperature and d) precipitation [Key as Figure 7.1].

Figure 7.2 shows the realisable predictive skill of precipitation for month-1 from 1st May. Strikingly, there are very few grids with $r$>0.40 (non-white areas), and there are fewer significant correlations over the land masses compared with temperature. Six out of eight models have significant skill over the Amazon basin, and all models have skill in the North American monsoon region. These two areas are also seen in the multi-model forecast. Figure 7.3 shows multi-model predictive skill of temperature and precipitation for month-1 and month-2 (second 30 day period) of May hindcasts. For month-1, high predictive skill of temperature over land ($r$>0.70) is found over the Amazon basin, Congo basin, south-central

Asia, central Europe and north-western and south-western North America. As lead time increases to 31 days (month-2 forecast), it is apparent that skilful temperature forecasts reduce back to the tropics (Figure 7.3b) and little skill exists for precipitation (Figure 7.3d). The multi-model tends to improve the predictive skill over the individual models. In general the land masses have negligible skill at a 31 day lead time, which is a relatively short lead time in terms of seasonal climate forecasting.

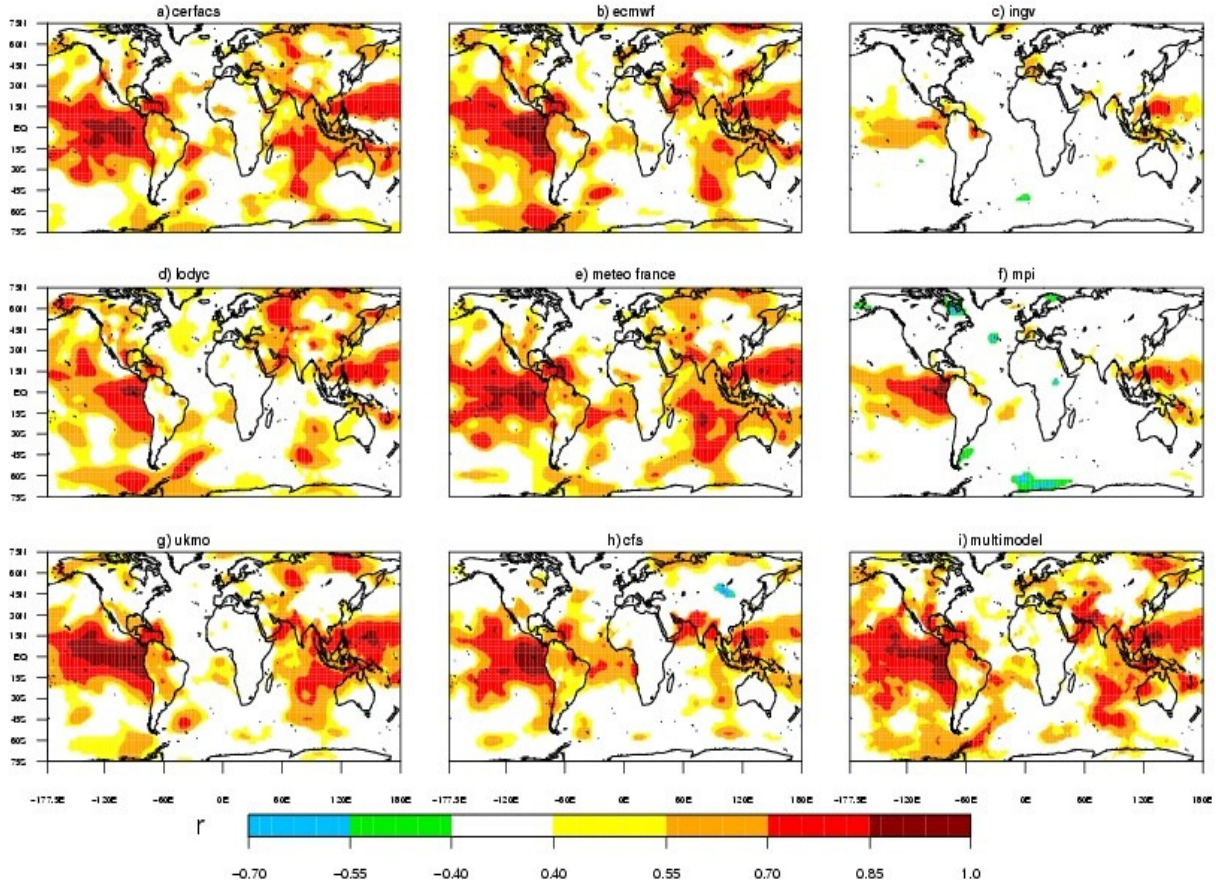


Figure 7.4: Actual predictive skill for each model grid point for 1981–2001 for a 30 day temporal average at a 1 day lead time for May MSLP forecasts for a) CERFACS, b) ECMWF, c) INGV, d) LODYC, e) METEO FRANCE, f) MPI, g) UKMO, h) CFS, and i) the MULTIMODEL [Key as Figure 7.1].

Figure 7.4 shows the realisable predictive skill of MSLP for month-1 from 1st May. Similar to temperature, high predictive skill of $r>0.70$ is predominantly confined to the oceans, especially over the tropical Pacific and in particular in the region synonymous with El Niño (eastern Pacific). A sector of high MSLP predictive skill is found over Russia in some models (e.g. ECMWF; Figure 7.4b), but in general little skill is seen over land regions for the first 30 day forecast period. As forecast lead time increases, the skilful MSLP forecasts shrink back to the tropics further indicating that the large-scale circulation as characterised by the MSLP has limited monthly predictive skill in current seasonal climate models.

Figure 7.5 shows the global grid scale idealised predictive skill for May temperature hindcasts for the first 30 day period. Idealised predictive skill in the DEMETER models is higher than that seen for the real climate system. This is true for the land masses and oceans and is particularly noticeable for the models shown in the left panels of Figure 7.5. Low idealised skill in the extratropical regions in the CFS model could be due to the ensemble initialisation, which produces members staggered throughout the month leading to members of varying ages. However, even with an ensemble of differing "initial" values, the members seem to forecast a similar climate state in the equatorial Pacific, which corroborates previous research by Shukla (1998). Idealised predictive skill of May precipitation for month-1 (not shown) exhibits much less idealised predictive skill than for temperature. As the lead time increases only a narrow region of the equatorial Pacific has idealised skill (not shown). This significant decrease in idealised predictive skill, more so for precipitation than temperature, demonstrates yet again the chaotic nature of climate (Lorenz, 1963) and the possible futility of long-lead seasonal climate forecasting.

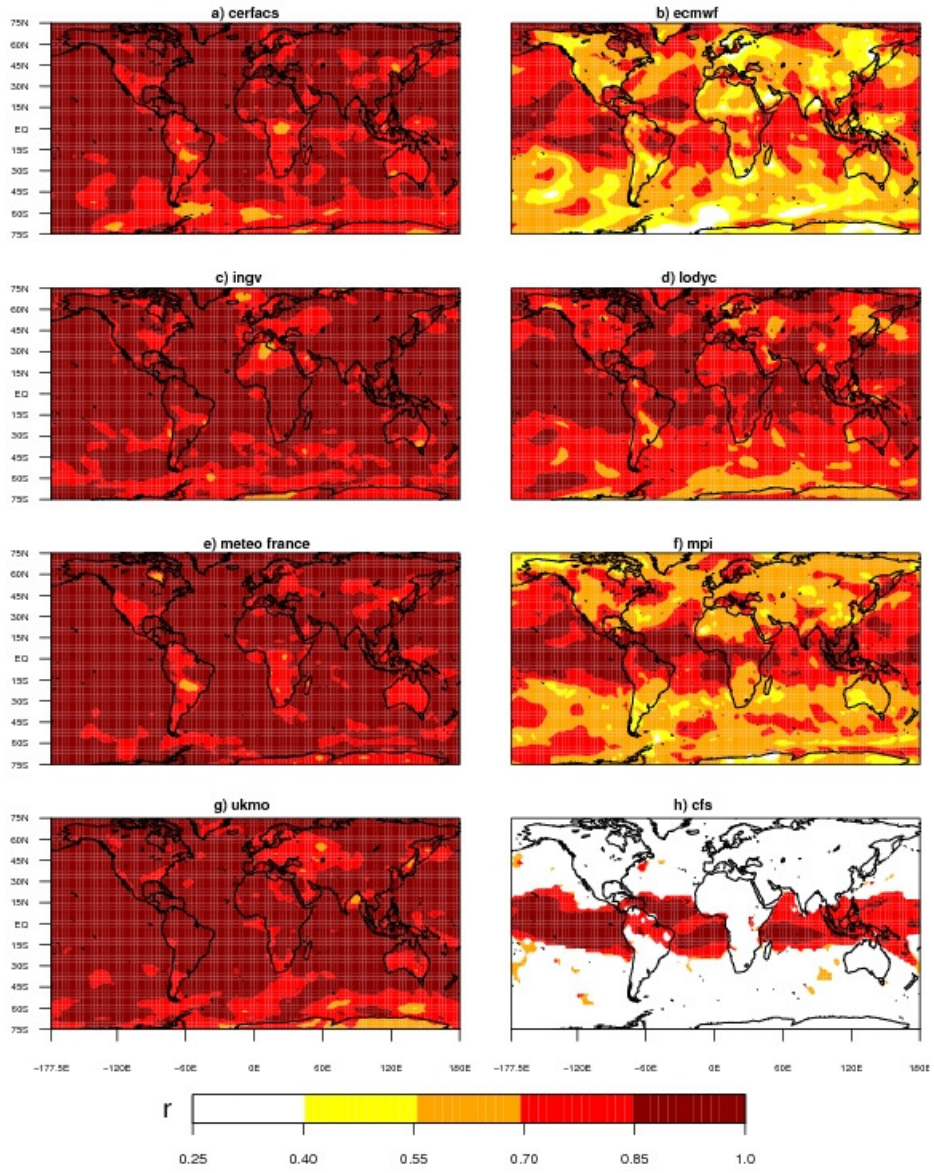


Figure 7.5: Idealised predictive skill for each model grid point for 1981–2001 for a 30 day temporal average at a 1 day lead time for May two metre temperature forecasts for a) CERFACS, b) ECMWF, c) INGV, d) LODYC, e) METEO FRANCE, f) MPI, g) UKMO, and h) CFS.

It appears that the high idealised predictive skill evident during month-1 is attributable to the skill present in the first two weeks of the forecast when the spread of ensemble members is small. This is confirmed by calculating the idealised skill on the first and second 15 day averages, which shows a large drop off in predictive skill in the second of these 15 day periods.

### 7.4 Discussion and Summary

This work has shown that limited realisable predictive skill of temperature, precipitation and MSLP is found in the DEMETER and CFS seasonal climate forecasting models. Globally for 30 day temporal averages the skill deteriorates with lead time becoming primarily located over the equatorial regions, in particular the eastern Pacific. In other words, these results suggest that the equatorial regions are predominately where a change can be detected in the conditional distribution of the observations given a seasonal forecast. Generally, only during the first month of the forecasts can a change in conditional distribution of the observations be seen over the land masses. Previous research concurs with the findings here showing higher predictive skill in the tropics (Peng *et al.*, 2000, Phelps *et al.*, 2004, Kumar *et al.*, 2007, Weigel *et al.*, 2008). Results also highlight that predictive skill in the idealised world is higher than in the real world, especially for the first month but degrades significantly after about 30 days. The idealised predictability estimates vary between the models (Figure 7.5) and depending on the noise inherent in the climate model system, the potential improvement in realisable seasonal climate predictability will also vary. However, if areas with higher idealised predictability (compared to realisable predictability) of temperature in the first month (cf. Figures 7.1 and 7.5) could be translated to the real climate system, then improved month-1 climate forecasts could be attained. This realisation of predictive skill would have benefits for decision making based on these forecasts.

Attempts are being made by the Global Land-Atmosphere Coupling Experiment (GLACE2; Koster *et al.* (2010)) to assess whether sub-seasonal predictive skill can be improved by having a more accurately initialised land surface. The Global Energy and Water Cycle Experiment (GEWEX; Sorooshian *et al.* (2005)) and the Hydrologic Ensemble Prediction Experiment (HEPEX; Schaake *et al.* (2007)) also aim to improve seasonal prediction

practices. There is potential in using a multi-model approach (Krishnamurti *et al.*, 2006), but the ideal way to combine the models is unresolved (Kirtman and Pirani, 2009). Given the actual skill demonstrated by operational seasonal climate forecasting models, it appears that only through significant model improvements can useful long-lead forecasts be provided that would be useful for decision makers – a quest that may prove to be elusive.

### 7.5 Chapter summary

This work has shown that skilful seasonal climate model forecasts are currently only available for the tropical regions with temperature and MSLP having higher predictive skill than precipitation. It is not advisable to use the predictions from these models for decision making in the extratropical regions near Great Britain. Also, due to the limited predictive skill of the large-scale atmospheric circulation (MSLP), it is not presently possible to use these climate forecasts with the uncovered statistical hydroclimatological relationships (Chapters 5 and 6) for "perfect prognosis" precipitation/discharge forecasting.

The low seasonal climate model predictive skill of precipitation highlights why River Dyfi discharge predictions driven by DEMETER models' precipitation were so poor (Chapter 4). Even though the research in Chapter 5 showed that more appropriate geographical areas could have been used for the River Dyfi precipitation downscaling in Chapter 4, the low MSLP predictive skill (a proxy for large-scale atmospheric circulation; similar to the geopotential at 500 hPa) also helps to explain why the downscaling did not yield river flow forecasts with greater skill than the historical river flow observations.

# 8. CONCLUSIONS AND FUTURE WORK

## 8.1 Introduction

Chapter 1 introduced the subject area and provided a rationale to undertake the work. A literature review that identified the research gaps for investigation was presented in Chapter 2. In light of the recognised knowledge gaps, the overarching *aim* of this thesis was to evaluate the potential for seasonal hydrological prediction in Great Britain. The data required and an overview of the statistical methods needed to fulfil the aim were described in Chapter 3. The specific objectives of the thesis (sections 1.2 and 2.6) were:

1) To undertake river flow prediction in Great Britain using a rainfall-runoff model and GCM output to in turn evaluate the current weaknesses of this approach. The evaluation of this physically realistic modelling system was the subject of Chapter 4.

2) To identify and quantify the spatiotemporal variability in hydroclimatological relationships across Great Britain and Europe. These were the topics of Chapters 5 and 6 respectively.

3) To assess at the global scale the current level of seasonal climate model predictive skill (specifically 2-metre temperature, precipitation and MSLP) for potential applications in sectors such as hydrology. This was presented in Chapter 7.

This final chapter draws conclusions on the research undertaken and identifies areas for further research.

## 8.2 Major research findings

Before detailing the conclusions in each chapter, the thesis's most significant findings and advancements in scientific understanding are identified and highlighted. Three principal outcomes from the research are as follows:

1) A rainfall-runoff model forced with GCM output (precipitation and downscaled precipitation) is currently unable to skilfully simulate observed river flow in a temperate basin such as the Dyfi in Wales. The climate-to-river modelling chain used here produced lower river flow forecast skill than historical river flow observations.

2) Confirmation of spatiotemporal variation of the hydroclimatological linkages across Britain and Europe. The identification of the large-scale climatic circulation that is related to British precipitation/river flow and European precipitation has improved process understanding, and has shown the benefit of using gridded climate fields as opposed to a fixed-point index (NAOI).

3) Seasonal climate models are shown to have low forecast skill over the land masses and over most extratropical regions for forecasts beyond month-1, with precipitation having a more pronounced drop in skill than 2-metre air temperature or mean sea level pressure. The results may be seen as a benchmark of current climate prediction capability using (dynamic) coupled models.

## 8.3 River flow prediction using a rainfall-runoff model forced with climate model data (Chapter 4)

This chapter evaluated river flow prediction by using the PDM rainfall-runoff model forced with direct and downscaled ERA-40 re-analysis and DEMETER climate models'

precipitation (i.e. a physically realistic modelling system), thus addressing research *objective 1*. It was found that climate model precipitation (ERA-40 and DEMETER) was not able to skilfully force the PDM rainfall-runoff model for the River Dyfi in West Wales, Great Britain. This precludes the direct use of GCM precipitation in river flow forecasting. The low seasonal climate model predictive skill of precipitation in Chapter 7 highlighted why the River Dyfi discharge forecasts driven by DEMETER models' precipitation were so poor (Figure 7.2).

A downscaling procedure (SDSM) was applied to produce more appropriate basin-scale (local-scale) precipitation time series. This downscaling process increased the river flow predictive skill compared to simply using GCM precipitation, but this analysis showed that river flow forecasts driven by downscaled DEMETER models' precipitation were not as skilful as forecasts based on historical river flow observations (climatology). Reasons for this result were expounded in Chapters 5 and 7. Chapter 5 showed that the geographical areas with strongest large-scale climatic control on Dyfi basin precipitation/discharge were not local to the Dyfi basin (i.e. nearest GCM grid point), but instead exhibited space-time variability. The regions with strongest statistical associations must be considered in future downscaling studies to attain the highest levels of precipitation or river flow forecast skill. Research in Chapter 7 showed that the large-scale atmospheric circulation (MSLP) in the DEMETER models had low predictive skill in the extratropics, which further explained the reason for inferior river flow forecast skill when using downscaled precipitation series compared to historical river flow observations.

### 8.4 Variation of hydroclimatological relationships across Great Britain (Chapter 5)

This part of the research investigated the linkages between the large-scale climatic circulation (ERA-40) and precipitation and river flow in 10 British river basins addressing *objective 2*. Monthly concurrent Spearman rank correlation analysis was performed between gridded ERA-40 re-analysis climate variables and British river basin precipitation and river flow. The statistical links between the large-scale climatic circulation, and precipitation and river flow shifted and varied in strength seasonally for the 10 study basins, with strongest associations evident in western Britain in winter. The month-to-month shift of strongest correlation highlighted changing precipitation and river flow generating weather systems throughout the year. An atmospheric index, such as the NAOI used herein, was unable to capture these seasonal movements due to the fixed station locations used for the index calculation. This was shown by the systematically lower monthly correlations obtained between the NAOI and precipitation and river flow compared to the gridded (ERA-40) large-scale climatic circulation variables (and in particular the comparable MSLP). Note that weaker large-scale atmospheric links are found with river flow compared to precipitation because of evapotranspiration control on river flow and due to basin properties (such as permeable geologies and basin steepness) that dampen the climate signal. The uncovered spatiotemporal variability in hydroclimatological relationships across Great Britain must be considered in future precipitation downscaling models to achieve the highest river flow forecast skill.

### 8.5 European precipitation connections with large-scale MSLP fields (Chapter 6)

As the relationships between the large-scale climatic circulation and basin precipitation had spatiotemporal variation across Great Britain (Chapter 5), the research was taken further to determine if this was true across Europe, thus completing *objective 2*. Monthly concurrent

Spearman rank correlation analysis was performed between gridded ERA-40 re-analysis MSLP and gridded European precipitation time series from the ENSEMBLES project. Results suggested that the large-scale climate-precipitation relationships had spatiotemporal variability across Europe. In winter a significant MSLP correlation dipole exists with European precipitation, with strongest links in coastal regions (e.g. western Scandinavia, British Isles and Iberian Peninsula) and weaker relationships inland. During spring, summer and autumn smaller MSLP correlation patterns were found with precipitation suggesting that precipitation is generated by smaller scale atmospheric dynamics. In the far north of Europe, in particular Scandinavia, the large-scale winter climatic circulation is in place for longer implying an extended winter season. The smaller regions of climatic control on precipitation in summer possibly indicate that convective weather systems contribute to precipitation receipt. Summer precipitation in Northwest (southern) Europe has a negative (positive) relationship with the SNAO pattern.

The strong significant statistical relationships between the large-scale MSLP and precipitation in some areas of Europe and in certain seasons has aided understanding of the process chain across Europe and demonstrated that precipitation variability is not random, but results from variations in the large-scale atmospheric circulation. This suggests that despite high precipitation variability in Europe, there is a certain degree of predictability of precipitation because of its relationship with MSLP, in particular in winter in western European coastal regions. This precipitation predictability is yet to be realised with the current generation of climate models (see Chapter 7).

### 8.6 Current level of seasonal climate model predictive skill for applications (Chapter 7)

To address *objective 3*, a careful analysis of the predictive skill of 2-metre air temperature, precipitation and MSLP was undertaken for eight seasonal climate forecast models (CFS and DEMETER) by using the joint distribution of observations and forecasts. Using the correlation coefficient, a shift in the conditional distribution of the observations given a forecast could be detected, which determines the usefulness of the forecast for applications. Results suggested that there is a deficiency of skill in the forecasts beyond month-1, with precipitation having a more pronounced drop in skill than temperature or MSLP. At long lead times only the equatorial Pacific Ocean exhibits significant skill. Higher skill is found for temperature in the "idealised" climate model system compared to the real climate system, and if this could be translated to the real climate system improved predictive skill in month-1 could be attained. The low level of predictive skill in the extratropical regions could have an influence on the planned use of seasonal forecasts in climate services and these results may also be seen as a benchmark of current climate prediction capability using (dynamic) coupled models.

### 8.7 Recommendations for future work

#### 8.7.1 Further evaluation of British and European hydroclimatological relationships

As strong concurrent hydroclimatological relationships have been found in Great Britain and Europe, lagged correlation analyses should be undertaken between large-scale climatic circulation and precipitation/river flow to determine whether climate or hydrological system memory provides additional insight on process understanding and precipitation/river flow prediction potential. Uncovering lagged links between the large-scale climatic circulation and river flow may especially be possible for permeable basins (generally basins with high BFI

values), where the rainfall-runoff transformation is strongly attenuated. Furthermore, in permeable basins such as the Dun used in Chapter 5, hydrological memory and thus river flow autocorrelation between successive months could be exploited in autoregressive moving average (ARMA) models for river flow prediction. ARMA models could also be incorporated, for example, in a regression-type model that uses other explanatory variables (e.g. MSLP, SST and sea-ice) of river flow to increase the predictive capability. To this end, it is also necessary to undertake exploratory analyses aimed at identifying geographical regions where slowly varying global boundary anomalies (e.g. SST) are significantly linked with British and European precipitation/river flow. Finally, the use of different temporal averaging periods (such as two-weekly, two-monthly or seasonal averages) for investigating hydroclimatological linkages should be considered to tease out and elucidate on process understanding and prediction potential.

### 8.7.2 Seasonal climate prediction

Based on the conclusions from the assessment of seasonal climate model forecast skill (Chapter 7), the following factors may lead to a larger portion of the inherent climate predictability being realised (i.e. higher predictive skill), and thus should be considered by the climate modelling community:

1) A concerted effort toward improving the understanding and modelling of global atmosphere-land and atmosphere-ocean interactions. As the slowly-varying lower boundary forcing is the premise for seasonal climate predictability (Palmer and Anderson, 1994), the results herein may indicate that the climate models' coupling between the lower boundary (land and ocean surfaces) and overlaying atmosphere may not currently be sufficient to transfer potential predictability from the land/ocean to the atmosphere.

2) A more accurate initialisation of the land surface so that the influence of the land on atmospheric development is more accurately simulated. Research in this vein is being undertaken as part of the GLACE2 experiment (Koster *et al.*, 2010).

3) Increased model resolution is required to more accurately capture regional-scale atmospheric processes. It is hoped that this will be feasible with ever-increasing computing power.

As datasets over a longer time period become available, it should also be feasible to build more stable downscaling models that capture a wider range of climate variability and therefore perform better in simulating future climate and hydrological extremes.

### 8.7.3 Bayesian merging of climate model forecasts for seasonal hydrological prediction

A seasonal hydrological prediction technique that could be tested for British river basins is a Bayesian approach. A Bayesian methodology can spatially downscale and bias correct the seasonal climate predictions, making them relevant for applications. This has been used with some success for seasonal hydrological prediction in North America (Luo *et al.,* 2007, Luo and Wood, 2008). If the seasonal climate predictions are not skilful then the resultant prediction from Bayesian merging (e.g. precipitation) will simply tend to the observed distribution or climatology (see Luo *et al.,* 2007).

## 8.8 Final remarks – current status of seasonal hydrological prediction in Great Britain

This research has shown that it is not currently possible to use seasonal climate model output (directly or downscaled) to skilfully force a rainfall-runoff model for hydrological prediction in Great Britain, underscoring the inherent difficulty in producing climate or hydrological predictions in the extratropics in the vicinity of Great Britain. The assessment of seasonal

climate model predictive skill for applications also highlighted the low climate model predictive skill in the mid-latitudes, and thus the caution that should be exercised when considering such predictions in decision making processes.

The strong significant statistical relationships found between the large-scale atmosphere and precipitation/river flow (in Great Britain and Europe) have improved process understanding and shown that it is necessary to use different geographical areas in each month when building precipitation downscaling models. If skilful seasonal climate predictions are realised in the coming years, then these concurrent hydroclimatological statistical relationships could be used in a "perfect prognosis" (Wilks, 2006) precipitation/river flow prediction approach. In the future it is hoped that seasonal hydrological prediction using a climate-to-river modelling chain could be improved through consideration of the uncovered spatiotemporal hydroclimatological variability, using different downscaling techniques and because of potential improvements to seasonal climate modelling.

# APPENDIX I

Table 1: The monthly multiple linear regression equations used in the SDSM downscaling process in Chapter 4.

| Month | Multiple Linear Regression Equation |
|---|---|
| January | 0.819U500 + 0.052V850 - 0.007Z500 - 0.057 |
| February | 0.767U500 + 0.120V850 + 0.006Z500 - 0.049 |
| March | 0.769U500 + 0.066V850 + 0.021Z500 - 0.100 |
| April | 0.650U500 + 0.148V850 + 0.055Z500 - 0.285 |
| May | 0.712U500 + 0.150V850 + 0.106Z500 - 0.350 |
| June | 0.905U500 + 0.198V850 + 0.088Z500 - 0.295 |
| July | 0.993U500 + 0.230V850 + 0.039Z500 - 0.380 |
| August | 0.916U500 + 0.203V850 + 0.009Z500 - 0.222 |
| September | 0.805U500 + 0.216V850 + 0.076Z500 - 0.207 |
| October | 0.844U500 + 0.053V850 + 0.017Z500 - 0.095 |
| November | 0.783U500 + 0.094V850 + 0.011Z500 - 0.103 |
| December | 0.831U500 + 0.073V850 + 0.015Z500 - 0.044 |

Table 2: Bias and Spearman rank correlation for the mean monthly river flow forecasts driven by the DEMETER 0–3 months and 4–6 months multi-model ensemble precipitation over May 1980 to April 2001. Bold values indicate significant correlation at $\alpha$=0.05 level.

| DEMETER Multi-Model | 0–3 months precipitation | | 4–6 months precipitation | |
|---|---|---|---|---|
| | Bias | Correlation | Bias | Correlation |
| January | -36.31 | 0.004 | -36.15 | -0.17 |
| February | -42.31 | 0.26 | -35.58 | -0.30 |
| March | -46.69 | 0.01 | -46.29 | -0.006 |
| April | -33.16 | 0.38 | -30.97 | 0.43 |
| May | -19.15 | 0.39 | -7.15 | 0.36 |
| June | -57.10 | 0.36 | -52.84 | 0.22 |
| July | -55.73 | 0.19 | -47.15 | 0.06 |
| August | -75.46 | 0.34 | -65.41 | 0.28 |
| September | -81.26 | 0.11 | -77.63 | -0.17 |
| October | -76.67 | -0.02 | -77.28 | -0.33 |
| November | -61.54 | 0.17 | -56.22 | -0.14 |
| December | -57.21 | -0.07 | -54.51 | -0.23 |

Table 3 (a) – (h): Contingency tables for July and August 1984 (low flow period) showing when daily forecasted (from downscaled 0–3 months DEMETER models) and observed river flow are above and below the daily median observed flow over the study period. Correct forecasts are in red font and the percent correct rate (%) is shown in the top right of each individual forecast box. DEMETER represents a forecast using the mean of downscaled ensemble members from all seven DEMETER models; M. FRA stands for METEO FRANCE.

| | (a) | Forecasts | | 50% |
|---|---|---|---|---|
| | **CERFACS** | >med | <med | Totals |
| Observed | >med | 0 | 31 | 31 |
| | <med | 0 | 31 | 31 |
| | Totals | 0 | 62 | 62 |

| | (b) | Forecasts | | 50% |
|---|---|---|---|---|
| | **ECMWF** | >med | <med | Totals |
| Observed | >med | 31 | 0 | 31 |
| | <med | 31 | 0 | 31 |
| | Totals | 62 | 0 | 62 |

| | (c) | Forecasts | | 50% |
|---|---|---|---|---|
| | **INGV** | >med | <med | Totals |
| Observed | >med | 31 | 0 | 31 |
| | <med | 31 | 0 | 31 |
| | Totals | 62 | 0 | 62 |

| | (d) | Forecasts | | 35% |
|---|---|---|---|---|
| | **LODYC** | >med | <med | Totals |
| Observed | >med | 22 | 9 | 31 |
| | <med | 31 | 0 | 31 |
| | Totals | 53 | 9 | 62 |

| | (e) | Forecasts | | 50% |
|---|---|---|---|---|
| | **M. FRA** | >med | <med | Totals |
| Observed | >med | 0 | 31 | 31 |
| | <med | 0 | 31 | 31 |
| | Totals | 0 | 62 | 62 |

| | (f) | Forecasts | | 50% |
|---|---|---|---|---|
| | **MPI** | >med | <med | Totals |
| Observed | >med | 31 | 0 | 31 |
| | <med | 31 | 0 | 31 |
| | Totals | 62 | 0 | 62 |

| | (g) | Forecasts | | 50% |
|---|---|---|---|---|
| | **UKMO** | >med | <med | Totals |
| Observed | >med | 31 | 0 | 31 |
| | <med | 31 | 0 | 31 |
| | Totals | 62 | 0 | 62 |

| | (h) | Forecasts | | 50% |
|---|---|---|---|---|
| | **DEMETER** | >med | <med | Totals |
| Observed | >med | 31 | 0 | 31 |
| | <med | 31 | 0 | 31 |
| | Totals | 62 | 0 | 62 |

Table 4 (a) – (h): Contingency tables for October and November 2000 (High flow period) showing when daily forecasted (from downscaled 0–3 months DEMETER models) and observed river flow are above and below the median observed flow over the study period (Key as in Table 3 in Appendix I).

| | (a) | Forecasts | | 50% |
|---|---|---|---|---|
| | **CERFACS** | >med | <med | Totals |
| Observed | >med | 0 | 30 | 30 |
| | <med | 0 | 30 | 30 |
| | Totals | 0 | 60 | 60 |

| | (b) | Forecasts | | 50% |
|---|---|---|---|---|
| | **ECMWF** | >med | <med | Totals |
| Observed | >med | 0 | 30 | 30 |
| | <med | 0 | 30 | 30 |
| | Totals | 0 | 60 | 60 |

| | (c) | Forecasts | | 50% |
|---|---|---|---|---|
| | **INGV** | >med | <med | Totals |
| Observed | >med | 0 | 30 | 30 |
| | <med | 0 | 30 | 30 |
| | Totals | 0 | 60 | 60 |

| | (d) | Forecasts | | 50% |
|---|---|---|---|---|
| | **LODYC** | >med | <med | Totals |
| Observed | >med | 0 | 30 | 30 |
| | <med | 0 | 30 | 30 |
| | Totals | 0 | 60 | 60 |

| | (e) | Forecasts | | 50% |
|---|---|---|---|---|
| | **M. FRA** | >med | <med | Totals |
| Observed | >med | 0 | 30 | 30 |
| | <med | 0 | 30 | 30 |
| | Totals | 0 | 60 | 60 |

| | (f) | Forecasts | | 50% |
|---|---|---|---|---|
| | **MPI** | >med | <med | Totals |
| Observed | >med | 0 | 30 | 30 |
| | <med | 0 | 30 | 30 |
| | Totals | 0 | 60 | 60 |

| | (g) | Forecasts | | 57% |
|---|---|---|---|---|
| | **UKMO** | >med | <med | Totals |
| Observed | >med | 6 | 24 | 30 |
| | <med | 2 | 28 | 30 |
| | Totals | 8 | 52 | 60 |

| | (h) | Forecasts | | 50% |
|---|---|---|---|---|
| | **DEMETER** | >med | <med | Totals |
| Observed | >med | 0 | 30 | 30 |
| | <med | 0 | 30 | 30 |
| | Totals | 0 | 60 | 60 |

# APPENDIX II

Lavers, D. A., Prudhomme, C. & Hannah, D. M. (2010) Large-scale Climatic Influences on Precipitation and Discharge for a British River Basin. *Hydrol. Processes,* 24**,** 2555-2563. (http://onlinelibrary.wiley.com/doi/10.1002/hyp.7668/abstract).

# APPENDIX III

Lavers, D. A., Prudhomme, C. & Hannah, D. M. (2010) Large-scale climate, precipitation and British river flows: identifying hydroclimatological connections and dynamics. *Journal of Hydrology*, 395, 242-255. (doi:10.1016/j.jhydrol.2010.10.036).

# APPENDIX IV

Lavers, D., Luo, L. F. and Wood, E. F. (2009). A multiple model assessment of seasonal climate forecast skill for applications. *Geophysical Research Letters,* 36**,** L23711, doi:10.1029/2009GL041365.
(http://www.agu.org/journals/ABS/2009/2009GL041365.shtml).

# LIST OF REFERENCES


Anderson, J., Van Den Dool, H. M., Barnston, A., Chen, W., Stern, W. and Ploshay, J. (1999). Present-Day Capabilities of Numerical and Statistical Models for Atmospheric Extratropical Seasonal Simulation and Prediction. *Bulletin of the American Meteorological Society,* 80**,** 1349-1361.

Archer, D. R. and Fowler, H. J. (2008). Using meteorological data to forecast seasonal runoff on the River Jhelum, Pakistan. *Journal of Hydrology,* 361**,** 10-23.

Barlow, M., Nigam, S. and Berbery, E. H. (2001). ENSO, Pacific Decadal Variability, and U.S. Summertime Precipitation, Drought, and Stream Flow. *Journal of Climate,* 14**,** 2105-2128.

Barlow, M. A. and Tippett, M. K. (2008). Variability and Predictability of Central Asia River Flows: Antecedent Winter Precipitation and Large-Scale Teleconnections. *Journal of Hydometeorology,* 9**,** 1334-1349.

Barnston, A. G. and Livezey, R. E. (1987). Classification, seasonality and persistence of low-frequency atmospheric circulation patterns. *Monthly Weather Review,* 115**,** 1083-1126.

Barnston, A. G., Van Den Dool, H. M., Zebiak, S. E., Barnett, T. P., Ming, J., Rodenhuis, D. R., Cane, M. A., Leetmaa, A., Graham, N. E., Ropelewski, C. R., Kousky, V. E., O'Lenic, E. A. and Livezey, R. E. (1994). Long-Lead Seasonal Forecasts - Where Do We Stand? *Bulletin of the American Meteorological Society,* 75**,** 2097-2113.

Barnston, A. G., Kumar, A., Goddard, L. and Hoerling, M. P. (2005). Improving seasonal prediction practices through attribution of climate variability. *Bulletin of the American Meteorological Society,* 86**,** 59-72.

Bartolini, E., Claps, P. and D'Odorico, P. (2009). Interannual variability of winter precipitation in the European Alps: relations with the North Atlantic Oscillation. *Hydrology and Earth System Sciences,* 13**,** 17-25.

Berg, P., Haerter, J. O., Thejll, P., Piani, C., Hagemann, S. and Christensen, J. H. (2009). Seasonal characteristics of the relationship between daily precipitation intensity and surface temperature. *Journal of Geophysical Research-Atmospheres,* 114**,** doi:10.1029/2009JD012008.

Bierkens, M. F. P. and Van Beek, L. P. H. (2009). Seasonal Predictability of European Discharge: NAO and Hydrological Response Time. *Journal of Hydrometeorology,* 10**,** 953-968.

Block, P. J., Souza, F. A., Sun, L. Q. and Kwon, H. H. (2009). A Streamflow Forecasting Framework using Multiple Climate and Hydrological Models(1). *Journal of the American Water Resources Association,* 45**,** 828-843.

Bouwer, L. M., Vermaat, J. E. and Aerts, J. C. J. H. (2006). Winter atmospheric circulation and river discharge in northwest Europe. *Geophysical Research Letters,* 33**,** L06403, doi:10.1029/2005GL025548.

Bouwer, L. M., Vermaat, J. E. and Aerts, J. C. J. H. (2008). Regional sensitivities of mean and peak river discharge to climate variability in Europe. *Journal of Geophysical Research,* 113**,** doi:10.1029/2008JD010301.

Bower, D., Hannah, D. M. and McGregor, G. R. (2004). Techniques for assessing the climatic sensitivity of river flow regimes. *Hydrological Processes,* 18**,** 2515-2543.

Bracken, C., Rajagopalan, B. and Prairie, J. (2010). A multisite seasonal ensemble streamflow forecasting technique. *Water Resources Research,* 46.

Bradford, R. B. and Marsh, T. J. (2003). Defining a network of benchmark catchments for the UK. *Proceedings of the Institution of Civil Engineers, Water and Maritime Engineering,* 156**,** 109-116.

Cantelaube, P. and Terres, J. M. (2005). Seasonal weather forecasts for crop yield modelling in Europe. *Tellus Series a-Dynamic Meteorology and Oceanography,* 57**,** 476-487.

Cardoso, A. O. and Silva Dias, P. L. (2006). The relationship between ENSO and Paraná River flow. *Advances in Geosciences,* 6**,** 189-193.

Carson, D. J. (1998). Seasonal forecasting. *Quarterly Journal of the Royal Meteorological Society,* 124**,** 1-26.

Céron, J.-P., Tanguy, G., Franchistéguy, L., Martin, E., Regimbeau, F. and Vidal, J.-P. (2010). Hydrological seasonal forecast over France: feasibility and prospects. *Atmospheric Science Letters***,** DOI:10.1002/asl.256.

Challinor, A. J., Slingo, J. M., Wheeler, T. R. and Doblas-Reyes, F. J. (2005). Probabilistic simulations of crop yield over western India using the DEMETER seasonal hindcast ensembles. *Tellus Series a-Dynamic Meteorology and Oceanography,* 57**,** 498-512.

Chandimala, J. and Zubair, L. (2007). Predictability of stream flow and rainfall based on ENSO for water resources management in Sri Lanka. *Journal of Hydrology,* 335**,** 303-312.

Chiew, F. H. S., Piechota, T. C., Dracup, J. A. and McMahon, T. A. (1998). El Nino/Southern Oscillation and Australian rainfall, streamflow, and drought: Links and potential for forecasting. *Journal of Hydrology,* 204**,** 138-149.

Chiew, F. H. S., Zhou, S. L. and McMahon, T. A. (2003). Use of seasonal streamflow forecasts in water resources management. *Journal of Hydrology,* 270**,** 135-144.

Chowdhury, S. and Sharma, A. (2009). Multisite seasonal forecast of arid river flows using a dynamic model combination approach. *Water Resources Research,* 45**,** W10428 10.1029/2008wr007510.

Coelho, C. A. S., Stephenson, D. B., Doblas-Reyes, F. J., Balmaseda, M., Guetter, A. and Van Oldenborgh, G. J. (2006). A Bayesian approach for multi-model downscaling: Seasonal forecasting of regional rainfall and river flows in South America. *Meteorological Applications,* 13**,** 73-82.

Colman, A. and Davey, M. (1999). Prediction of summer temperature, rainfall and pressure in Europe from preceding winter North Atlantic Ocean temperature. *International Journal of Climatology,* 19**,** 513-536.

Davies, J. R., Rowell, D. P. and Folland, C. K. (1997). North Atlantic and European seasonal predictability using an ensemble of multidecadal atmospheric GCM simulations. *International Journal of Climatology,* 17**,** 1263-1284.

Dettinger, M. D. and Diaz, H. F. (2000). Global Characteristics of Stream Flow Seasonality and Variability. *Journal of Hydrometeorology,* 1**,** 289-310.

Devineni, N., Sankarasubramanian, A. and Ghosh, S. (2008). Multimodel ensembles of streamflow forecasts: Role of predictor state in developing optimal combinations. *Water Resources Research,* 44**,** 10.1029/2006wr005855.

Doblas-Reyes, F. J., Weisheimer, A., Deque, M., Keenlyside, N., McVean, M., Murphy, J. M., Rogel, P., Smith, D. and Palmer, T. N. (2009). Addressing model uncertainty in seasonal and annual dynamical ensemble forecasts. *Quarterly Journal of the Royal Meteorological Society,* 135**,** 1538-1559.

Dutta, S. C., Ritchie, J. W., Freebairn, D. M. and Abawi, G. Y. (2006). Rainfall and streamflow response to El Nino Southern Oscillation: a case study in a semiarid

catchment, Australia. *Hydrological Sciences Journal-Journal Des Sciences Hydrologiques,* 51**,** 1006-1020.

Efron, B. and Tibshirani, R. J. (1998). An Introduction to the Bootstrap. CRC Press, Boca Raton, FL.

Eldaw, A. K., Salas, J. D. and Garcia, L. A. (2003). Long-Range Forecasting of the Nile River Flows Using Climatic Forcing. *Journal of Applied Meteorology,* 42**,** 890-904.

Fleig, A. K., Tallaksen, L. M., Hisdal, H. and Hannah, D. M. in press. Regional hydrological drought in north-western Europe: linking a new Regional Drought Area Index with weather types. *Hydrological Processes*

Folland, C. K., Colman, A., Rowell, D. P. and Davey, M. (2001). Predictability of Northeast Brazil Rainfall and Real-Time Forecast Skill, 1987–98. *Journal of Climate,* 14**,** 1937-1958.

Folland, C. K., Knight, J., Linderholm, H. W., Fereday, D., Ineson, S. and Hurrell, J. W. (2009). The Summer North Atlantic Oscillation: Past, Present, and Future. *Journal of Climate,* 22**,** 1082-1103.

Fowler, H. J. and Kilsby, C. G. (2002). Precipitation and the North Atlantic Oscillation: a study of climatic variability in northern England. *International Journal of Climatology,* 22**,** 843-866.

Gámiz-Fortis, S., Pozo-Vázquez, D., Trigo, R. M. and Castro-Díez, Y. (2008). Quantifying the Predictability of Winter River Flow in Iberia. Part II: Seasonal Predictability *Journal of Climate,* 21**,** 2503-2518.

Gámiz-Fortis, S. R., Esteban-Parra, M. J., Trigo, R. M. and Castro-Díez, Y. (2010). Potential predictability of an Iberian river flow based on its relationship with previous winter global SST. *Journal of Hydrology,* 385**,** 143-149.

Goddard, L., Mason, S. J., Zebiak, S. E., Ropelewski, C. F., Basher, R. and Cane, M. A. (2001). Current Approaches To Seasonal-To-Interannual Climate Predictions. *International Journal of Climatology,* 21**,** 1111-1152.

Graham, R. J., Gordon, C., Huddleston, M. R., Davey, M., Norton, W., Colman, A., Scaife, A. A., Brookshaw, A., Ingleby, B., McLean, P., Cusack, S., McCallum, E., Elliott, W., Groves, K., Cotgrove, D. and Robinson, D. (2006). The 2005/06 winter in Europe and the United Kingdom: Part 1 - How the Met Office forecast was produced and communicated. *Weather,* 61**,** 327-336.

Grantz, K., Rajagopalan, B., Clark, M. and Zagona, E. (2005). A technique for incorporating large-scale climate information in basin-scale ensemble streamflow forecasts. *Water Resources Research,* 41.

Gustard, A., Bullock, A. and Dixon, J. M. (1992). Low flow estimation in the United Kingdom. Report No. 108. Wallingford: Institute of Hydrology, 88pp. + Appendices.

Gutiérrez, F. and Dracup, J. A. (2001). An analysis of the feasibility of long-range streamflow forecasting for Columbia using El Niño-Southern Oscillation indicators. *Journal of Hydrology,* 246**,** 181-196

Hagedorn, R., Doblas-Reyes, F. J. and Palmer, T. N. (2005). The rationale behind the success of multi-model ensembles in seasonal forecasting - I. Basic concept. *Tellus Series a-Dynamic Meteorology and Oceanography,* 57**,** 219-233.

Hannaford, J. (2004). Development of a strategic data management system for a national hydrological database, the UK national river flow archive. In Liong, Phoon and Babovic (Ed). . Proceedings of 6th International Conference on Hydroinformatics, World Scientific Publishing: p. 637 – 644.

Hannaford, J. and Marsh, T. J. (2008). High-flow and flood trends in a network of undisturbed catchments in the UK. *International Journal of Climatology,* 28**,** 1325-1338.

Harrison, M. (2005). The development of seasonal and inter-annual climate forecasting. *Climatic Change,* 70**,** 201-220.

Hastenrath, S. (1990). Diagnostics and Prediction of Anomalous River Discharge in Northern South America. *Journal of Climate,* 3**,** 1080-1096.

Haylock, M. R., Hofstra, N., Klein Tank, A. M. G., Klok, E. J., Jones, P. D. and New, M. (2008). A European daily high-resolution gridded dataset of surface temperature and precipitation. *Journal of Geophysical Research-Atmospheres,* 113.

Helsel, D. R. and Hirsch, R. M. (1992). *Statistical methods in water resources,* Amsterdam, Elsevier.

Hewitt, C. D. and Griggs, D. J. (2004). Ensembles-based predictions of climate changes and their impacts. *Eos, Transactions, AGU,* 85**,** doi:10.1029/2004EO520005.

Hewitson, B. C. and Crane, R. G. (1996). Climate downscaling: techniques and application. *Climate Research,* 7**,** 85-95.

Hisdal, H., Tallaksen, L. M., Clausen, B., Peters, E. and Gustard, A. (2004). Hydrological Drought Characteristics, in: *Hydrological Drought Processes and Estimation Methods for Streamflow and Groundwater*, Tallaksen, L. M. and Van Lanen, H. A. J. (Eds.), Amsterdam, Elsevier, 139-198.

Holton, J. R. (1992). *An Introduction to Dynamic Meteorology,* San Diego, Academic Press.

Hough, M. N. and Jones, R. J. A. (1997). The United Kingdom Meteorological Office rainfall and evaporation calculation system: MORECS version 2.0 - an overview. *Hydrology and Earth System Sciences,* 1**,** 227-239.

Hurrell, J. W. (1995). Decadal Trends in the North Atlantic Oscillation: Regional Temperatures and Precipitation. *Science,* 269**,** 676-679.

Hurrell, J. W. and Van Loon, H. (1997). Decadal variations in climate associated with the North Atlantic oscillation. *Climatic Change,* 36**,** 301–326.

Hurrell, J. W., Kushnir, Y., Ottersen, G. and Visbeck, M. (2003). An Overview of the North Atlantic Oscillation, in: *The North Atlantic Oscillation Climatic Significance and Environmental Impact*, Hurrell, J. W., Kushnir, Y., Ottersen, G. and Visbeck, M. (Eds.), American Geophysical Union, Washington DC, 1-36.

Ionita, M., Lohmann, G. and Rimbu, N. (2008). Prediction of Elbe discharge based on stable teleconnections with winter global temperature and precipitation. *Journal of Climate,* 21**,** 6215–6226.

Jaagus, J., Briede, A., Rimkus, E. and Remm, K. (2010). Precipitation pattern in the Baltic countries under the influence of large-scale atmospheric circulation and local landscape factors. *International Journal of Climatology,* 30**,** 705-720.

Jones, S. B. (1983). The estimation of catchment average point rainfall profiles. Institute of Hydrology, Report 87.

Jones, P. D., Jonsson, T. and Wheeler, D., 1997. Extension to the North Atlantic Oscillation using early instrumental pressure observations from Gibraltar and south-west Iceland. *International Journal of Climatology,* 17**,** 1433-1450.

Kahya, E. and Dracup, J. A. (1994). The influences of Type 1 El Niño and La Niña events on streamflows in the Pacific Southwest of the United States. *Journal of Climate,* 7, 965-976.

Kiem, A. S. and Franks, S. W. (2001). On the identification of ENSO-induced rainfall and runoff variability: a comparison of methods and indices. *Hydrological Sciences Journal,* 46**,** 715-727.

Kim, J., Miller, N. L., Farrara, J. D. and Hong, S. Y. (2000). A seasonal precipitation and stream flow hindcast and prediction study in the western United States during the 1997/98 winter season using a dynamic downscaling system. *Journal of Hydrometeorology,* 1**,** 311-329.

Kingston, D. G., McGregor, G. R., Hannah, D. M. and Lawler, D. M. (2006a). River flow teleconnections across the northern North Atlantic region. *Geophysical Research Letters,* 33**,** L14705, doi:10.1029/2006GL026574.

Kingston, D. G., Lawler, D. M. and McGregor, G. R. (2006b). Linkages between atmospheric circulation, climate and streamflow in the northern North Atlantic: research prospects. *Progress in Physical Geography*, 30(2): 143-174.

Kingston, D. G., McGregor, G. R., Hannah, D. M. and Lawler, D. M. (2007). Climatic controls on New England streamflow. *Journal of Hydrometeorology*, 8: 367-379.

Kingston, D. G., Hannah, D. M., Lawler, D. M. and McGregor, G. R. (2009). Climate-river flow relationships across montane and lowland environments in northern Europe. *Hydrological Processes*, 23: 985-996.

Kirono, D. G. C., Chiew, F. H. S. and Kent, D. M. (2010). Identification of best predictors for forecasting seasonal rainfall and runoff in Australia. *Hydrological Processes,* 24**,** 1237-1247.

Kirtman, B. P. and Pirani, A. (2009). The State of the Art of Seasonal Prediction: Outcomes and Recommendations from the First World Climate Research Program Workshop on Seasonal Prediction. *Bulletin of the American Meteorological Society,* 90**,** 455-458.

Koster, R. D., Suarez, M. J., Liu, P., Jambor, U., Berg, A., Kistler, M., Reichle, R., Rodell, M. and Famiglietti, J. (2004). Realistic Initialization of Land Surface States: Impacts on Subseasonal Forecast Skill. *Journal of Hydrometeorology,* 5**,** 1049-1063.

Koster, R. D., Mahanama, S. P. P., Yamada, T. J., Balsamo, G., Berg, A. A., Boisserie, M., Dirmeyer, P. A., Doblas-Reyes, F. J., Drewitt, G., Gordon, C. T., Guo, Z., Jeong, J. H., Lawrence, D. M., Lee, W. S., Li, Z., Luo, L., Malyshev, S., Merryfield, W. J., Seneviratne, S. I., Stanelle, T., van den Hurk, B., Vitart, F. and Wood, E. F. (2010). Contribution of land surface initialization to subseasonal forecast skill: First results from a multi-model experiment. *Geophysical Research Letters,* 37**,** L02402, doi:10.1029/2009GL041677.

Krishnamurti, T. N., Chakraborty, A., Krishnamurti, R., Dewar, W. K. and Clayson, C. A. (2006). Seasonal Prediction of Sea Surface Temperature Anomalies Using a Suite of 13 Coupled Atmosphere–Ocean Models. *Journal of Climate,* 19**,** 6069-6088.

Kumar, A. and Hoerling, M. P. (1995). Prospects and Limitations of Seasonal Atmospheric GCM Predictions. *Bulletin of the American Meteorological Society,* 76**,** 335-345.

Kumar, A., Jha, B., Zhang, Q. and Bounoua, L. (2007). A new methodology for estimating the unpredictable component of seasonal atmospheric variability. *Journal of Climate,* 20**,** 3888-3901.

Kundzewicz, Z. W. and Robson, A. J. (2004). Change detection in hydrological records–a review of the methodology. *Hydrological Sciences Journal,* 49**,** 7-19.

Kundzewicz, Z. W., Mata, L. J., Arnell, N. W., Döll, P., Kabat, P., Jiménez, B., Miller, K. A., Oki, T., Sen, Z. and Shiklomanov, I. A. (2007). Freshwater resources and their management. *Climate Change 2007: Impacts, Adaptation and Vulnerability. Contribution of Working Group II to the Fourth Assessment Report of the*

*Intergovernmental Panel on Climate Change*, In Parry, M. L., Canziani, O. F., Palutikof, J. P., Van Der Linden, P. J. and Hanson, C. E. (Eds.), Cambridge University Press, Cambridge, UK, 173-210.

Kuo, C. C., Gan, T. Y. and Yu, P. S. (2010). Seasonal streamflow prediction by a combined climate-hydrologic system for river basins of Taiwan. *Journal of Hydrology,* 387**,** 292-303.

Lamb, H. H. (1972). British Isles weather types and a register of the daily sequences of circulation patterns. 1861-1971. *Geophysical Memoirs*, 116: 85 pp.

Landman, W. A., Mason, S. J., Tyson, P. D. and Tennant, W. J. (2001). Statistical downscaling of GCM simulations to Streamflow. *Journal of Hydrology,* 252**,** 221-236.

Lavers, D., Luo, L. F. and Wood, E. F. (2009). A multiple model assessment of seasonal climate forecast skill for applications. *Geophysical Research Letters,* 36**,** L23711, doi:10.1029/2009GL041365.

Lettenmaier, D. P. and Wood, E. F. (1993). Hydrologic Forecasting, in: *Handbook of Hydrology*, Maidment, D. R. (Ed.), New York, McGraw-Hill.

Leung, L. R., Hamlet, A. F., Lettenmaier, D. P. and Kumar, A. (1999). Simulations of the ENSO Hydroclimate Signals in the Pacific Northwest Columbia River Basin. *Bulletin of the American Meteorological Society,* 80**,** 2313-2329.

Li, H. B., Luo, L. F., Wood, E. F. and Schaake, J. (2009). The role of initial conditions and forcing uncertainties in seasonal hydrologic forecasting. *Journal of Geophysical Research-Atmospheres,* 114**,** 10.1029/2008jd010969.

Livezey, R. E. and Chen, W. Y. (1983). Statistical Field Significance and its Determination by Monte Carlo Techniques. *Monthly Weather Review,* 111**,** 46-59.

Lloyd-Hughes, B. and Saunders, M. A. (2002). Seasonal prediction of European spring precipitation from El Niño - Southern Oscillation and local sea-surface temperatures. *International Journal of Climatology,* 22**,** 1-14.

Lorenz, E. N. (1963). Deterministic nonperiodic flow. *Journal of the Atmospheric Sciences,* 20**,** 130-141.

Lorenzo, M. N., Taboada, J. J. and Gimeno, L. (2008). Links between circulation weather types and teleconnection patterns and their influence on precipitation patterns in Galicia (NW Spain). *International Journal of Climatology,* 28**,** 1493-1505.

Luo, L., Wood, E. F. and Pan, M. (2007). Bayesian merging of multiple climate model forecasts for seasonal hydrological predictions. *Journal of Geophysical Research,* 112**,** D10102, doi:10.1029/2006JD007655.

Luo, L. F. and Wood, E. F. (2008). Use of Bayesian Merging Techniques in a Multimodel Seasonal Hydrologic Ensemble Prediction System for the Eastern United States. *Journal of Hydrometeorology,* 9**,** 866-884.

Marsh, T. J. (2004). The January 2003 flood on the Thames. *Weather,* 59**,** 59-62.

Marsh, T. J., Cole, G. and Wilby, R. L. (2007). Major droughts in England and Wales, 1800-2006. *Weather,* 62**,** 87-93.

Marsh, T. J. (2008). A hydrological overview of the summer 2007 floods in England and Wales. *Weather,* 63**,** 274-279.

Marshall, J., Kushner, Y., Battisti, D., Chang, P., Czaja, A., Dickson, R., Hurrell, J., Mccartney, M., Saravanan, R. and Visbeck, M. (2001). North Atlantic climate variability: Phenomena, impacts and mechanisms. *International Journal of Climatology,* 21**,** 1863-1898.

Mason, I. B. (2003). Binary Events, in: *Forecast Verification: A Practitioner's Guide in Atmospheric Science*, Jolliffe, I. T. and Stephenson, D. B. (Eds.), New York, Wiley, 37-76.

Mayes, J. and Wheeler, D. (1997). The anatomy of regional climates in the British Isles, in: *Regional Climates of the British Isles*, Wheeler, D. and Mayes, J. (Eds.), New York, Routledge, 9-44.

McGregor, G. R. and Phillips, I. D. (2004). Specification and prediction of monthly and seasonal rainfall over the South West Peninsula of England. *Quarterly Journal of the Royal Meteorological Society*, 130: 193-210.

McKerchar, A. I., Pearson, C. P. and Fitzharris, B. B. (1998). Dependency of summer lake inflows and precipitation on spring SOI. *Journal of Hydrology,* 205**,** 66-80.

Moore, R. J. (2007). The PDM rainfall-runoff model. *Hydrology and Earth System Sciences,* 11**,** 483-499.

Murphy, A. H. and Winkler, R. L. (1987). A General Framework for Forecast Verification. *Monthly Weather Review,* 115**,** 1330-1338.

Murphy, A. H., Brown, B. G. and Chen, Y.-S. (1989). Diagnostic Verification of Temperature Forecasts. *Weather and Forecasting,* 4**,** 485-501.

Murphy, A. H. (1993). What Is a Good Forecast? An Essay on the Nature of Goodness in Weather Forecasting. *Weather and Forecasting,* 8**,** 281-293.

Murphy, S. J. and Washington, R. (2001). United Kingdom and Ireland precipitation variability and the North Atlantic sea-level pressure field. *International Journal of Climatology,* 21**,** 939-959.

Nakaegawa, T., Kusunoki, S., Sugi, M., Kitoh, A., Kobayashi, C. and Takano, K. (2007). A study of dynamical seasonal prediction of potential water resources based on an atmospheric GCM experiment with prescribed sea-surface temperature. *Hydrological Sciences Journal,* 52**,** 152-165.

Nash, J. E. and Sutcliffe, J. V. (1970). River flow forecasting through conceptual models part I — A discussion of principles. *Journal of Hydrology,*10 (3), 282–290.

Opitz-Stapleton, S., Gangopadhyay, S. and Rajagopalan, B. (2007). Generating streamflow forecasts for the Yakima River Basin using large-scale climate predictors. *Journal of Hydrology,* 341**,** 131-143.

Palmer, T. N. and Anderson, D. L. T. (1994). The prospects for seasonal forecasting - A review paper. . *Quarterly Journal of the Royal Meteorological Society,* 120**,** 755-793.

Palmer, T. N., Alessandri, A., Andersen, U., Cantelaube, P., Davey, M., Délécluse, P., Déqué, M., Díez, E., Doblas-Reyes, F. J., Feddersen, H., Graham, R., Gualdi, S., Guérémy, J.-F., Hagedorn, R., Hoshen, M., Keenlyside, N., Latif, M., Lazar, A., Maisonnave, E., Marletto, V., Morse, A. P., Orfila, B., Rogel, P., Terres, J.-M. and Thomson, M. C. (2004). Development of a European Multimodel Ensemble System for Seasonal-to-Interannual Prediction (DEMETER). *Bulletin of the American Meteorological Society,* 85**,** 853-872.

Peng, P., Kumar, A., Barnston, A. G. and Goddard, L. (2000). Simulation Skills of the SST-Forced Global Climate Variability of the NCEP–MRF9 and the Scripps–MPI ECHAM3 Models. *Journal of Climate,* 13**,** 3657-3679.

Phelps, M. W., Kumar, A. and O'Brien, J. J. (2004). Potential Predictability in the NCEP CPC Dynamical Seasonal Forecast System. *Journal of Climate,* 17**,** 3775–3785.

Phillips, I. D. and McGregor, G. R. (2002). The relationship between monthly and seasonal South-west England rainfall anomalies and concurrent North Atlantic sea surface temperatures. *International Journal of Climatology,* 22**,** 197-217.

Phillips, I. D., McGregor, G. R., Wilson, C. J., Bower, D. and Hannah, D. M. (2003). Regional climate and atmospheric circulation controls on the discharge of two British rivers, 1974-97. *Theoretical and Applied Climatology,* 76**,** 141-164.

Purdie, J. M. and Bardsley, W. E. (2010). Seasonal prediction of lake inflows and rainfall in a hydro-electricity catchment, Waitaki river, New Zealand. *International Journal of Climatology,* 30**,** 372-389.

Regimbeau, F., Habets, F., Martin, E. and Noilhan, J. (2007). Ensemble streamflow forecasts over France. *ECMWF Newsletter,* 111**,** 21-27.

Reimann, C., Filzmoser, P., Garrett, R. and Dutter, R. (2008). Statistical Data Analysis Explained. Wiley, Chichester, 361 pp.

Rodwell, M. J. and Folland, C. K. (2002). Atlantic air-sea interaction and seasonal predictability. *Quarterly Journal of the Royal Meteorological Society,* 128**,** 1413-1443.

Roy, M. (1997). The Highlands and Islands of Scotland. in: *Regional Climates of the British Isles*, Wheeler, D. and Mayes, J. (Eds.), London, Routledge, 228-253.

Rudolf, B., Beck, C., Grieser, J. and Schneider, U. (2005). Global Precipitation Analysis Products. Global Precipitation Climatology Centre (GPCC), DWD. *Internet publication***,** 1-8.

Ruiz, J. E., Cordery, I. and Sharma, A. (2007). Forecasting streamflows in Australia using the tropical Indo-Pacific thermocline as predictor. *Journal of Hydrology,* 341**,** 156-164.

Saha, S., Nadiga, S., Thiaw, C., Wang, J., Wang, W., Zhang, Q., Van Den Dool, H. M., Pan, H.-L., Moorthi, S., Behringer, D., Stokes, D., Peña, M., Lord, S., White, G., Ebisuzaki, W., Peng, P. and Xie, P. (2006). The NCEP Climate Forecast System. *Journal of Climate,* 19**,** 3483-3517.

Sankarasubramanian, A., Lall, U. and Espinueva, S. (2008). Role of Retrospective Forecasts of GCMs Forced with Persisted SST Anomalies in Operational Streamflow Forecasts Development. *Journal of Hydrometeorology,* 9**,** 212–227.

Sankarasubramanian, A., Lall, U., Devineni, N. and Espinueva, S. (2009). The Role of Monthly Updated Climate Forecasts in Improving Intraseasonal Water Allocation. *Journal of Applied Meteorology and Climatology,* 48**,** 1464-1482.

Sapiano, M. R. P., Stephenson, D. B., Grubb, H. J. and Arkin, P. A. (2006). Diagnosis of Variability and Trends in a Global Precipitation Dataset Using a Physically Motivated Statistical Model. *Journal of Climate*, 19: 4154-4166.

Schaake, J. C., Hamill, T. M., Buizza, R. and Clark, M. (2007). HEPEX: The Hydrological Ensemble Prediction Experiment. *Bulletin of the American Meteorological Society,* 88**,** 1541-1547.

Shukla, J. (1998). Predictability in the Midst of Chaos: A Scientific Basis for Climate Forecasting. *Science,* 282**,** 728-731.

Smith, K. (1972). *Water in Britain,* London, MacMillan Press LTD.

Sorooshian, S., Lawford, R. G., Try, P., Rossow, W., Roads, J., Polcher, J., Sommeria, G. and Schiffer, R. (2005). Water and energy cycles: investigating the links. *WMO Bulletin,* 54**,** 58-64.

Spearman, C. E. (1904). "General Intelligence" objectively determined and measured. *American Journal of Psychology,* 15**,** 201-293.

Steinemann, A. C. (2006). Using Climate Forecasts for Drought Management. *Journal of Applied Meteorology and Climatology,* 45**,** 1353-1361.

Stockdale, T. N., Balmaseda, M. A. and Vidard, A. (2006). Tropical Atlantic SST Prediction with Coupled Ocean-Atmosphere GCMs. *Journal of Climate,* 19**,** 6047-6061.

Sumner, G. (1997). Wales, in: *Regional Climates of the British Isles*, Wheeler, D. and Mayes, J. (Eds.), London, Routledge, 131-157.

Svensson, C. and Prudhomme, C. (2005). Prediction of British summer river flows using winter predictors. *Theoretical and Applied Climatology,* 82**,** 1-15.

Tang, Y., Lin, H. and Moore, A. M. (2008). Measuring the potential predictability of ensemble climate predictions. *Journal of Geophysical Research,* 113**,** D04108, doi:10.1029/2007JD008804.

Thomson, M. C., Doblas-Reyes, F. J., Mason, S. J., Hagedorn, R., Connor, S. J., Phindela, T., Morse, A. P. and Palmer, T. N. (2006). Malaria early warnings based on seasonal climate forecasts from multi-model ensembles. *Nature,* 439**,** 576-579.

Tootle, G. A., Piechota, T. C. and Gutiérrez, F. (2008). The relationships between Pacific and Atlantic Ocean sea surface temperatures and Colombian streamflow variability. *Journal of Hydrology,* 349**,** 268-276.

Toth, Z., Pena, M. and Vintzileos, A. (2007). Bridging The Gap Between Weather And Climate Forecasting - Research Priorities for Intraseasonal Prediction. Camp Springs, Maryland, *Bulletin of the American Meteorological Society*

Troccoli, A. (2010). Seasonal climate forecasting. *Meteorological Applications,* 17, 251-268

Tufnell, L. (1997). North-west England and the Isle of Man, in: *Regional Climates of the British Isles*, Wheeler, D. and Mayes, J. (Eds.), London, Routledge, 181-204.

Uppala, S. M., Kållberg, P. W., Simmons, A. J., Andrae, U., Da Costa Bechtold, V. D., Fiorino, M., Gibson, J. K., Haseler, J., Hernandez, A., Kelly, G. A., Li, X., Onogi, K., Saarinen, S., Sokka, N., Allan, R. P., Andersson, E., Arpe, K., Balmaseda, M. A., Beljaars, A. C. M., Van De Berg, L., Bidlot, J., Bormann, N., Caires, S., Chevallier, F., Dethof, A., Dragosavac, M., Fisher, M., Fuentes, M., Hagemann, S., Hólm, E., Hoskins, B. J., Isaksen, L., Janssen, P. A. E. M., Jenne, R., McNally, A. P., Mahfouf, J. -F., Morcrette, J. -J., Rayner, N. A., Saunders, R. W., Simon, P., Sterl, A., Trenberth, K. E., Untch, A., Vasiljevic, D., Viterbo, P. and Woollen, J. (2005). The ERA-40 re-analysis. *Quarterly Journal of the Royal Meteorological Society,* 131**,** 2961-3012.

Uvo, C. B. (2003). Analysis and Regionalization of northern European winter precipitation based on its relationship with the North Atlantic Oscillation. *International Journal of Climatology*, 23: 1185-1194.

Van Oldenborgh, G. J., Burgers, G. and Klein Tank, A. (2000). On the El Niño Teleconnection to Spring Precipitation in Europe. *International Journal of Climatology,* 20**,** 565-574.

Van Oldenborgh, G. J., Balmaseda, M. A., Ferranti, L., Stockdale, T. N. and Anderson, D. L. T. (2005). Evaluation of Atmospheric Fields from the ECMWF Seasonal Forecasts over a 15-Year Period. *Journal of Climate,* 18**,** 3250-3269.

Vicente-Serrano, S. M. and Lopez-Moreno, J. I. (2008). Nonstationary influence of the North Atlantic Oscillation on European precipitation. *Journal of Geophysical Research-Atmospheres,* 113**,** D20120, doi:10.1029/2008jd010382.

Wallace, J. M. and Hobbs, P. V. (2006). Atmospheric Science An Introductory Survey. International Geophysics Series, 92. Academic Press, London.

Wang, G. and Eltahir, E. A. B. (1999). Use of ENSO Information in Medium- and Long-Range Forecasting of the Nile Floods. *Journal of Climate,* 12**,** 1726-1737.

Wang, Q. J., Robertson, D. E. and Chiew, F. H. S. (2009). A Bayesian joint probability modeling approach for seasonal forecasting of streamflows at multiple sites. *Water Resources Research,* 45.

Wedgbrow, C. S., Wilby, R. L., Fox, H. R. and O'Hare, G. (2002). Prospects for seasonal forecasting of summer drought and low river flow anomalies in England and Wales. *International Journal of Climatology,* 22**,** 219-236.

Wedgbrow, C. S., Wilby, R. L. and Fox, H. R. (2005). Experimental seasonal forecasts of low summer flows in the River Thames, UK, using Expert Systems. *Climate Research,* 28**,** 133-141.

Weigel, A. P., Baggenstos, D., Liniger, M. A., Vitart, F. and Appenzeller, C. (2008). Probabilistic Verification of Monthly Temperature Forecasts. *Monthly Weather Review,* 136**,** 5162-5182.

Weisheimer, A., Doblas-Reyes, F. J., Palmer, T. N., Alessandri, A., Arribas, A., Deque, M., Keenlyside, N., Macvean, M., Navarra, A. and Rogel, P. (2009) ENSEMBLES: A new multi-model ensemble for seasonal-to-annual predictions-Skill and progress beyond DEMETER in forecasting tropical Pacific SSTs. *Geophysical Research Letters,* 36**,** L21711, doi:10.1029/2009GL040896.

Wheeler, D. (1997). North-East England and Yorkshire. In: D. Wheeler and J. Mayes (Editors), Regional Climates of the British Isles. Routledge, New York, pp. 158-180.

Whitaker, D. W., Wasimi, S. A. and Islam, S. (2001). The El Niño-Southern Oscillation and long-range forecasting of flows in the Ganges. *International Journal of Climatology,* 21**,** 77-87.

Wibig, J. (1999). Precipitation in Europe in relation to circulation patterns at the 500 hPa level. *International Journal of Climatology,* 19**,** 253-269.

Wilby, R. L., O'Hare, G. and Barnsley, N. (1997). The North Atlantic Oscillation and British Isles climate variability, 1865-1996. *Weather,* 52**,** 266-276.

Wilby, R. L. (2001). Seasonal forecasting of river flows in the British Isles using North Atlantic pressure patterns. *Journal of the Chartered Institution of Water and Environmental Management,* 15**,** 56-63.

Wilby, R. L., Dawson, C. W. and Barrow, E., M. (2002). SDSM - a decision support tool for the assessment of regional climate change impacts. *Environmental and Modelling Software***,** 145 - 147.

Wilby, R. L., Wedgbrow, C. S. and Fox, H. R. (2004). Seasonal predictability of the summer hydrometeorology of the River Thames, UK. *Journal of Hydrology,* 295**,** 1-16.

Wilks, D. S. (2006). *Statistical Methods in the Atmospheric Sciences,* Burlington, MA, Academic Press.

Wood, A. W., Maurer, E. P., Kumar, A. and Lettenmaier, D. P. (2002). Long-range experimental hydrologic forecasting for the eastern United States. *Journal of Geophysical Research,* 107**,** (D20), 4429, doi:10.1029/2001JD000659.

Wood, A. W., Kumar, A. and Lettenmaier, D. P. (2005). A retrospective assessment of National Centers for Environmental Prediction climate model-based ensemble hydrologic forecasting in the western United States. *Journal of Geophysical Research,* 110**,** D04105, doi:10.1029/2004JD004508.

Wood, A. W. and Lettenmaier, D. P. (2006). A test bed for new seasonal hydrologic forecasting approaches in the western United States. *Bulletin of the American Meteorological Society,* 87**,** 1699-1712.

Wu, R., Kirtman, B. P. and Van Den Dool, H. M. (2009). An Analysis of ENSO Prediction Skill in the CFS Retrospective Forecasts. *Journal of Climate,* 22**,** 1801-1818.

Zubair, L. (2003). Sensitivity of Kelani streamflow in Sri Lanka to ENSO. *Hydrological Processes,* 17**,** 2439-2448.

Zveryaev, II. (2004). Seasonality in precipitation variability over Europe. *Journal of Geophysical Research-Atmospheres,* 109**,** D05103, doi:10.1029/2003jd003668

Zveryaev, II. and Allan, R. P. (2010). Summertime precipitation variability over Europe and its links to atmospheric dynamics and evaporation. *Journal of Geophysical Research,* 115**,** D12102, doi:10.1029/2008JD011213.